OPTIMIZATION OF RESIDUAL STRESSES IN CNC TURNING OF AISI 8620 STEEL

A DISSERTATION

SUBMITTED IN PARTIAL FULFILLMENT OF THE REQUIREMENTS FOR THE AWARD OF THE DEGREE

OF

MASTER OF TECHNOLOGY

IN

[**PRODUCTION ENGINEERING**]

Submitted by

[**TUSHARJEET SINGH KALRA**]

(**Roll No. 2K17/PIE/17**)

Under the supervision

of

Prof. QASIM MURTAZA

(Professor)

Dr. SAURABH AGRAWAL

(Assistant Professor)

DEPARTMENT OF MECHANICAL ENGINEERING

DELHI TECHNOLOGICAL UNIVERSITY

(Formerly Delhi College of Engineering)

Bawana Road, Delhi-110042

CANDIDATE'S DECLARATION

I, **Tusharjeet Singh Kalra**, 2K17/PIE/17 hereby declare that the major project Dissertation titled "**OPTIMIZATION OF RESIDUAL STRESSES IN CNC TURNING OF AISI 8620 STEEL**" submitted to the department of MECHANICAL, PRODUCTION & INDUSTRIAL ENGINEERING, Delhi Technological university, Delhi in partial fulfillment of the requirement for the award of the **Master of Technology**, in **Production Engineering** was original and not copied from any source without proper citation. This was further to declare that the work embodied in this report has not previously formed the basis for the award of any Degree, Diploma, Fellowship or other similar title or recognition.

Place: Delhi **Tusharjeet Singh Kalra**

Date: (2K17/PIE/17)

CERTIFICATE

We hereby certify that the major project entitled **"OPTIMIZATION OF RESIDUAL STRESSES IN CNC TURNING OF AISI 8620 STEEL",** in partial fulfillment of the requirements for the award of the Degree of **Master of Technology** in **Production Engineering** and submitted to the Department of Mechanical, Production and Industrial Engineering of Delhi Technological University has been an authentic record work of **Mr. Tusharjeet Singh Kalra (2K17/PIE/17)** carried out under our supervision.

It is to further certify that the matter embodied in this report has not been submitted to any other university or institution by him for the award of any other Degree/Certificate and the declaration made by him is correct to the best of our knowledge and belief.

Prof. Qasim Murtaza
Professor
Department of Mechanical Engineering
Delhi Technological University

Dr. Saurabh Agrawal
Assistant Professor
Department of Mechanical Engineering
Delhi Technological University

Place: Delhi

Date:

ACKNOWLEDGMENT

I would like to express my special thanks of gratitude to **Prof. Qasim Murtaza** and **Dr. Saurabh Agrawal** for their guidance, unwavering support and encouragement. This project work could not have attained its present form, both in content and presentation, without his active interest, direction and guidance. His personal care has been the source of great inspiration. He has devoted his invaluable time and took personal care in motivating me whenever I was disheartened.

I would also like to thank Prof. Vipin, HOD (Mechanical Engineering Department), Prof. Ranganath M. Singari, Mr. K.Srinivas, Mr. Parvez Ali for their support and guidance, although they had a very busy schedule in managing the corporate and academic affairs.

I am thankful to the technical staff of Delhi Technological University, Mr Virendra, Mr. Roshan, Mr. Suneel for their support.

My deep and sincere gratitude to my family for their continuous and unparalleled love, help and support. I am grateful to my brother for always being there for me as a friend and always with me in every situation. I am forever indebted to my parents for giving me the opportunities and experiences that have made me who I am. They selflessly encouraged me to explore new directions in life and seek my own destiny. This journey would not have been possible if not for them, and I dedicate this milestone to them. I cannot forget to take the name of my cousins for helping me to manage the time and managing my journey to complete the project work.

I also want to thank all those who are directly or indirectly support me for my project.

Tusharjeet Singh Kalra

(2K17/PIE/17)

TABLE OF CONTENTS

LIST OF TABLES

LIST OF FIGURES

ABBREVIATIONS

ANN	Artificial Neural Network
ANOVA	Analysis of Variance
CBN	Cubic Boron Nitride
CCD	Central Composite Design
CNC	Computer Numerical Control
CS	Cutting Speed
DOC	Depth of Cut
DOE	Design of Experiment
FR	Feed Rate
HSS	High Speed Steel
MCU	Machine Control Unit
MRR	Material Removal Rate
OA	Orthogonal Array
RS	Residual Stress
RSM	Response Surface Methodology
SF	Surface Finish
SR	Surface Roughness

ABSTRACT

In the present world, it is observed that quality and productivity plays a vital role in today's industrial applications. Customer satisfaction remains the primary goal for industry which is directly under the influence of quality, whereas the profit margin of the industry relies subsequently on the productivity of the process. Thus for every industry to survive in this competitive world, optimisation is the key element to control the functional parameters simultaneously.

This dissertation is focused on optimising quality characteristics through the use of Response surface methodology. Turning operation on CNC lathe machine is the centre of focus for the study, while the output factors chosen are surface roughness and residual stress.

Surface quality is the major concern for every customer which is rather hard to quantify, thus surface finish is kept as a crucial indicator for CNC Lathe performance. Various input parameters considered for the experimentation is cutting speed, feed rate and depth of cut. Suitable design matrix is prepared using Central Composite Design through RSM including the input parameters for CNC turning on AISI 8620 steel.

The effect of the selected process parameters on the surface finish and residual stress is prepared on RSM. Furthermore ANOVA is used to analyze the performance characteristics in CNC turning operation. Since the p value for the output parameter is less than 0.05 which indicates that model is maintained significant while lack of fit is kept insignificant. Eventually, for obtaining the optimum values for various responses, F value was taken in order to investigate the dominating parameter. Finally the conclusions were drawn which reveals that cutting speed should be raised while feed rate and depth of cut be dropped in order to optimise the output responses.

Keywords: Turning operation, CNC Lathe machine, Response Surface Methodology, ANOVA, Surface Roughness, Residual Stress.

CHAPTER 1
INTRODUCTION

1.1 Introduction

The primary difficulties of the metal-based sector are to increase the productivity and performance of the machined components; there has been enhanced concern in tracking all elements of the machining method. Turning is the most commonly used process of cutting. The determination of machinability of materials is done by measure of SF and material removal rate; Surface finishing is a significant product quality metric as it significantly affects mechanical components performance as well as manufacturing costs. Optimizing machining parameters improves the cost-effectiveness of machining and also greatly improves the product quality.

The objective in contemporary sector is to produce high-quality products at small price in a short time. For this intent, automated and flexible production devices were used along with CNC; computers capable of attaining elevated precision and very small handling moment. Turning was the most popular cutting technique, particularly for machined components for completing [1].

Turning is the first most popular cutting technique, particularly for machined components for completing. To achieve strong reducing efficiency, it is essential to pick reducing parameters in switching procedure. Cutting parameters reflect surface roughness, ground composition and material size variation [2]. The surface finish obtained during the manufacturing process depends primarily on the combination of two aspects: the ideal SF provided by the marks produced by the manufacturing process on the surface and the actual SF produced, taking into account the irregularities and deficiencies that may occur during the manufacturing process, changing the initial production process conditions [3].

The surface of each portion involves some sort of texture produced by any mixture of the previous variables: the material's microstructure, the behavior of the cutting tool, instrument milling distortion, instrument guide mistakes and deformations induced by the component's stress models.

An architectural component's ground composition was very crucial. The machining procedures impacted it by modifications in the product or machine circumstances [4]. A machined texture contains a ton of useful method data including wear of tools, built-up edge, earthquakes, harmed machine components, etc. Under stable machining circumstances, the texture of the substrate modifications significantly owing to wear-induced modifications in the form of the cutting tool.

Because the cutting tool works straight on the workpiece during machining, it impacts the workpiece Texture of the ground of the workpiece which offers accurate and detectable data on the situation of the instrument for the classifications. A machined board is therefore a slicing rim copy that holds precious data about the condition of the instrument (i.e., shortness or bluntness).

Turning was a commonly used machining method that extracts content from the ground of the spinning cylindrical workpiece by a single point cutting tool. In a rotating procedure it is necessary to determine three slicing parameters, i.e. spindle velocity, load frequency and slice length. Common techniques for assessing the efficiency of machining in a rotating procedure are focused on the previous efficiency features: tool lives, cutting power, and surface rigidity. Tool lives, cutting power and SR are basically heavily correlated with slicing parameters such as CS, load frequency, cutting angle [5].

1.2 Turning Operation

Turning is removing metal from the spinning cylindrical workpiece's exterior diameter. Turning is used to reduce the workpiece's diameter, usually to a specified size, and to produce a smooth metal SF. The workpiece is often transformed to have distinct diameters in neighboring parts.

Turning is the process of machining which generates cylindrical components. It can be described in its fundamental shape as the processing of an internal layer

- With the rotation of the workpiece.
- With a single point cutting tool, and
- With the cutting tool flowing adjacent to the workpiece matrix and at a range to clear the job layer.

Taper Turning is almost the same, except that at an angle to the job column the cutter route is the same. Similarly, the range between the cutter and the job unit is diverse in contour spinning to create the required form. Although a single point instrument is a defined, various instrument setups are not excluded, which are often used in rotating. In such configurations, each instrument works as a separate point cutter separately.

1.3 Adjustable Cutting Factors in Turning

In any fundamental rotating procedure, the three main considerations are velocity, load and cutting distance. Of course, other variables such as product type and instrument sort have a big impact, but these are the three that the user can alter by changing the handle straight on the device.

1.3.1 Speed

Speed relates to the spindle and workpiece at all times. It informs their spinning velocity when specified in cycles per minute (rpm). But the ground velocity, or the velocity at which the workpiece fabric moves passed the cutting tool, is the significant characteristic for a specific rotating procedure. It is merely the result of the spinning velocity moments the workpiece circumference before starting the chop. It is expressed in meter per minute (m / min). Every different diameter on a workpiece will have a different CS, although the speed of rotation is the same.

$$V = \frac{\pi DN}{1000} \text{ m/min}$$

In this case, V is the CS in turning; D is the workpiece's initial diameter in mm, and N is the RPM spindle speed.

1.3.2 Feed

Feed is always the cutting tool and it is the speed at which the instrument progresses along its drafting route. The feed rate is immediately associated with slicing velocity on most power-fed laths and is measured in mm (instrument progress) per revolution (of the spindle) or mm / rev.

$$\mathrm{F} = \mathrm{f} \times \mathrm{N} \ \mathrm{mm/min}$$

Here, F is the feed in the mm per minute, *f* is the feed in mm/rev and N is the spindle speed in RPM.

1.3.3 Depth of Cut

DOC is almost self-explanatory. It is the thickness of the layer to be removed from the workpiece (in a single pass) or the distance from the work's uncut to the cut surface, expressed in mm. However, it is essential to notice that the workpiece's diameter is lowered by twice the cutting range as this coating is separated from both ends of the job.

$$d_{cut} = \frac{\mathrm{D} - \mathrm{d}}{2} \ \mathrm{mm}$$

In this case, D and d are the initial and final diameters in mm of the work.

1.4 Computer Numerical Control (CNC)

CNC is one that controls a machine tool's features and movements through a ready program that contains alphanumeric written information. CNC can regulate workpiece or instrument movements, interface parameters like feed, slice volume, velocity, and features like switching on / off spindle, switching on / off coolant.

1.4.1 Applications

CNC's apps include regions for both machine tool and non-machine instrument. CNC is commonly used for lathe, drill press, processing device, processing unit, laser, sheet metal press operating system, tube bending machine etc. in the machine tool classification. Highly automated machine tools have been created, such as switching center and machining center that automatically alter the cutting tools under CNC command. CNC apps in the non-machine instrument group include welding devices, position assessment devices, electronic installation, touch setting, and composite filament winding systems, etc.

1.4.2 Advantages and Limitations

Benefits of CNC are following below:-

- High Accuracy
- Short production time, greater flexibility
- Simpler fixturing
- Contour machining(225 Axis Machining)
- Reduction of human error

The drawbacks include high cost, maintenance and the requirement of skilled part programmer.

1.4.3 Elements of a CNC

A typical CNC system consists of the 6 elements.

- Part Program
- Program Input Device
- MCU
- Drive System
- Machine Tool
- Feedback Device

1.5 Cutting Tool Materials

HSS Tool, cobalt-based alloys, cemented carbides, ceramics, polycrystalline CBN and polycrystalline diamond are presently used for machining. Different apps of machining involve varying components of working tools. The perfect drafting instrument fabric should have all the previous features

- Harder than the job it is drawing
- High heat strength
- Resist friction and heat stress
- Impact resistant

To efficiently pick a device manufacturer's or engineer's machine tools, specific information mus t be provided on:

- Start and complete portion form
- Work piece hardness
- Material tensile strength
- Material abrasives
- Chip sort produced
- Work keeping configuration
- Machine tool power and velocity capability

Some popular cutting tool materials are outlined below:-

1.5.1 Carbon Steel

Carbon Steels have been used since the 1880's for cutting tools. However, carbon steels start to soften at a temperature of about 180^{o}C. This limitation means that such tools are rarely used for metal cutting operations. Plain Carbon Steel Tools, containing about 0.9% Carbon and about 1% Manganese, Hardened to about 62 Rc, are widely used for wood working and they can be used in a router to machine aluminium sheet of upto about 3 mm thick.

1.5.2 High Speed Steels (HSS)

HSS instruments are so appointed for being designed for cutting at greater rates. The most extremely alloyed instrument steels developed around 1900 HSS. The tungsten (T-Series) was first created and typically includes 12-18% tungsten comprising about 4% chromium and 1-5% vanadium. Most grades comprise about 0.5% of molybdenum and the majority of grades comprise 4-12% of cobalt. Approximately 95 percent of all HSS instruments are therefore produced from grades of the M- series. These comprise 5-10% molybdenum, 1.5-10% tungsten,

1-4% vanadium, 4% chromium. HSS instruments are hard and appropriate for disrupted processing and are used to produce complicated shaped instruments such as presses, reamers, presses, presses and equipment cutters. Tools can also be covered to enhance wear strength. HSS represents the biggest tonnage of presently used instrument components. Typical velocity of slicing; 10-60 m / min.

1.5.3 Cast Cobalt Alloys

These alloys have proportions of about 40-55 percent cobalt, 30 percent chromium and 10-20 percent tungsten introduced in the beginning 1900s. Maximum 55-64Rc hardness score. They have excellent work strength, but they are not as hard as HSS but can be used at rates that are somewhat greater than HSS. Now used only in restricted quantities.

1.5.4 Carbides

Also described as cemented carbide or sintered carbide were launched in the 1930s and have elevated strength over a broad heat spectrum, elevated heat conductivity and elevated youth module. Making them an efficient instrument for a broad spectrum of apps and die content. Tungsten carbide and copper carbide are the two groups used for machining; both kinds may be covered or uncoated. Particles of tungsten carbide (1-5 micrometer) are linked together using oxide metallurgy in a silver framework. Pressing and sintering the material to the necessary envelope form. In order to impart unique characteristics, titanium and niobium carbides may also be included. For various apps, a broad variety of grades are accessible. The dominant form of fabric used in slicing is the sintered carbide guides. Cobalt ratio (the usual matrix substance) has a important impact on carbide tool characteristics. Cobalt matrix of 3-6 percent provides better hardness while cobalt matrix of 6-15 percent provides more toughness while reducing hardness, tear resistance and strength.

Carbide tungsten instruments are widely used for metal, cast iron and non-ferrous abrasive products. Typical slicing rates when covered are 30-150m / min or 100-250 m / min.

1.5.5 Coatings

Coatings are often added to advice on carbide tools to enhance the lives of the instrument or to allow greater working rates. Typically, coated hints have life 10 times higher than uncoated advice. Common fabric products, generally 2-15 micrometer dense, include titanium nitride, zinc carbide and aluminum oxide.

1.5.6 Cermets

Developed in the 1960s, it typically includes 70 percent oxide of aluminum and 30 percent carbide of titanium. Some formulations contain carbide of molybdenum, carbide of niobium and carbide of tantalum. Performance appears to give few advantages between those of carbides and ceramics and coatings. Typical rates of slicing; 150-350 m / min.

1.5.7 Ceramics

1.5.7.1 Alumina

For cutting tools, two classes were introduced in the early 1950s; fine-grained high-purity aluminum oxide (Al2O3) and silicon nitride (Si3N4) were pressed into insert tip shapes and sintered at high temperatures. Titanium carbide and zirconium oxide (ZrO2) additions may be produced to enhance characteristics, but while ZrO2 increases the toughness of the fracture, it decreases the hardness and thermal conductivity. To improve toughness and thermal shock resistance, Silicon Carbide (SiC) whiskers can be introduced. Typical rates of slicing; 150-650 m / min.

1.5.7.2 Silicon Nitride

A instrument design was created in the 1970s depending on silicon nitride, which may also comprise aluminum oxide, yttrium oxide and zinc carbide. SiN has an iron bond and is not appropriate for steel processing which contains the components of silicon, aluminum, oxygen and nitrogen. These have greater heat shock strength than carbon nitride and are suggested at medium slicing rates for machining wrought steel and nickel-based super alloys.

1.5.7.3 Cubic Boron Nitride (CBN)

The second hardest material accessible after diamond was introduced in the mid 1960s. CBN instruments can be used either in the shape of tiny strong guides or as a 0.5 to 1 mm dense coating of polycrystalline boron nitride sintered onto a carbide surface under stress. In the latter event the carbide offers crash resistance and the CBN coating offers very large slip resistance and slicing border stability. Typical rates of slicing: 30-310 m / min.

1.5.7.4 Diamond

Diamond is the easiest recognized material, although single crystal platinum has been used as a instrument, it is fragile and must be installed in the right crystal position in order to achieve optimum instrument lives. Single glass laser instruments were predominantly substituted by PCD.

This comprises of very tiny synthetic crystals linked to a density of between 0.5 and 1 mm and attached to a carbide substratum by a elevated temperature elevated stress method. The results are comparable to those of CBN instruments. The diamond crystalline accidental direction stops track propagation, enhancing toughness. Cutting rates typically: 200-2000 m / min.

Developments with whisker strengthening, such as silicon nitride enhanced with silicon carbide whiskers, are being held out to enhance the toughness of instruments. As metal extraction levels have risen, the need for heat-resistant cutting tools has also risen.

The outcome was a transition from HSS to carbide, as well as from ceramics and other super hard materials. HSS trimmed the carbon steels they substituted four times quicker.

Over 30 grades of HSS are available in three primary classifications: grades centered on tungsten, molybdenum and molybdenum-cobalt. In sector today, in most apps, carbide instruments have substituted HSS. These carbide and carbide covered instruments slice quicker than high-speed steels about 3 to 5 times.

Ceramic tools are more resistant to heat than carbides, but more brittle. They are suitable for cast iron, tough steels and super alloys machining. There are two kinds of ceramic extraction instruments accessible: alumina and silicon-nitride-based ceramics. Alumina-based ceramics are used to finish ferrous and some non-ferrous products at elevated velocity semi-and complete. Ceramics based on silicon nitride are usually used to make cast iron and super alloys rougher and lighter.

1.6 Response Surface Methodology

This optimization methodology comprises of several mathematical and statistical techniques that facilitate problem analysis where the answers or results depend on different entry factors and the aim is to optimize the answers. RSM is widely used in locations where the entry factors directly depend on the answers that determine the products performance features. Generally speaking, RSM involves more than 1 entry element in the scientific or experimental strategy. By starting a low-order polynomial, RSM attempts to establish a connection between factors and reactions. For example

A first-order model with 2 independent variables can be expressed as

$$Y = b_0 + b_1x_1 + b_2x_2 + e \quad (1.1)$$

If there is a curvature in the response surface, then a higher degree polynomial should be used. The approximating function with 2 variables is called a second-order model:

$$Y = b_0 + b_1 + b_2 + b_{11}.x^2_{11} + b_{22}.x^2_{22} + b_{12}.x_{12} + e \quad (1.2)$$

Least square method is used for the highest estimate between reaction and variable of the polynomial relationship. Data collection in an organized manner enables to determine the most precise polynomial relationship [6].

1.6.1 Central Composite Design

A CCD usually referred to as a focal composite setup includes an embedded factorial or fragmentary factorial sketch with concentrate points that is expanded by a collection of point concentrate that allows arch assessment. If the distance for each variable from the focal stage of the sketch room to a factorial stage is ±1 division, the distance from the focal stage of the schedule room to a target stage is ±α. The exact estimation of α is based on the desired specific properties for the plan and the quantity of included components. Furthermore, the amount of concentrate stage the project operates is to include actually depends on specific properties needed for the plan [6].

1.7 Surface Structure and Properties

SR is a significant indicator of product quality as it significantly affects mechanical components efficiency as well as price of manufacturing. Surface roughness affects mechanical characteristics such as fatigue behavior, strength to corrosion, creep existence, etc. It also impacts other components operational characteristics such as friction, touch, reflection of color, transmission of heat etc. It is also essential to address characteristics before surface roughness, since they are strongly linked.

After closely examining a metal piece's layer, it can be discovered that it usually consists of several parts. The features of these strands are described here shortly:

(i) Bulk glass, also recognized as the metal substrate, has a framework that relies on the metal's record of composition and handling.

(ii) There is a coating above this mass metal that has generally been deformed plastically and worked to a higher level during the production phase. The work-hardened layer's size and characteristics (the concrete structure) rely on variables such as the handling technique used.

The use of strong instruments and the choice of suitable handling parameters lead to littler-free substrates. During production activities, non-uniform texture distortion or serious heat gradients generally trigger remaining stress in the coating.

(iii) The metal is processed and stored in an inert environment or is a noble metal such as gold or platinum, an oxide layer forms over a hard layer of work.

(iv) The ground oxide sheets are usually coated with dissolved gas and moisture strands under ordinary climate circumstances.

Therefore, substrates have characteristics that are usually very hard from substrate ones. The oxide from the substratum on a metal layer is usually very hard. Oxide is usually much difficult on a metal layer than base metal. Oxides therefore appear to be brittle and abrasive.

Surface performance is an significant parameter for assessing the efficiency of tool instruments and machined components, thus achieving the required soil value for the mechanical components ' operational conduct. The ground roughness is the item performance index and affects several characteristics such as fatigue strength, strain ratio, lubrication, corrosion resistance and machine component wear resistance. Special focus is now given to spatial precision and surface finishing in the manufacturing industry.

The measurement and characterization of the surface finish is therefore regarded to be the predictor of the results of machining.

1.8 Factors affecting surface finishing

Whenever two machined surfaces fall into touch with each other, the quality of the binding components performs a major part in the efficiency and carry of the coupling components. The height, size, structure and orientation on the workpiece of these ground defects depends on a variety of variables such as:

1.8.1 Depth of Cut

Increasing the working range improves the strength to slicing and the vibration amplitude. As a result, the temperature reduction also increases. Therefore, ground performance is anticipated to deteriorate.

1.8.2 Feed

Experiments demonstrate that because of the rise in working power and vibration, surface roughness also improves as the feed rate rises.

1.8.3 Cutting Speed

Increasing the CS usually increases the performance of the surface.

1.8.4 Engagement of the cutting tool

This variable operates in the same manner as cutting thickness.

1.8.5 Cutting Tool Wears

The cutting edge defects owing to strain are displayed on the ground of the machine. In addition, as tool wear rises, there will be other vibrant events such as increased noise, which will further deteriorate ground performance.

1.8.6 Use of Cutting Fluid

The cutting fluid is usually advantageous in terms of SR because it has three distinct effects on the cutting method. First, it absorbs the heat generated during the cutting process by mainly cooling the tool point and the working surface. In addition, the cutting fluid can reduce the friction between the rake face and the chip and between the flank and the machined surface. Finally, the cutting fluid's laundry intervention is significant as it involves separating chip pieces and wearing droplets. Therefore, it is anticipated that the performance of a ground machined with the existence of working fluid is greater than that acquired from wet processing.

The required slicing parameters are generally chosen depending on the handbook's knowledge or use. But by modeling the surface roughness and optimizing slicing parameters, a stronger outcome can be accomplished. Several mathematical models were built to identify the connection between reducing efficiency and slicing parameters depending on statistical regression or neural network methods.

Since Turning is the main procedure in most of the industry's manufacturing cycle, surface finishing of turning parts has a higher impact on product quality. The SF in Turning has been discovered to be affected by a variety of variables such as load frequency, work hardness, volatile built-up edge, velocity, slicing thickness, slicing moment, use of working liquids, etc.

1.9 Quality and Productivity

Quality and productivity have been seen for years as two significant corporate efficiency indexes, particularly in manufacturing sectors. They are always stressed individually, though. The primary causes that value and productivity are not emphasized at the same time are that the goals and indicate a favorable connection between value and productivity.

- Importance of productivity
- Keep expenses down for profit improvement and/or price reduction.
- Makes it possible for companies to invest more on enhancing customer service and additional facilities.
- Quality Importance:-

- Increase faithful customer repetition buys.
- Allows a company to distinguish its products.

Effectively managing performance was a main determinant in the search of reduced overall costs and enhanced customer satisfaction by an organization. In previous days, performance problems were predominantly specified or processed and related to machinery being unable to manufacture performance customer-desired parts and products in a credible fashion to a required standard. This was mainly a task for the company and was addressed as such. The difficulties of today are quite distinct. The performance of a commodity today relies not only on the operations performed on it within the company, but also on the value chain at every point.

The performance of its item is the concern of every manufacturing organization. While it is essential to satisfy the volume demands and the manufacturing timetable, it is similarly essential that the completed item meets the specifications that have been developed. It is because the fulfillment of the customer is obtained from products and facilities of value. Strict rivalry at domestic and global stage and consciousness of clients involve the company's existence and development to produce value products and facilities. It is more probable that performance and productivity will give wealth to the nation and enhance the standard of work life.

However, by operating its company at the required financial stage, the leadership seeks to attain client fulfillment. Both can be achieved through the growth of the value of wealth equity, performance retention, and product quality improvement.

It should be borne in mind that efficiency is affected by many variables such as skills of the worker, motive and commitment, techniques of employment used, performance of workmanship, development of employees, equipment used and leadership efficiency. Productivity is the cornerstone of any nation's financial development. Higher productivity results in greater living standards.

Higher productivity findings in cost reduction as well as enhanced marketing opportunities, enhanced customer service responsiveness, improved cash flow and revenues. Increasing achievement in current company can contribute to operational growth and an boost in the amount of employment. If salaries rise without a rise in productivity, it will result in higher item costs and contribute to inflation.

1.10 Work piece Material

AISI 8620 Steel is a stainless steel with small alloy nickel, chromium, molybdenum case, usually provided with peak HB 255max hardness as folded situation and provides elevated external resistance and excellent internal strength, rendering it extremely susceptible to carry. The key resistance of AISI 8620 steel is greater than that of grades 8615 and 8617.

During hardening procedures, AISI 8620 stainless metal is versatile, allowing enhancement of case / core characteristics. Pre-hardened and strengthened (uncarburized) 8620 may be further dried by nitriding, but owing to its low carbon material, it will not react satisfactorily to the hardening of fire or induction. Steel 8620 is suitable for apps requiring a mixture of wear resistance and toughness. This grade is usually delivered in round bar [7].

Figure 1.1: Work piece Material of AISI 8620 steel

1.10.1 Properties of Material AISI 8620

- High strength

- High toughness
- Good hardenability
- Stability against overheating
- Complex chemical composition
- High concentration of alloy elements, such as Cr, Ni and Mo

1.10.2 Application of AISI 8620 Steel

AISI 8620 steel fabric for light to intermediate strained parts and pipes needing elevated layer wear resistance with decent core strength and effect characteristics is widely used by all business industries.

Typical apps include: Arbors, Bearings, Bushings, Cam Shafts, Differential Pinions, Guide Pins, Piston Pins, Gears, Splined Shafts, Ratchets, Sleeves and other apps where a steel can be easily machined and carburized to regulated situation levels is useful [7].

1.11 Force analysis

1.11.1 Cutting force (F_C)

This force is in the direction of primary motion. The cutting force constitutes about 70~80 % of the total force F and is used to calculate the power P required to perform the machining operation,

$P = VF_C$

Where V=velocity of tool

Fc=cutting force

1.11.2 Thrust force (F_t)

This force is in direction of feed motion in orthogonal cutting. The thrust force is used to calculate the power of feed motion.

1.11.3 Feed force (F_f)

In the longitudinal path, the axial or feed power operates. Its also called the push power as its in the tools flow path. The radial or torque power is radial and appears to move the device back from the workpiece.

1.12 Surface Roughness Measuring Instrument

The Surtronic 3 + is a portable and is suitable for workshop and laboratories use. Accessible parameters for evaluating the texture of the ground are: Ra, Rq, Rz (DIN), Ry and Sm. The instruments evaluation parameters and other features are focused on microprocessor. The results

of the measurement are displaced on an LCD screen and for further results can be output to a voluntary printer or other computer.

An alkaline non-rechargeable battery usually powers the device. If chosen, it is possible to us a rechargeable Ni-Cad battery[8][9].

Figure 1.2: Surface roughness measurement apparatus in Metrology Lab

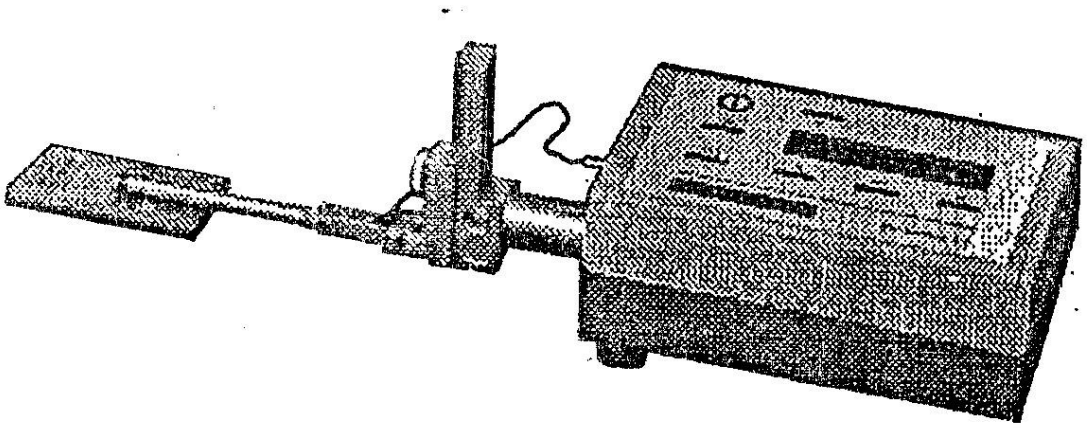

Figure 1.3: Surface roughness measurement apparatus (Referred from Instrument Manual)

1.12.1 Display-Transverse Unit

The display-traverse units bottom board holds a control board of the mesh sort and a screen of liquid crystal. The system contains the electronics for managing the test process, calculating the

test information and displaying the outcomes, or the RS232 port for use with a printer (when included) or a laptop for further evaluation.

The system also includes a ride engine that crosses the ground to be evaluated through the bin.The stroke of measurement always begins from the severe locations outside.

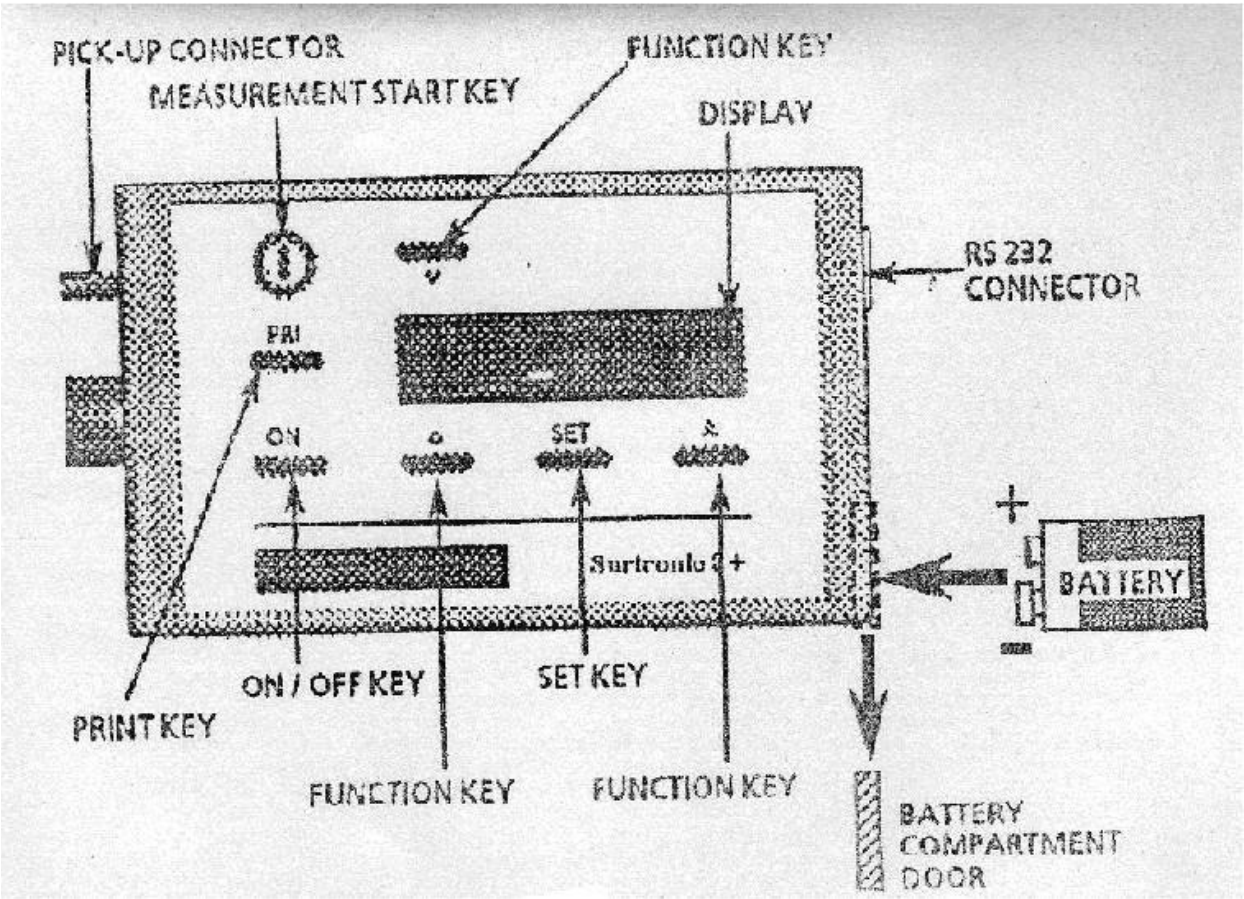

Figure 1.4: Display Transverse Unit (Referred from Instrument Manual)

The pickup returns to this position prepared for the next measurement at the end of the measurement. The duration of the crossing is determined by cut-off (Lc) or duration (Ln) choices. Available Taylor Hobson Surtronic 3 + device has a skid pickup that is used to automatically move through a ride engine. Thus such transport would involve at approximately 10 mm of range. Therefore, on switched job item, we involve suitable ground transport length. These dimensions were engaged to keep the stylus traveling on the best surface as the cutting at the beginning or at the end could be improper. This could also reduce the mistake in estimation and there is less possibility of measuring the wrong side values.

1.12.2 Pick-Up Mounting Components

The pick-up is fastened to the drive shaft.

1.12.3 Mounting Bracket

Through a knurled button, this is attached to the drive shaft. Although usually used horizontally, the pick-up can be switched to angle or remove it from the center line. If the right-angle pick-up is in use, it can also be installed sideways on the drive shaft.

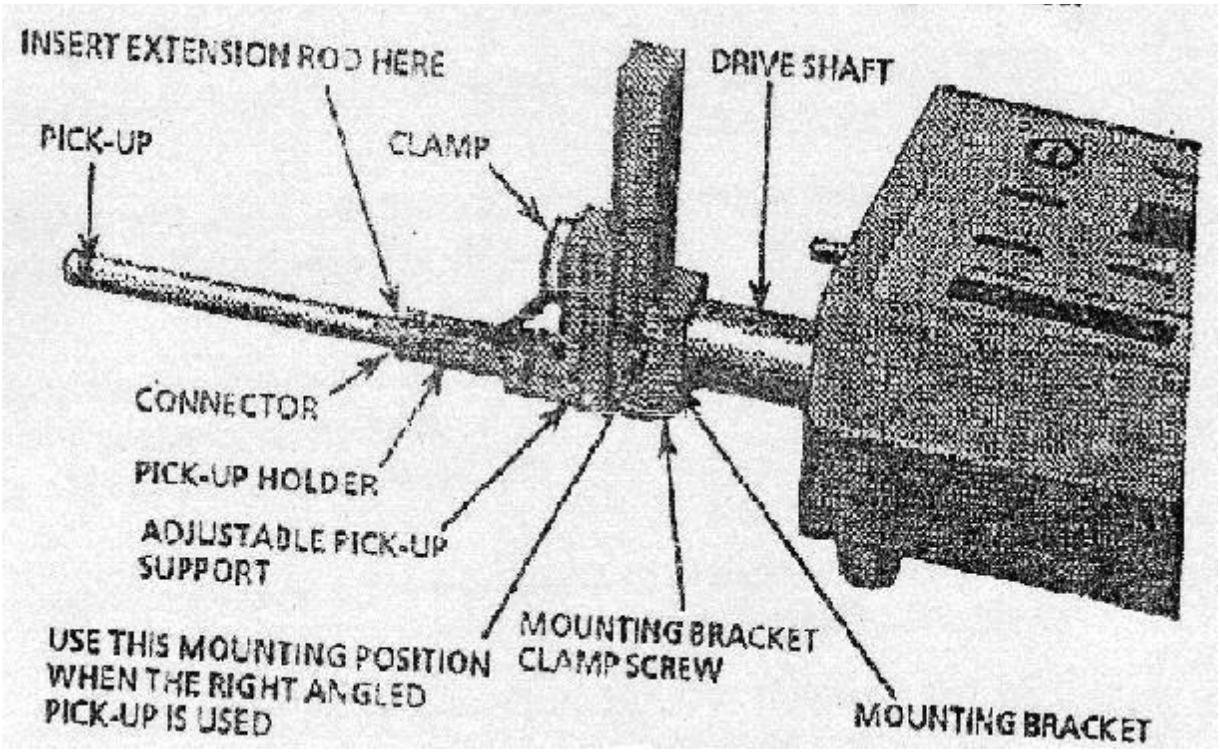

Figure 1.5: Mounting Bracket (Referred from Instrument Manual)

1.12.4 Adjustable Support

This can be clamped at any positions on the slide of the mounting bracket to provide pick-up height adjustment.

1.12.5 Pick-up Holder

This fits into the crutch of the pick-up support and is held in place by a spring plunger.

1.12.6 Connector

The pick-up ribbon loop is screwed into the pick-up unit and placed into the pick-up shelf unit, with the result coming out through the holder pocket. Connecting the guide first to the display-traverse device and then to the pick-up is advisable. The brief pick-up is not needed when using the expansion cord and the top of the tube itself is placed into the container.

1.12.7 DIP switch settings

When powering up with a fresh batteries, the standard device configurations are fixed via DIP buttons inside the display-traverse device. Menu / pushbutton activities can change the choices. Access to the DIP switches is done by screwing the three feet off the base of the display-traverse unit, then removing the screws partially covered by the feet.

1.12.8 Pick-up

The pickup is a variable reticence style transducer that is backed on the ground to be evaluated by a skid, a bent base projected in the area of the stylus from the bottom of the pickup. As the pickup traverses the floor, the stylus motions compared to the skid are identified and transformed into a corresponding electrical signal. The skids curvature radius is much larger than the spacing of roughness. This allows it to run almost uninfluenced by the roughness across the ground and gives a data depicting the overall ground shape. Even so, it will be necessary to use the pickup with the shoe in conjunction with the 2.5 mm (0.1 in) cut-off when the waviness is commonly distributed.

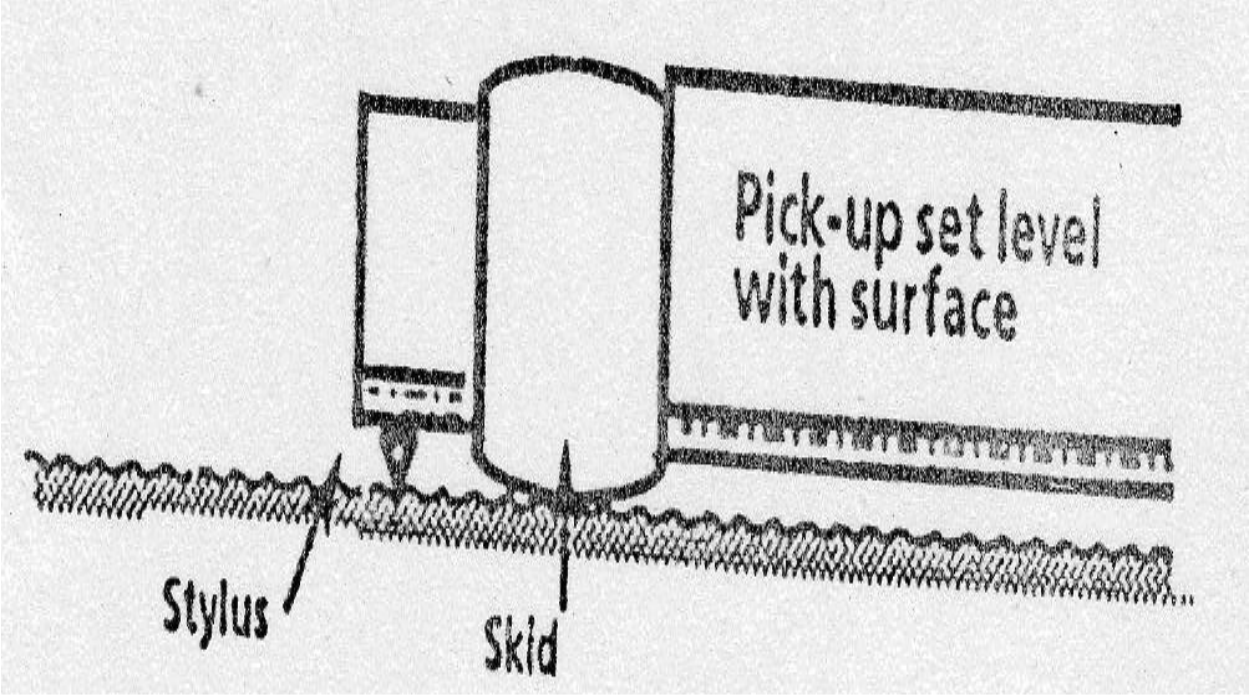

Figure 1.6: Pick-up (Referred from Instrument Manual)

Table 1.1 Surtronic 3+ Specifications (Referred from Instrument Manual)

Battery	Alkaline: Minimum 600 Measurements of 4mm Measurements Lengths. Ni-Cad: Minimum 200 Measurement of 4mm Length Size: 6 LR 61 (USA/Japan), Fixed Battery External Charger (Ni-Cad Only) 110/240V, 50/60 Hz
Traverse Unit	Traverse Speed: 1mm/Sec
Measurement	Metric/Inch Preset by DIP-Switch
Cut-Off Values	0.25mm, 0.8mm, and 2.50mm
Traverse Length	1, 3, 5, 10, Or 25.4 + 0.2mm At 0.8mm Cut-Off
Display	LCD-Matrix. 2lines * 16 Characters
Keyboard	Membrane Switch Panel Tactile
Filters	Digital Gauss Filters or 2CR Filter (ISO) Selectable By DIPSwitch
Parameters	Ra, Rq, Rz (DIN), Ry and Sm.
Calculations Time	Less Than Reversal Time Or 2 Sec Which Ever Is The Longer

1.13 Methods of measuring residual stresses in components

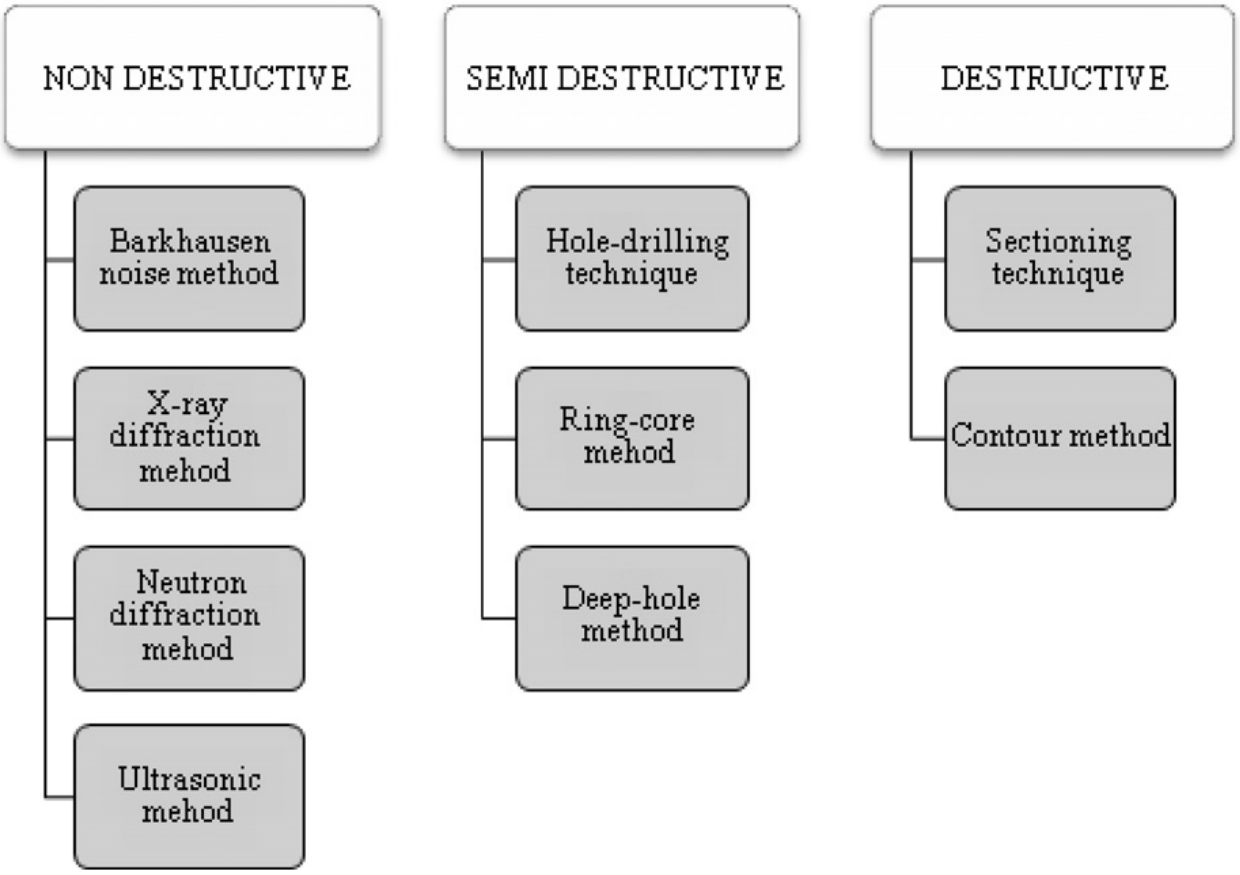

Figure 1.7: Methods of measuring Residual Stress adopting by [9]

RS can be defined as stresses that, in the absence of external forces or thermal gradients, remain within a material or body after fabrication and material processing. They can also be generated by service loading, resulting in inhomogeneous deformation of plastic in the portion or sample.

RS can be described either as macro or micro stresses and both can be available at any moment in an element [10].

1.13.1 Causes of residual stresses

During most manufacturing procedures, RS are produced requiring plastic deformation, thermal therapy, machining or handling activities that convert the form or alter materials characteristics. They come from a variety of causes and may be available in the unprocessed raw material, produced during manufacturing or result from in-service loading [10].

It is classified the origin of RS in the following way:

- differential plastic flow;
- differential cooling rates;
- bulk change phase etc

CHAPTER 2

LITERATURE REVIEW

2.1 Influence the Input process parameter of CNC Turning through Response Surface Methodology

The Literature Review of the project in the form of Paragraph consists of the selection of the material of work piece and different research work added in the area of interest of topic of this project.

Vijay Kumar et al. [11] preferred working on EN19 stainless steel for turning through using carbide tool. The author selected FR, CS, lubricant and DOC as the initial input parameters while SR and MRR were expected to be the output parameters. Tagauchi's L18 mixed type OA experimental design is chosen for identification and finally ANOVA is applied for validity of process parameters on response variable.

E. Garcia Plaza et al. [12] implemented CNC turning operation through online platform for mitigation of inspection time and reduction of cost, cutting force signals were transmitted based on wavelet packet transform (WPT) which is further classified as G-WPT, E-WPT, SE-WPT. In the process G-WPT was responsible for the calculation meant for cutting force analysis, whereas E-WPT and SE-WPT is responsible for the reduction of signal processing time.

Rajesh Kumar et al. [13] used high carbon high chromium steel (HCHCr) material and performed CNC turning operation taking the inputs for analysis as CS, DOC and FR , while the output parameters selected for the optimization purpose are the Surface Roughness maintained after turning and the rate of material removal during turning operation using the Tagauchi Technique. The tools handled for the turning operation are the carbide inserts. Optimization is achieved using the regression and the variance analysis and finally L9 orthogonal array was used.

B C Routara et al. [14] investigated EN-8 steel for turning on CNC, in order to calculate the surface roughness under optimum cutting variables. RSM was preferred for analysis of surface roughness prediction by developing second order mathematical model. The model was examined and consulted using F test and ensured analysis was performed using ANOVA. Cutting parameters was essentially analysed using Genetic Algorithm.

N. Satheesh et al. [15] worked on Carbon Alloy Steel through CNC turning in order to understand the effect of FR and CS on the SR. Author chose five different categories of carbon

alloy steels namely SAE8620, EN8, EN24, EN19 and EN47. Results reveal that SR is directly dependent on the FR whereas it shows a reverse relationship with the cutting speed.

M. Nataraj et al. [16] developed a composite consisting of alumina(Al_2O_3) and molybdenum disulphide (MoS_2) reinforcement with aluminum alloy LM6 which is turned further and then the information is supplemented to Design of Experiment for analyzing, which is perhaps linked with Response Surface Method. Experimentation was done taking inputs such as CS, FR and DOC while the output parameters considered for the purpose are Specific cutting pressure (SCP) and SR (R_a).

K. Venkatesan et al. [17] worked with Inconel 617 alloy by turning using MQL for the investigation of machinability using the CNC turning via special carbide insert tool. Both RSM and L9 orthogonal array was preferred for the optimisation purpose. Results implied the dependency of Cutting velocity and force upon the SR and tool wear. Other keen observation regarding the research is that as the lubricant quality was lowered and tool friction was increased, there was a sharp rise in curl diameter.

Roopa Tulasi et al. [18] worked on EN24 steel for gathering information on Surface Roughness which is affected through various parameters such as CS, FR, DOC, Nose Radius and Rake angle. Experimentation was carried out on conventional lathe and method adopted for optimization was Tagauchi's approach. The cutting parameters considered for the process are likely to be at 400 rpm cutting velocity, feed is maintained at 0.25mm/rev and finally DOC is maintained close to 0.5 mm

C.L. He et al. [19] tried developing a model for checking surface roughness through turning. Surface Roughness is primarily studied through analytics via modeling part and then practically considered through ISO standards, thereby finally the modeling factors are categorised into easy and difficult ones. The author finally discussed about the advantages and disadvantages of the modeling and also mentioned about the future scope of the current work.

D. Palanisamy et al. [20] initiated the process by working on PH stainless steel using the grey fuzzy approach which is occupying the power of sustaining mixed profits of both fuzzy logic approach as well as grey system. Taguchi analysis including the L27 OA is implemented for the purpose of designing and performing of experiment. CS, FR and DOC is provided as the initial incoming parameter whereas SR and power consumption is used as the output responses. Taguchi method tried to frame coordination between input variable and output responses using

grey system approach.

Surendra et al. [21] performed the CNC turning operation on Aluminium alloy 8011 using L27 Taguchi OA for performing of experiment in which the inputs like CS, FR and DOC were adjusted while the output parameters for the experiment was SR and MRR. For the valid experimentation, Taguchi fuzzy application was chosen for the optimisation. Results manifested that feed remained the dominant factor besides DOC and finally comes the speed of operation.

Korimilli et al.[22] worked on Aluminium 7075 alloy for the purpose of determining the surface performance and stress induced once it is turned on CNC by varying inputs such as CS and DOC and calculating RS and micro hardness at different circumferential points of the specimen using Digital Vickers Micro-hardness tester. Residual stress is calculated using X-Ray diffraction method. Results calculated helps in identifying the service life.

Sudhansu et al. [23] worked on AISI 4340 steel using CVD for the purpose of investigating various factors including chip morphology, flank wear and surface roughness by application of L9 OA for developing the design platform with 3 levels of inputs selected namely the CS, FR and DOC. Results displayed that CS and FR of operations played dominant role in manipulating the SR and flank wear. Experimentations were carried forward using Scanning electron microscope for invigilating chip structuring. MRA was used for optimisation purposes of the mathematical model prepared. Gilberth approach is used cost compatibility of the experiment.

D. Palanisamy et al. [24] worked on peak age PH stainless steel by considering various process parameters such as CS, FR and nose radius and responses as an output considered are cutting force, SR and micro-hardness for the purpose of acquiring knowledge regarding machinability performance. Results manifested that hardness saw a substantial hike for the initial height of specimen then a fine drop at the sub surface, finally it settled for the base metal hardness. Conclusions that can be drawn out of the experiment is with higher nose radius and cutting speeds and with lower feed rates, surface finish can be developed significantly.

P. Bhanu Prakash et al. [25] worked on AlSi7Mg with an objective of determining optimisation methods while performing CNC turning operation and using Taguchi's design of experiment and L27 OA for performing the optimisation operations. The input parameters or process parameters considered are CS, FR and DOC while the responses generated are material removal rate and surface roughness. Two essential techniques considered for study are Taguchi's S/N

ratio for generating relationship between the various independent process parameters while the grey relational analysis is used for extracting optimisation characteristics.

R.K. Bharilya et al. [26] turned Carburised Mild Steel, aluminium alloys and brass using CNC and then the force analysis is performed using the cutting force dynamometer. For the experimentation purpose, force dynamometer is implemented to achieve a drop in cutting force and enhance cutting speed wherein the objective stands to accomplish finer surface finish. Author in this context took CS, FR and DOC as the input parameter while responses mentioned are SF and uniformity of the specimen.

G. Kartheek et al. [27] worked on Inconel 718 with tool inserts usually made up of cemented carbide namely TiCN-Al_2O_3 coated cemented carbide inserts with the objective of mitigating residual stresses, improving surface finish and optimising material removal rate. Author has implemented L9 orthogonal array along with grey relational theory which empowers optimum parameters for improving surface finish and developing lower residual stresses. Grey Relational analysis is best suitable as optimization tool.

Vallabh D. Patel et al. [28] analysed AISI D2 steel which is operated on hard turning using the CBN tool for the purpose of Surface Roughness. Specimens were tested on variable CS, FR and nose radius while the DOC is maintained same throughout. Results manifested that there was a simultaneous dependency in various parameters. Feed of cut played the major role in maintaining SR in companionship with the CS and tool nose radius.

Asit Kumar Parida et al. [29] worked on Monel-400 by heating it up using oxygen and LPG before turning operation, machining parameters such as CS, FR, DOC and temperature are taken as the inputs while surface roughness and flank wear are taken down as the output variables for performing RSM operations via central composite design, ANOVA is implemented for the purpose of shear analysis. Eventually after obtaining the regression equation, the model is conceived to be satisfactory with minor errors arising between the experimental and simulated results.

Aimin Yang et al. [30] investigated Titanium alloy TC11 through finish turning. The input parameters under consideration were CS, DOC and FR while the response parameter maintained was SR. The author suggested using RSM for mathematical modeling to develop regression equations among various parameters and the responses; finally ANOVA was adopted for

precision checking. Results manifested that desired MRR can be achieved at the optimum condition derived from the experimentation without compromising the surface finish.

K. Manikanda et al. [31] worked on EN31 steel by performing the turning operations, author choose to optimize the experimentation through the Taguchi and RSM. The input variable selected for the process is CS, DOC and FR whereas SR and Material Removal Rates are maintained as the output response. Results manifested that cutting speed had a major role to deliver in SR while FR and DOC is responsible to handle MRR more diligently. Since the error quoted in the entire experimentation is less than 6% which implies that model clears the feasibility test.

Lianjie Ma et al. [32] studied the impact of turning Ceramics which is brittle in nature and thus cultivates pits while machining. The study concentrates on statistical analysis of stress generation and energy requirements during fracture and chips formations. Author took into consideration Fluorophlogopite while turning on CNC lathe with PCD tool. Results manifested that as the CS and DOC were raised, ductile shearing turned into brittle fracturing. It also declared that turning force and surface structure played a vital role in material removal. At the transition point, huge amount of force needs to be dedicated for material removal.

S.P. Leo et al. [33] worked on C360 Copper alloy for the puopose of turning through Tungusten Carbide inserts. The input parameters selected are CS, FR and DOC while the output responses taken were SR and material removal rates. The author chose to work on Taguchi L27 OA for the optimisation purpose while working pins were structured using micromachining. Results manifested that Lower range of process variables holds responsible for maintaining good surface finish while upper range holds responsibility of generating higher MRR.

Aezhisai Vallavi et al. [34] worked on Metal matrix composites by investigating the factors responsible for impacting cutting force and SF. Author chose to have CS, DOC, FR and silicon carbide percentage as their process parameters. RSM is deployed for developing the mathematical model while analysis of variance is applied for verifying the experimentation.

Eva M. Rubio et al. [35] worked on Titanium Alloy bars Ti6Al4V which are prepared by turning using inputs as DOC, FR, CS, type of cooling system, type of tool and the measurement location. DOE is adopted for working with full factorial design so as to visualise all possible variations with surface roughness. Results manifested that feed rate, spindle speed and

measurement location plays keen role in determining the surface roughness while factors like type of cooling system and the tool type are negligently favourable to the process.

H. Joardar et al. [36] worked on Aluminium Metal Matrix composites with TiB2 as the reinforcement used. Mathematical modelling was executed using the RSM with the initial input parameters as CS, DOC and FR while SR is kept as the response. ANOVA verifies the applicability for the model as the error margin was maintained quite negligible. Results manifested that CS followed by FR played significant role in influencing SR. Conclusion that came out quite clearly was surface roughness can be improved by mitigating feed rates while upgrading the cutting speeds and depth of cut.

C.L. He et al. [37] worked on investigating surface roughness of turned specimens through influencing factors and by modeling methods. Modeling processes are divided under two categories namely theoretical and emperical solutions. Finally the various factors are further classified as ‘easy’ or ‘difficult’. Eventually the discussion is laid down to pros and cons of the theoretical model.

Ashwin J. Makadia et al. [38] worked on AISI 410 steel by indulging various input process parameters like FR, tool nose radius, CS using DOE. RSM is adopted for the purpose of mathematical modeling and gaining the perspective of influencing factors driving the surface roughness. In fact, Response surface contours are also generated for determining the optimum conditions. Results manifested that feed rate followed by tool nose radius manipulates the SR of specimens. ANOVA was considered for feasibility which showed that error was found less than 6%.

Mite Tomov et al. [39] worked on 42CrMo (EN) for the purpose of analysing the roughness during longitudinal turning. Author considered two kinds of Roughness in the context namely Rdistorting and Rkinem-geomet. The surface roughness is achieved because of various factors namely the feed, the nose radius and various other angles. Observations were made using various modes i.e firstly the visual comparison, secondly the material ratio curves and finally the histograms.

Suleyman Neseli et al. [40] worked on AISI 1040 steel by performing turning operation in order to check the effects of tool geometry on SR. RSM is adopted for the purpose of mathematical modelling and eventually surface roughness model was constructed. Results manifested close

proxomity in Predicted and Measured values of surface roughness. Error detected comes under the range of 5%, thus the feasibility issue stands sorted.

A. K. Parida et al. [41] worked on GFRP composite by drilling in order to determine the surface roughness. Mathematical modelling is achieved using Tagauchi's L27 orthogonal array and the inputs used for the experimentation are CS, FR, diameter of drill. ANOVA is taken into consideration for validating the results which displays that spindle speed is primarily influencing factor followed by diameter of drill and then the feed comes into action which is rather insignificant for the surface finish. RSM is used to develop second order mathematical model which is further verified using the F-Test and then by the ANOVA.

C.L. He et al. [42] laid emphasis on surface roughness model which considers the input parameters as kinematics, plastic side flow and material spring back in diamond turning. Author tried to manage the material spring back through yield stress and minimum undeformed chip thickness, similarly plastic side flow is managed using minimum chip thickness, tool nose radius. Coarse grains ensure larger and stronger particles in the fixture. Results manifested that at a larger feed rates, it's observed that pit defects are visible and deep grooves are formed on the SF, while at lesser feed rates it's observed that hard particles tends to bulge out.

C. R. Prakash et al. [43] worked on metal matrix composites (MMC's) by turning operation using reinforcement of Silicon Carbide. The following composite is generally useful in automobile, aviation and marine application for its strength to weight ratio. Turning process is performed to achieve the specimen desired specification and desired surface roughness. Results were calculated and conclusions were drawn out.

Ramanuj Kumar et al. [44] worked on AISI D2 grade tool steel using carbide tool inserts where the primary focus of the author is to gather information on flank wear, average SR and chip tool interfacing temperature. RSM and ANN models are implemented for the purpose of mathematical modeling and forecasting. Results manifested that ANN predicted better results for flank wear generation while RSM models are superior for SF and chip tool interface temperature.

S. Xavierarockiaraj et al. [45] worked on SKD 11 tool steel which is turned using special technology named as laser assisted turning. The input parameter chosen for the purpose is surface temperature. RSM is adopted for mathematical modelling while full factorial design is taken into account. Various input parameters which were suitable in the study are laser power, CS and FR. Results manifested that laser power carries maximum influence over the surface

temperature followed by CS and finally the FR. Response surface contours are plotted for start optimisation while ANOVA is used to validate the reliability of the experimentation.

Ashish Kumar Srivastava et. al. [46] worked on metal matrix composite using wire electric discharge turning along with abrasive waterjet turning for a particular set of rotational speed. Author mentioned that various forms of comparison modes were adopted for calculation of Surface Roughness i.e. by optical profilometry, Laser confocal microscope and finally the FE-SEM analysis. Residual Stress measurement is also processed using the XRD machines for the analysis. Results manifested that microhardness is dropped while the tensile residual stress were generated while in abrasive water jet machining a slight variation is seen in microhardness and compressive stresses were generated.

Rogério Pontes Araújo [47] focussed on cooling fluids using VCRS which is present in the liquid state. The author wish to chose this method over others due to several reasons some of which are due to its relatively lower cost in comparison to cryogenic systems, similarly convective coefficient of fluid carries higher values in comparison to compressed air, thus making the system more worthwhile. The specimen taken for the experimentation is SAE 1045 steel for turning operation on CNC. The cutting fluid used is primarily for maintaining the temperature constant. Results were evaluated by considering temperature generation, surface roughness maintained and finally the tool wear which is analysed using Scanning Electron Microscopy.

C. Moganapriya et. al. [48] worked on AISI 1015 mild steel with initial inputs as FR, CS and the coating material while the output responses maintained are MRR and SR using a titanium tool for turning operation. Author selected Tagauchi technique which is also referred as L9 Orthogonal Array Tagauchi Optimisation. Observations manifested that coating material has a major role in deciding the quality of output parameters. The experimentation is also useful in correlating MRR and surface roughness.

Supriya Sahu et. al. [49] worked on AISI 4340 steel by turning it using coated tool with multilayered TiN. The inputs considered for the operations are CS, FR and DOC while the response used for the experimentation is Surface Roughness. Optimisation is done using the Tagauchi method which is SEM is used for the purpose of understanding the surface texture and to evaluate the tool wear. Results manifested that coated tools can help in improving the surface finish for hard metals while operating at incremental speeds and smaller feeds.

Murat Sarikaya et. al. [50] investigated the impact of parameters such as cooling conditions, CS, FR and DOC on various output parameters related to SR like Average SR and the mean highest height of the profile. Author selected AISI 1050 steel for performing the operation where the conditions are varied such as dry cutting, conventional wet cutting. Analysis was performed using L16 orthogonal array and ANOVA was performed for analysis of feasibility of the existing mathematical model. Results were also verified using 3D surface generation, S/N ratio and finally by graphs corresponding to means.

Ilhan Asilturk et al. [51] worked on AISI 4140 by considering the initial inputs as CS, FR and DOC. The output responses generated are SR with its two varients. Optimization is carried out using Tagauchi method using the L9 orthogonal array. Feasibility is verified using ANOVA along with SNR is also brought to action. Finally the impact of the two factor collaboration is done i.e. is with CS and FR and the other one being DOC.

Messias Borges et al. [52] worked on SAE 52100 hardened steel for the purpose of turning by considering firstly the number of radials units, secondly method for selection of radial centres and finally method for considering the spread factor of the function. The output responses considered in the process is Roughness Average. ANN was opted for the judgement of SR quite accurately. Finally it can be marked out that design of experiment proves out to be better in terms of approach for running RBF networks.

Ilhan Asilturk et al. [53] worked on an alloy Co28Cr6Mo which is specifically used in the hospitals. Specimens were turned on CNC lathes while keeping the input parameters as CS, FR, DOC and finally the tool tip radius. The output response considered for the process is Surface Roughness with its two varients being Ra, Rz. For the purpose of developing the model RSM was used which is based on Tagauchi Orthogonal array test. Finally ANOVA is adopted for feasibility of model. Finally optimum parametes were noted and concluded.

Ilhan Asilturk et al. [54] worked on AISI 304 alloy specimens by using tools of coated carbide inserts under non-wet conditions. The input parameters taken are CS, DOC and FR which is inserted in the Tagauchi's model. The output response taken for the study is the surface roughness. Eventually RSM is also chosen for constructing the model between the input parameters and the responses. Finally the feasibility is checked using ANOVA for the developed model. Results manifested that the most influencing factor amongst all the considered ones will

be feed rate on the SR. The obtained results also demonstrated the error percentage to be quite insignificant.

Sanchit Kumar Khare et al. [55] worked on AISI 4340 steel by turning it through cryogenic technologies. The various input parameters considered during studies were CS, DOC, FR and the rake angle while the output response parameters nominated was the SR. Author adopted various optimisation techniques including the L9 OA, the signal to noise ratio (S/N) and finally the Qualitek-4 were used . Results manifested that CS and DOC were the most prominent factor to contribute towards the SR. To conclude the experiment, author preferred to use Confirmation Experiment, in order to compare the results from the predicted ones to the actual database.

L. C. Moreira et al. [56] developed a model based on Artificial Intelligence which is basically a smart invigilation controller that can regulate the process parameters in real time in order to target the required surface quality on specimens. Controller is designed in such a way that surface roughness is optimised while marking the variation in the input parameter appropriately. Finally the results manifested improved surface finish being achieved using the above algorithm.

Sujan Debnath et al. [57] worked on mild steel for the purpose of CNC turning using titanium carbide tool. The inputs kept for investigation are CS, FR, DOC and the cutting fluid used for the process. The output response parameters are set out to be surface finish and tool wearing rate. Author choose to pick tagauchi orthogonal array for the purpose of optimisation. Results depicted that feed rate and cutting fluid flow rate have a influential role to play in the SR. While the CS and DOC variation doesn't reflect dominancy for the surface finish achieved. Optimised results can be derived if the CS is maintained high while FR and flow rate of cutting fluid should be maintained low.

Anupam Agrawal et al. [58] worked on AISI 4340 steel workpiece using the CBN inserts by preparing various specimens and installed in the CNC lathe setup for performing the experiment. The entire experiment is performed in non-wet conditions while the roughness is measured using the Form Talysurf. For the purpose of optimisation various models are suggested such as the multiple; random and finally the Quantile regression. The input parameter under consideration is FR, DOC and the CS while the output response maintained is SR for which a model is developed to monitor the correlation between them. Results manifested that random regression analysis had dominancy over the others.

Abbas Razavykia et al. [59] developed particulate metal matrix composites (PMMC) consisting of Aluminium, Magnesium and Silicon. The inputs considered for the experiment are CS, FR and the amount of Strontium addition to the composite while the output responses are maintained to be surface roughness. DOE is selected as the preferred methodology for optimisation while the feasibility is judged using the ANOVA analysis. Results manifested that due to the addition of Strontium particle there was significant variation in size, shape and distribution of Mg2Si particles. Reliability achieved is also quite satisfactory upto 95% which is known through the conformational test.

Harsh Y Valera et al. [60] worked on EN-31 alloy steel for the purpose of turning. The input parameters selected for the operations are CS, FR and DOC while the response maintained are SF quality and power consumption. For performing the experiment the author wish to keep 1 parameter to five different variations while keeping the other two parameters constant. Thus 15 specimens were taken and optimum condition is realised.

2.2 Research Gap

On the basis of literature survey the following research gap have been identified

- The experimental analysis on AISI 8620 has not been explored in the literature.
- The surface characteristics of AISI 8620 have not been explored in the literature.
- The Residual stress in metal of AISI 8620 has not been investigated in the literature.
- The machinability in CNC turning has not been investigated.
- Chip tool interface temperature during machining has not been studied thoroughly.

2.3 Research Objective

On the basis of detailed study of research survey the following research objective have been drawn

- To prepare the CCD Design matrix including the input factors i.e. CS, FR and DOC.
- To perform the experiment on CNC machine by varying the different input factors i.e. CS, FR and DOC.
- To study the effect of process parameter such as CS, FR and DOC on the surface roughness and residual stress during CNC turning of the AISI 8620 steel metal.
- Statistical analysis of process parameters in CNC turning.

CHAPTER 3

RESEARCH METHODLOGY

3.1 CNC Turning

Machining is basically the extraction from the fabric workpiece, mostly metal, using one or more cutting tools to obtain the required sizes. There are different machining processes, such as rotating, friction, squeezing, etc. In all these cases, metal is removed by a shearing process due to the relative motion between the workpiece and the tool. In general, one of the two rotates at a defined and generally quick speed. The other moves through the workpiece relatively softly to affect metal removal. Processing velocity, demand and decreasing duration are important parameters. The previous image shows the conversion methods important geometry. The CS, a study of the cut portions surface velocity relative to the tool. Speed is a tool that can be defined in meters / min for translational motion velocity. The variety of slicing, DOC is the water plunging the machine into the floor. Feed explains the cutting tools relative lateral movement to the workpiece. The feed thus determines, as the case may be, the cross-section of the material removed for each rotation of the work or tool, cutting depth. Figure 3.1 shown the turning operations in following below.

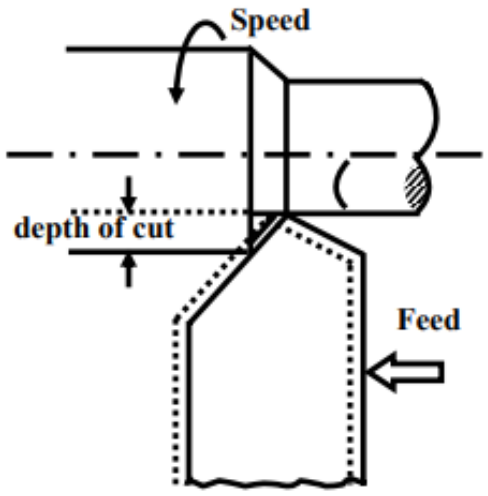

Figure 3.1: Turning Operations adopted by [61]

The automatic command of a machine tool based on a set of pre-programmed machining and movement rules is acknowledged as numerical control, or NC. In a typical NC scheme called a component program, the movement and machining directions and the associated numerical data were published on a punched tape. The part program is structured in the shape of data sections, each connected to a specific procedure, in a series of activities required to create a mechanical component. One portion of the punched tape was uploaded at a time.

Each segment supplied information in a particular syntax required to handle a particular machining instruction such as part length, CS, availability, extra characteristics associated with coolant stream, spindle speed, part clamping are also provided. Punched tapes are now mainly obsolete and are replaced by magnetic disks and optical drives.

CNC instrument tools, present versions of NC computers have an integrated scheme that involves various microprocessors and related equipment such as the MCU. In CNC, multiple microprocessors and programmable logic controllers work in combination for simultaneous servo place and velocity monitoring of different components of a contour milling device as well as monitoring the drafting technique and machine tool.

3.1.1 Advantages of CNC Machine

The Advantages of the CNC Machine are following below:

- Improved performance
- Improved quality
- Reduced volume of landfill
- Reliable and secure operation
- Smaller footprint

3.1.2 Limitations of CNC Machine

Limitations of CNC Machine are following below:

- Relatively higher cost compared to manual versions
- More complicated service due to the difficulty of the methods
- Skilled programmers of components are needed.

3.1.3 Classification of CNC Machine

It is possible to classify CNC machine instrument devices in different respects:

1. Point-to-point or contouring: based on whether metal is cut off by the device while the workpiece passes close to instrument

2. Incremental or complete: the parameterization of movement instructions depends on the sort of coordinate system taken.

3. Open loop or closed loop: based on the control system used to power the movement of the object.

3.1.4 G & M Codes

G Codes

G00 - Rapid move (not cutting)

G01 - Linear move

G02 - Clockwise circular motion

G03 - Counter clockwise circular motion

G04 – Dwell

G05 - Pause (for operator intervention)

G08 – Acceleration

G09 - Deceleration

G17 - x-y plane for circular interpolation

G18 - z-x plane for circular interpolation

G19 - y-z plane for circular interpolation

G20 - turning cycle or inch data specification

G21 - thread cutting cycle or metric data specification

G24 - face turning cycle

G25 - wait for input to go low

G26 - wait for input to go high

G28 - return to reference point

G29 - return from reference point

G31 - Stop on input

G33-35 - thread cutting functions

G35 - wait for input to go low

G36 - wait for input to go high

G40 - cutter compensation cancel

G41 - cutter compensation to the left

G42 - cutter compensation to the right

G43 - tool length compensation, positive

G44 - tool length compensation, negative

G90 - absolute dimension program

G91 - incremental dimensions

G92 - Spindle speed limit

G93 - Coordinate system setting

G94 - Feed rate in ipm

G95 - Feed rate in ipr

G96 - Surface cutting speed

G97 - Rotational speed rpm

G98 - withdraw the tool to the starting point or feed per minute

G99 - withdraw the tool to a safe plane or feed per revolution

M Codes

M00 - program stop

M01 - optional stop using stop button

M02 - end of program

M03 - spindle on CW

M04 - spindle on CCW

M05 - spindle off

M06 - tool change

M07 - flood with coolant

M08 - mist with coolant

M08 - turn on accessory (e.g. AC power outlet)

M09 - coolant off

M09 - turn off accessory

M10 - turn on accessory

M11 - turn off accessory or tool change

M17 - subroutine end

M20 - tailstock back

M20 - Chain to next program

M21 - tailstock forward

M22 - Write current position to data file

M25 - open chuck

M26 - close chuck

M30 - end of tape (rewind)

3.1.5 Main Parts of CNC Machine

Important parts of CNC are described in the following below Table 3.1 and shown in following given below Figure 3.2.

Table 3.1: Main Parts of CNC Machine

S. No.	Main Parts of CNC Lathe Machine
1	Headstock
2	CNC Lathe Bed
3	Chuck
4	Tailstock
5	Tailstock Quill
6	Foot Switch or Foot Pedals
7	CNC Control Panel
8	Tool Turret

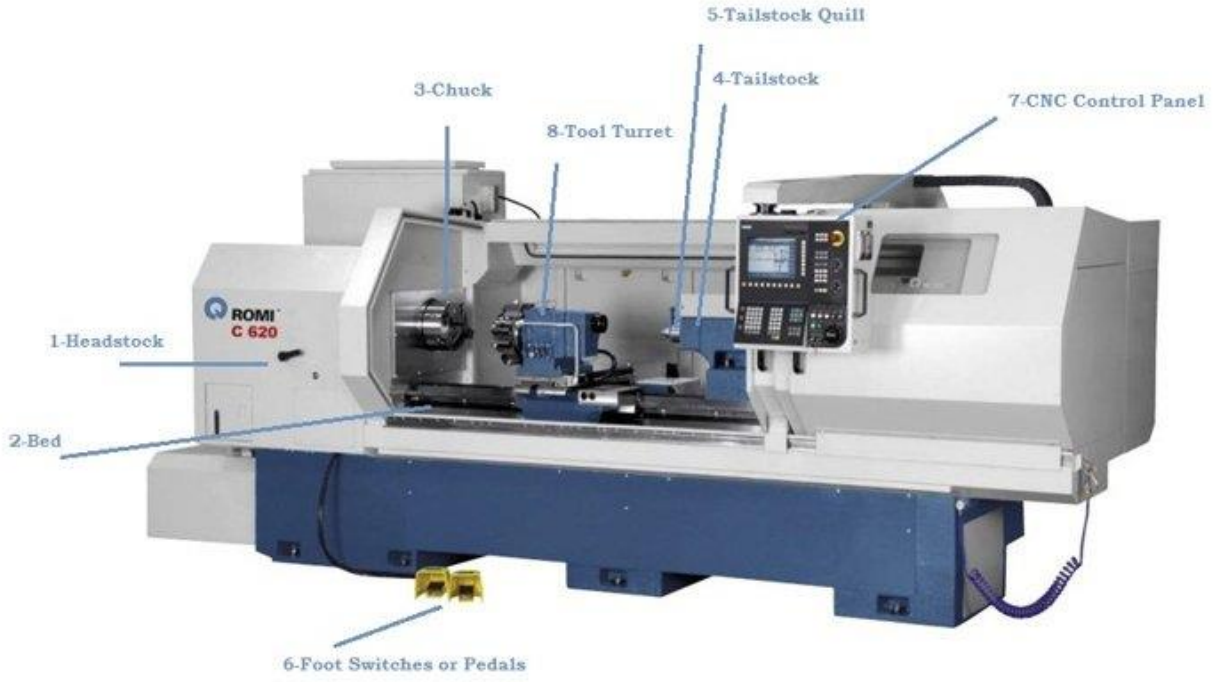

Figure 3.2: CNC Lathe adopted by [62]

3.2 Surface Roughness

SR is a surface texture component that is often lowered to roughness. It is quantified by the deviations in the route of the ordinary matrix of a real surface from its ideal form. When these deviations are large, the texture is rough; if they are small, the texture is smooth. Roughness is typically considered in surface metrology as the component of a loaded soil which is high-frequency, short-wavelength. In practice, however, it is often necessary to know both the amplitude and the frequency to ensure that a surface is fit for a purpose. There are many different parameters of roughness in use, but it is by far the most common, although this is often due to historical reasons and not particular valuation Ra, as the ancient roughness meters could only be evaluated. Other common parameters include Rq, Rt, and Rz. Only in some industries or in some countries are some parameters used.

Surface finish is the shape of a soil, also known as surface texture or topography. It involves the small local deviations of a surface from the ideal (a real plane) totally fluid. Surface roughness is a surface texture component that is often lowered to roughness. It is quantified by the deviations in the route of the ordinary matrix of a real surface from its ideal form. When these deviations are large, the fabric is rough; if they are small, the fabric is smooth. Waviness is the metric of the bigger spaced component of the surface texture.

It is a broader roughness view because it is more strictly defined as the artifacts whose spacing is greater than the roughness inspection length set is the direction of the floor system generally determined by the manufacturing method.

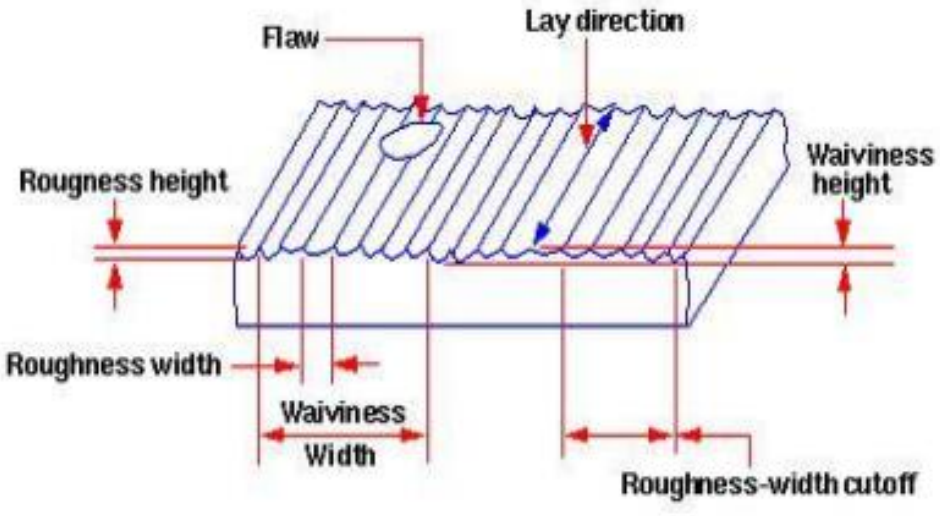

Figure 3.3: Surface Characteristics adopted by [63]

3.2.1 Methods to calculate Roughness

3.2.1.1 Root Means Square roughness (Ra or RMS)

- Closely linked to the median roughness (Ra)
- Square the lengths, count them, and determine the count base of the consequence
- The subsequent valuation is a ground fabric comparative coefficient that is generally 11% greater than the Ra score.

3.2.1.2 Maximum Peak to Valley Roughness (Rmax or Rt)

- Determine the difference between the lines contacting the highest outer and center boundary of the profile
- Second most prevalent industry method

3.2.1.3 Ten Point Height (Rz)

Means the range within the recording duration between the five highs and five lowest villages.

3.2.2 Taylor Hobson Talysurf

A skid or shoe sliced across the workpiece coating to match the grounds general contours as tightly as needed. The skid also provides the stylus A stylus datum that runs over the floor along with the skid, so its motion is vertically near to the skid. This variable enables the stylus to track contours of surface roughness irrespective of surface waviness. An amplifier to magnify the stylus A monitoring machines movements to produce a hint or record of the floor picture.

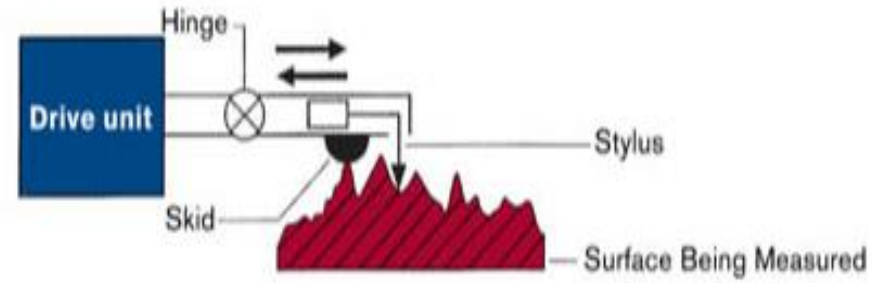

Figure 3.4: Surface Roughness measurement adopted by [64]

A stylus is linked to an armature spinning around the middle of a stamping portion shaped E. The outer feet of the e-shaped stamping are injured by electrical coils. A predetermined cost of rotating present (current excitation) is given to the coils. The coils are part of a bridge loop. A skid or shoe provides information for mapping the grounds roughness. An electric motor can cross a linear path through the experiment bar. The armature is also pressed due to surface defects as the stylus moves up and down. This generates variation in the air divide and generates an imbalance in the connection circuit. The bridge loops subsequent output consists only of compression.

3.2.3 Analysis of Surface Traces

3.2.3.1 Centre Line Average (Ra) Value

Ra is the roughness parameter that is widely acknowledged. Roughness median Ra is the arithmetic average of the standard numbers of the ordinates of roughness analysis.

- Roughness Average, Ra, is the arithmetic average of absolute height of the profile over the duration of the evaluation.
- RMS Roughness, Rq, is the root mean square average of the profile heights over the evaluation Length
- Maximum heights within the sampling length, Rti, the vertical distance between the highest and lowest profile points within the sampling length.
- Average Maximum Profile Height, Rz, is calculated on average over the length of evaluation of successive Rti values. This parameter is the same as Rz (DIN) if there are five sampling times within the duration of the evaluation.

3.3 X-RAY Diffraction

Using the portable phones μ-X360, the residual tensions are assessed up to 30μm elevations by assessing the fabrics inter-atomic spacing. X-rays have the same wavelength order as inter planar ranges of material. When X-rays strike the material surface it gets scattered to form a diffracted beam constructive to destructive interference. The device also tests the angle of peak interference with diffraction. To measure inter-planar distances (d0), the angles measured from interferences are used. The existence of residual stress in the sample alters the d spacing that can be assessed using the law of bragg. The distinction in d-spacing is immediately equal to the strain that can be used to calculate residual stress.

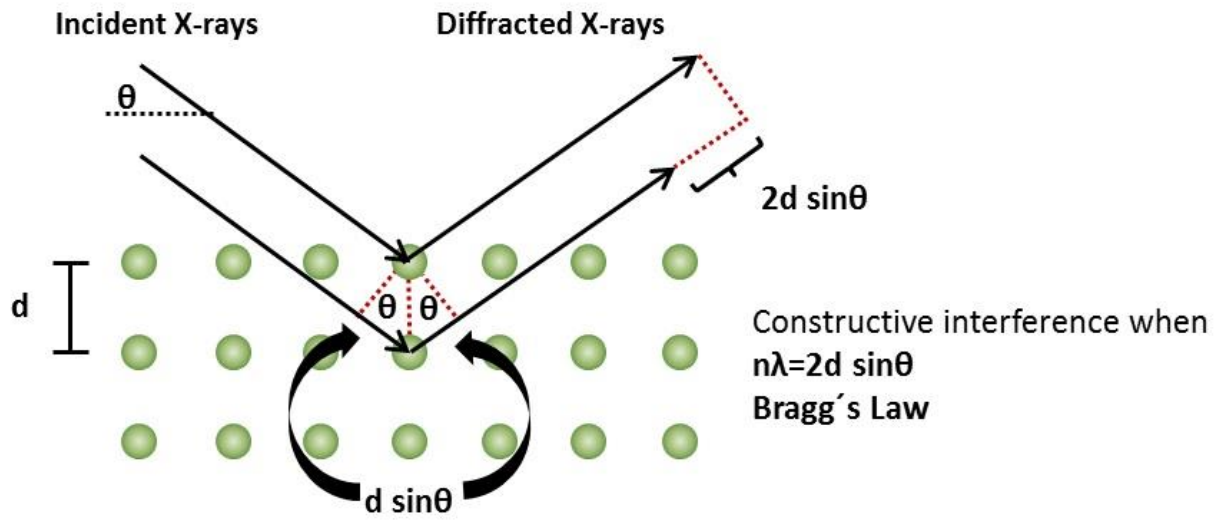

Figure 3.5: Schematic diagram of X-Ray diffraction adopted by [65]

3.3.1 Cos α Method

The standard Sin2ψ case method with a point sensor (diffract meter) requires a series of measurements with separate sample orientations with respect to the diffract meter to accomplish the projection of the strain tensor along the different separate scattering vector orientations, and these instructions are chosen to simplify subsequent assessment.

Since each object in the Debye loop arises from a distinct angle of the resulting matrix for a specified test profile in studio locations, the entire Debye loop can be used in a separate test when using a 2D sensor and a range of propagation matrix orientations are simultaneously tested. Because of its convenience of use, the use of mobile residual stress analyzers has now risen. The cosα technique has emerged as a quicker and simpler technique of experimentally assessing remaining stress by using mobile equipment because of its capacity to detect a whole Debye loop at once from the two-dimensional sensor, thus needing no various test tilts as in the event of Sin2ψ technique.

3.3.2 Portable X-Ray Device to Measure Residual Stress by using Cos α method

A portable industrial company from Pulstec. Ltd. Remaining stress analyzer (μ-X360) mounted on a strong board is used to evaluate the residual stress after Turning of AISI 8620 steel specimen. After swinging along the tube shaft, different marks on the Turning specimens are

labeled throughout the length of the sample. The detector gun of the stress analyzer is inclined to obtain accurate results for the ferrous metal at an angle of 35 °.

The sample is put on the operating panel allowing the layer to be evaluated for residual stress creating a red laser place on the mark where the X-ray beam is to be performed.

Table 3.2: Specifications of the X-ray machine (μ-X360) adopted from lab manual

X-ray Tube Voltage, Current	30 KV, 1.0 mA
Target Material	Chromium (Cr)
Beam Wavelength (Energy)	λ= 2.29 Å (E = 5.4 KeV)
Collimator and Beam Spot Size	1 mm and 2 mm diameter
Sample to Detector Distance Approx.	35-40 mm
Typical Data Acquisition + Readout Time	90 seconds

3.3.3 Principle of residual stress by the Cos α method

The complete Debye-Sherrer circle is acquired by this technique. A Debye-Scherre loop is acquired using an picture panel (IP) and the picture information as tested to determine the stress significance. Due to the 2D planar geometry of the test, the conversion of the test scheme (diffractometer scheme) into the sample scheme is actually more complicated. Figure 3.6 shown the geometric representation of the angles on the Debye ring.

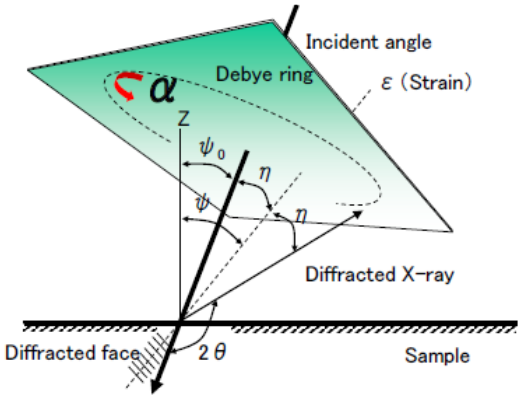

Figure 3.6: Geometric representation of the angles α, Ψ, η and 2θ on the Debye ring adopted by [10]

The expression for the translation of strain,

$\varepsilon_\alpha = n_i\, n_j\, \varepsilon_{ij}$

Where n is the diffraction vector, which can be expressed in the form

$$n = \begin{bmatrix} \cos\eta \sin\psi_o + \sin\eta \cos\psi_o \cos\alpha \\ \cos\eta \sin\psi_o sin\emptyset_o + \sin\eta \cos\psi_o \sin\psi_o \cos\alpha + sin\eta cos\emptyset_o\, sin\alpha \\ \cos\eta \cos\psi_o - \sin\eta \sin\psi_o \cos\alpha \end{bmatrix}$$

Now this value of n can be inserted into Hooke's law to form

$$\varepsilon_\alpha = \frac{1+\upsilon}{E} n_i n_j \varepsilon_{ij} - \frac{\upsilon}{E}\sigma_{kk}$$

The magnitude of strain is determined from the detected position of the Debye-Scherrer ring. Calculate using the following formula.

$$\varepsilon_{\alpha 1} = \frac{1}{2}\{(\varepsilon_{\alpha} - \varepsilon_{\pi+\alpha}) + (\varepsilon_{-\alpha} - \varepsilon_{\pi-\alpha})\}$$

$$\varepsilon_{\alpha 2} = \frac{1}{2}\{(\varepsilon_{\alpha} - \varepsilon_{\pi+\alpha}) - (\varepsilon_{-\alpha} - \varepsilon_{\pi-\alpha})\}$$

Hence the value of stress is calculated from the strain using proper elastic and other constants.

$$\boxed{\sigma_x = -\frac{E}{1+\upsilon} \cdot \frac{1}{\sin 2\eta} \cdot \frac{1}{\sin 2\psi_o} \cdot \left(\frac{\partial \varepsilon \alpha_1}{\partial \cos \alpha}\right)}$$

CHAPTER 4

EXPERIMENTAL METHOD

4.1 Design of Experiment (DOE)

Several CNC Turning research has demonstrated that machining parameters such as Speed, Feed, and Depth of Cut etc. have a important impact on manufactured materials mechanical characteristics. To study the impact of individual factors, one can simply choose traditional experiment design technique in which one parameter varies at a time and the others remain the same. This method needs multiple laboratory cycles and takes time. Furthermore, in this method, interaction effects of system parameters are ignored.

The purpose of the experimentation is to see the effects of input parameters and to generate mathematical models to describe the relationship among various parameters.

For achieving above objectives, following are the steps were carried out:

1. Identification of essential process control factors
2. Deciding the working scope of the procedure control factors, viz. Speed, Feed and Depth of Cut
3. Developing the design matrix
4. Conducting the examinations according to the design matrix
5. Recording the reactions viz. Surface Roughness, Residual Stress
6. Developing the numerical models
7. Checking the adequacy of the models
8. Finding the significance of coefficient
9. Developing the final proposed models
10. Plotting of diagrams and drawing conclusion
11. Discussion of the outcomes

4.1.1 Identification of numerous process control factors

Based on the effect on CNC turning machining, ease of design and desire-level maintenance ability, three independently controllable system parameters were identified as particular, cutting speed, feed and cutting depth. For this examination, CNC turning geometry parameters were Surface ruggedness and residual stress.

4.1.2 Deciding the range of the process factors

Preliminary flows were resulted by simultaneously differentiating one of the system parameters while maintaining the steady significance of whatever survives. By inspecting the geometry of the Turning process for a smooth appearance and the non-appearance of obvious deformities, the working range was fixed.

The upper and lower limits were individually coded as+ 1 and -1. From the situation, where, Xi is the necessary specified estimate of a variable X, when X is any estimate of the variable from Xmin to Xmax; Xmax and Xmin are the most severe and lowest of the variables.They chose procedure parameters and their upper and lower restrains together with documentations and units are given in Table 4.1.

Table 4.1: Process control parameters and their breaking points

S.NO.	Parameters	Units	Notations	-1	0	+1
1.	Speed	m/min	A	80	120	160
2.	Feed	mm/rev	B	0.03	0.05	0.07
3.	Depth of Cut	mm	C	0.2	0.3	0.4

4.1.3 Developing the design framework

For the test, a fully rotatable block of 3 factors and 3 levels was used. A CCD matrix includes more remarkable layout room than the factory design matrix grid, resulting in greater accuracy of the defined relationship. Table 4.2 shows the 20 mapped circumstances used to display the coded outline-

Table 4.2: Design matrix

Std	Run	Coded value of Speed	Coded value of Feed	Coded value of Depth of Cut	Actual value of Speed (m/min)	Actual value of Feed (mm/rev)	Actual value of Depth of Cut (mm)
1	4	-1	-1	-1	80	0.03	0.2
2	13	1	-1	-1	160	0.03	0.2
3	11	-1	1	-1	80	0.07	0.2
4	15	1	1	-1	160	0.07	0.2

5	6	-1	-1	1	80	0.03	0.4
6	12	1	-1	1	160	0.03	0.4
7	20	-1	1	1	80	0.07	0.4
8	17	1	1	1	160	0.07	0.4
9	1	-1	0	0	80	0.05	0.3
10	9	1	0	0	160	0.05	0.3
11	8	0	-1	0	120	0.03	0.3
12	10	0	1	0	120	0.07	0.3
13	16	0	0	-1	120	0.05	0.2
14	2	0	0	1	120	0.05	0.4
15	3	0	0	0	120	0.05	0.3
16	14	0	0	0	120	0.05	0.3
17	19	0	0	0	120	0.05	0.3
18	7	0	0	0	120	0.05	0.3
19	5	0	0	0	120	0.05	0.3
20	18	0	0	0	120	0.05	0.3

4.2 Workpiece composition and its properties

AISI 8620 Steel is a stainless steel with small alloy nickel, chromium, molybdenum case, usually provided with peak HB 255max hardness as folded situation. SAE steel 8620 provides elevated external resistance and excellent internal strength, rendering it extremely susceptible to carry. The core strength of AISI 8620 steel is greater than that of grades 8615 and 8617.

During hardening procedures, SAE 8620 stainless metal is versatile, allowing enhancement of case / core characteristics. Pre-hardened and strengthened (uncarburized) 8620 may be further dried by nitriding, but owing to its low carbon material, it will not react satisfactorily to the hardening of fire or induction. Steel 8620 is suitable for apps requiring a mixture of wear resistance and toughness. This grade is usually delivered in round bar [7].

Table 4.3: Chemical Composition (in wt. %) of AISI 8620 steel [66]

Compo Sition	C	Si	Mn	S	P	Cr	Ni	Cu	Mo	Fe
Percent (wt.%)	0.20	0.30	0.87	0.015	0.013	0.57	0.44	0.08	0.19	Balance

4.3 Horizontal Lathe Specifications

LMW LL20T L3

Figure 4.1: CNC Lathe in Metal Cutting Lab

Figure 4.2: Specimen after the cutting operation performed on the basis of Design Matrix

Table 4.4 Specification of Horizontal CNC Machine adopted by Metal Cutting Lab manual

CAPACITY	
Swing Over bed	510 mm
Chuck dia. Max	210 mm
Max. Turning diameters	320 mm
Max. Turning Length	310 mm
Admit between Centers	420 mm
SPINDLE	
Spindle nose type	A2-6
Hole through spindle	61 mm
Spindle speed	3000 to 3500 RPM
Spindle motor power	11 / 7.5 to 10.5 / 7
FEED	
Cross travel X-axis	185 mm
Longitudinal travel Z-axis	370 mm
Rapid traverse rate X/Z axes	30 m/min
TURRET	
No. of stations nos	8
Tool shank size mm	25 x 25 mm
Max. Boring bar dia	40 mm
Turret Indexing type	Bi-directional
Turret Indexing time	1.0 sec
TAILSTOCK	
Quill dia	75 mm
Quill stroke	100 mm
Quill taper	MT-4
CNC SYSTEM	
Controller	Fanuc / (Siemens)
MACHINE SIZE	
Front x Side	2065 x 1650 x 1920 mm
Weight	3200 Kg

4.4 Experimental Procedure of Surface Roughness

SR was measured by following below steps of experimentation. Steps are described below:

- Taylor Hobson portable tool is used to measure ground roughness. For writing, three marks are labeled on each samples finest completed layer.
- Samples are put for adequate assistance and stabilization between the V-blocks.
- A typical surface sampling device consists of a tiny point stylus, a gage or transducer, a crossing data and a cpu.
- The floor is assessed by shifting the stylus across the ground traveling in a direct row to and from the ground, the transducer transforms this motion into a message that is then transmitted to a computer that transforms it into a code and generally a spectral representation.
- The gage must move over the substrate in a direct row for right information compilation, so that only the point of the stylus touches the layer under study.
- The Ra score is gathered for each sample after closure of the exam and the median is gathered.

4.4.1 Specification of Surface Roughness measuring instrument

The instrument was used in Metrology Lab, DTU. The Taylor Hobson Talysurf instrument of SURTRONIC S-100 SERIES is available in Metrology Lab.

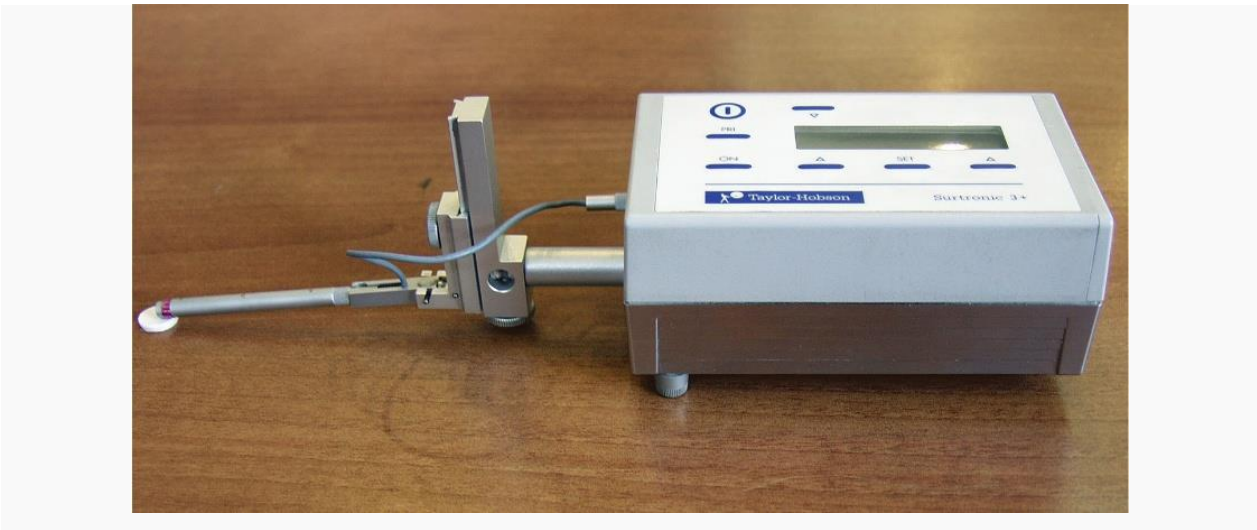

Figure 4.3: Taylor Hobson Talysurf instrument in Metrology Lab

The specifications of measuring instrument of SR are following below:

- Measurement capability
- Gauge Range=200 μm / 100 μm / 10 μm
- Resolution=100 nm / 20 nm / 10 nm
- Noise floor (Ra)=250 nm / 150 nm / 100 nm
- Repeatability (Ra)=1 % of value + noise
- Pickup type=Inductive
- Gauge force=150-300 mg
- Stylus tip radius=5 μm (200 μin)
- Measurement type=Skidded
- Calibration Process=Automated software calibration routine
- Standards=Able to calibrate to ISO 4287 roughness standards
- Evaluation length=0.25 mm - 17.5 mm (0.01 in - 0.70 in)
- Measuring speed=1 mm / sec (0.04 in / sec)
- Returning speed=1.5 mm / sec (0.06 in / sec)
- Analysis capability
- Standards=ISO 4287, ISO 13565-1, ISO 13565-2, ASME 46.1, JIS 0601, N31007
- ISO basic=Ra, Rv, Rp, Rz, Rt, Rq, Rsk, Rmr, Rdq, Rpc, RSm, Rz1max
- Units=μm / μin

4.5 Experimental Procedure of Residual Stress

RS was measured by following below steps of experimentation. Steps are described below:

- RS measurement is done using portable X-ray machine (μ-X360)
- In order to measure the RS in the prepared sample, four marking are done on the surface of the sample
- Samples are put on the V-block under the laser.
- Focus of collimator is done on specimen using laser in order to Irradiated the marked point.
- After a particular time, diffraction-peak location and stress values are detected and recorded.

Figure 4.4: Experimental set-up for residual stress measurement using portable X-ray machine (μ-X360) in Precision Lab

Table 4.5: Specifications of the X-ray machine (μ-X360) in Precision Lab

X-ray Tube Voltage, Current	30 KV, 1.0 mA
Target Material	Chromium (Cr)
Beam Wavelength (Energy)	λ= 2.29 Å (E = 5.4 KeV)
Collimator and Beam Spot Size	1 mm and 2 mm diameter
Sample to Detector Distance Approx.	35-40 mm
Typical Data Acquisition + Readout Time	90 seconds

4.6 Recording of responses

Recording of responses occurred after the experiments of Surface Roughness and Residual Stress. Responses are in this experiment i.e. Cutting Speed, Feed and Depth of Cut. All these responses are very important on the basis of mechanical properties. Responses were recorded in Design Expert Software Trial Version and shown following below in the Table 3.6, furthermore graphs are also plotted in Appendix.

Table 4.6: Recording of responses

Std	Run	Coded value of Speed	Coded value of Feed	Coded value of Depth of Cut	Actual value of Speed (m/min)	Actual value of Feed (mm/rev)	Actual value of Depth of Cut (mm)	Response 1 Surface Roughness (micro meter)	Response 2 Residual Stress (MPa)
1	4	-1	-1	-1	80	0.03	0.2	3.5	-0.345
2	13	1	-1	-1	160	0.03	0.2	1.05	-39
3	11	-1	1	-1	80	0.07	0.2	3.679	-27
4	15	1	1	-1	160	0.07	0.2	1.935	92
5	6	-1	-1	1	80	0.03	0.4	3.4	3.666
6	12	1	-1	1	160	0.03	0.4	1.76	-103.333
7	20	-1	1	1	80	0.07	0.4	3.59	-5.666
8	17	1	1	1	160	0.07	0.4	2.115	32
9	1	-1	0	0	80	0.05	0.3	3.62	31
10	9	1	0	0	160	0.05	0.3	2.05	-0.666
11	8	0	-1	0	120	0.03	0.3	2.46	-20.666
12	10	0	1	0	120	0.07	0.3	2.97	25
13	16	0	0	-1	120	0.05	0.2	2.75	33
14	2	0	0	1	120	0.05	0.4	3.135	-0.333
15	3	0	0	0	120	0.05	0.3	3.04	12
16	14	0	0	0	120	0.05	0.3	2.94	17
17	19	0	0	0	120	0.05	0.3	2.915	24.333
18	7	0	0	0	120	0.05	0.3	3.11	35
19	5	0	0	0	120	0.05	0.3	2.96	10
20	18	0	0	0	120	0.05	0.3	2.845	13.666

CHAPTER 5

STATISTICAL ANALYSIS

5.1 Response 1: Surface Roughness

Table 5.1: ANOVA for Reduced Quadratic model for Surface Roughness

Source	**Sum of Squares**	**df**	**Mean Square**	**F-value**	**p-value**	
Model	9.11	6	1.52	97.85	< 0.0001	significant
A-Speed	7.88	1	7.88	507.88	< 0.0001	
B-Feed	0.4490	1	0.4490	28.93	0.0001	
C-Depth of Cut	0.1179	1	0.1179	7.60	0.0163	
AB	0.0948	1	0.0948	6.11	0.0280	
AC	0.1455	1	0.1455	9.38	0.0091	
B^2	0.4222	1	0.4222	27.20	0.0002	
Residual	0.2018	13	0.0155			
Lack of Fit	0.1577	8	0.0197	2.23	0.1958	not significant
Pure Error	0.0441	5	0.0088			
Cor Total	9.32	19				

Factor coding is **Coded**.

Sum of squares is **Type III - Partial**

The Model **F-value** of 97.85 shows the significance of the present model under inquiry. Small percentage of the incidence of the greater F score could occur due to sound, i.e. 0.01%.

P value should not reach 0.05. It is noted that key / significant conditions were A, B, C, AB, AC, B^2. If the P-values reach above the figure of 0.1; it reflects that model stands insignificant. Therefore, if the number of insignificant terms in any model is higher, shortening the model is recommended by decreasing the parameter to enhance the model.

Finally, in comparison with the pure error, the **Lack of fit F value** should remain insignificant for a model. We obtained 19.58 percent opportunity of absence of match F-value for the present model, which could result mainly from noise variables.

Table 5.1.1 Fit Statistics of Surface Roughness

Std. Dev.	0.1246	**R^2**	0.9783
Mean	2.79	**Adjusted R^2**	0.9683
C.V. %	4.46	**Predicted R^2**	0.9095
		Adeq Precision	35.6899

The price of the **predicted R^2** is near to the price of the **Adjusted R^2** with a small difference of 0.2.

Adeq Precision allows the S / N proportion to be calculated by the customer. This percentage is appropriate for a required price of 4, which in our situation is 35.6899, so it is quite desirable to get the message accomplished. In addition, this model is entitled to be satisfactory in the development region.

Final Equation in Terms of Coded Factors

Surface Roughness =+2.94-0.5279* A+0.1260 *B+0.0646* **C**+0.0385* **AB**+0.0477 *AC-0.1027 *B^2

Equations acquired in terms of labeled variables are appropriate for making statements about information for each parameters specified concentrations. The greater parameters are usually encoded as + 1 while the reduced parameters are encoded with-1. Evaluation of the factor coefficient is useful in quantifying the comparative impact of the variables in given formulas.

Final Equation in Terms of Actual Factors

Surface Roughness=+4.95884-0.039118* Speed+66.91375* Feed-2.96025* Depth of Cut+0.136094* Speed * Feed+0.033719 *****Speed * Depth of Cut-726.50000* $Feed^2$

The equation created due to the real parameters can be used to frame the hypothesis of the yield information for each parameters specified stage. It is necessary to quantify each amount for each parameter in their corresponding ranges. This equation should be excluded from examining the comparative impact of each parameter as the original coefficient is magnified to merge with each parameters parts while the median is not adapted to the layout areas center.

5.2 Response 2: Residual Stress

Table 5.2: ANOVA for Reduced Quadratic model of Residual stress

Source	**Sum of Squares**	**df**	**Mean Square**	**F-value**	**p-value**	
Model	26020.62	6	4336.77	46.46	< 0.0001	Significant
A-Speed	42.66	1	42.66	0.4570	0.5109	
B-Feed	7618.26	1	7618.26	81.61	< 0.0001	
C-Depth of Cut	1750.88	1	1750.88	18.76	0.0008	
AB	11424.67	1	11424.67	122.38	< 0.0001	
AC	2800.44	1	2800.44	30.00	0.0001	
B^2	2383.71	1	2383.71	25.53	0.0002	
Residual	1213.58	13	93.35			
Lack of Fit	767.35	8	95.92	1.07	0.4910	not significant
Pure Error	446.23	5	89.25			
Cor Total	27234.20	19				

Factor coding is **Coded**.

Sum of squares is **Type III - Partial**

The Model **F-value** of 46.46 shows the significance of the present model under inquiry. Small percentage of the incidence of the greater F score could occur due to sound, i.e. 0.01%.

P value should not reach 0.05. It is noted that key / significant conditions were A, B, C, AB, AC, B^2. If the P-values are above the 0.1 line; it represents the insignificance of the model. Therefore, if the number of insignificant terms in any model is higher, shortening,the model is recommended by decreasing the parameter to enhance the model.

Finally, in comparison with the pure error, the **Lack of fit F value** should remain insignificant for a model. We obtained 49.10 percent opportunity of absence of match F-value for the present model, which could result mainly from noise variables.

Table 5.2.1: Fit Statistics of Residual Stress

Std. Dev.	9.66	**R^2**	0.9554

Mean	6.58	**Adjusted R^2**	0.9349
C.V. %	146.77	**Predicted R^2**	0.8842
		Adeq Precision	34.0561

The value of the **Predicted R^2** is near to the value of the **Adjusted R^2** with a small difference of 0.2.

Adeq Precision allows the S / N proportion to be calculated by the customer. This percentage is appropriate at a required price of 4, which in our situation is 34.0561, so it is quite desirable to get the message accomplished. In addition, this model is entitled to be satisfactory in the development region.

Final Equation in Terms of Coded Factors

Residual Stress=+17.50-1.23 *A+16.41 *B-7.87 *C+13.36 *AB-6.61 *AC-7.72 *B^2

Equations acquired in terms of labeled variables are appropriate for making statements about information for each parameters specified concentrations. The greater parameters are usually encoded as + 1 while the reduced parameters are encoded with-1. Evaluation of the factor coefficient is useful in quantifying the comparative impact of the variables in given formulas.

Final Equation in Terms of Actual Factors

Residual Stress=-27.03825-1.01028*Speed+1170.16000*Feed+428.97150*Depth of Cut+47.23750* Speed * Feed-4.67744* Speed * Depth of Cut-54586.00000* $Feed^2$

The equation created due to the real parameters can be used to frame the hypothesis of the yield information for each parameters specified stage. It is necessary to quantify each amount for each parameter in their corresponding ranges. This equation should be excluded from examining the comparative impact of each parameter as the original coefficient is magnified to merge with each parameters parts while the median is not adapted to the layout areas center.

CHAPTER 6

RESULT ANALYSIS AND DISCUSSION

6.1 Analysis of Result

6.1.1 Effect of analysis on Surface Roughness

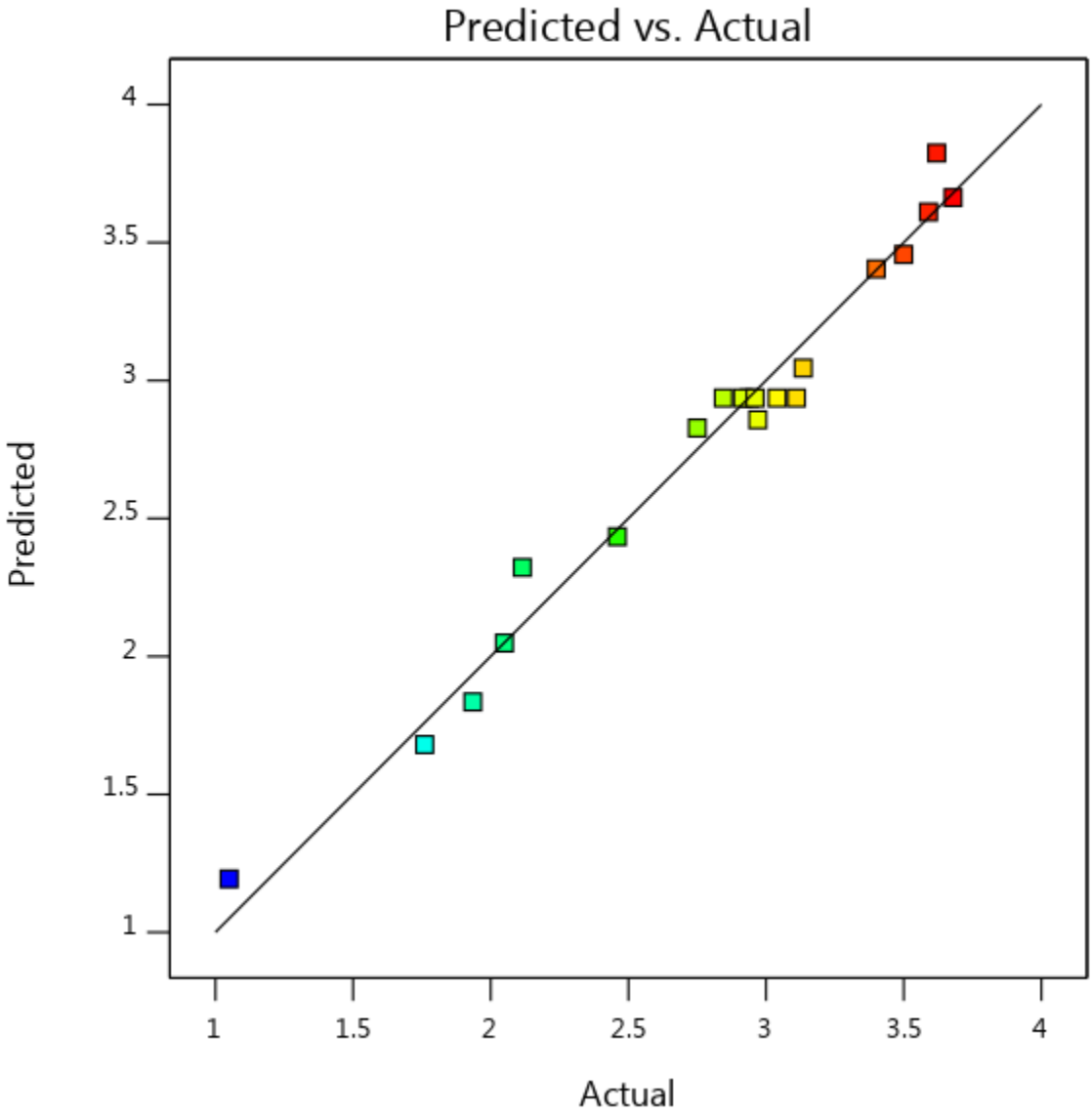

Figure 6.1: A plot between Predicted vs. Actual points of SR

The graph above shows real Surface Roughness information on the x-axis while Surface Roughness information on the y-axis is anticipated. Red spots are Surface Roughness greatest valuation while a blue spot constitutes Surface Roughness lowest levels. It is obvious from the graph that the real information is similar to the expected information. The chart demonstrates the

predicted and actual information scores connection.

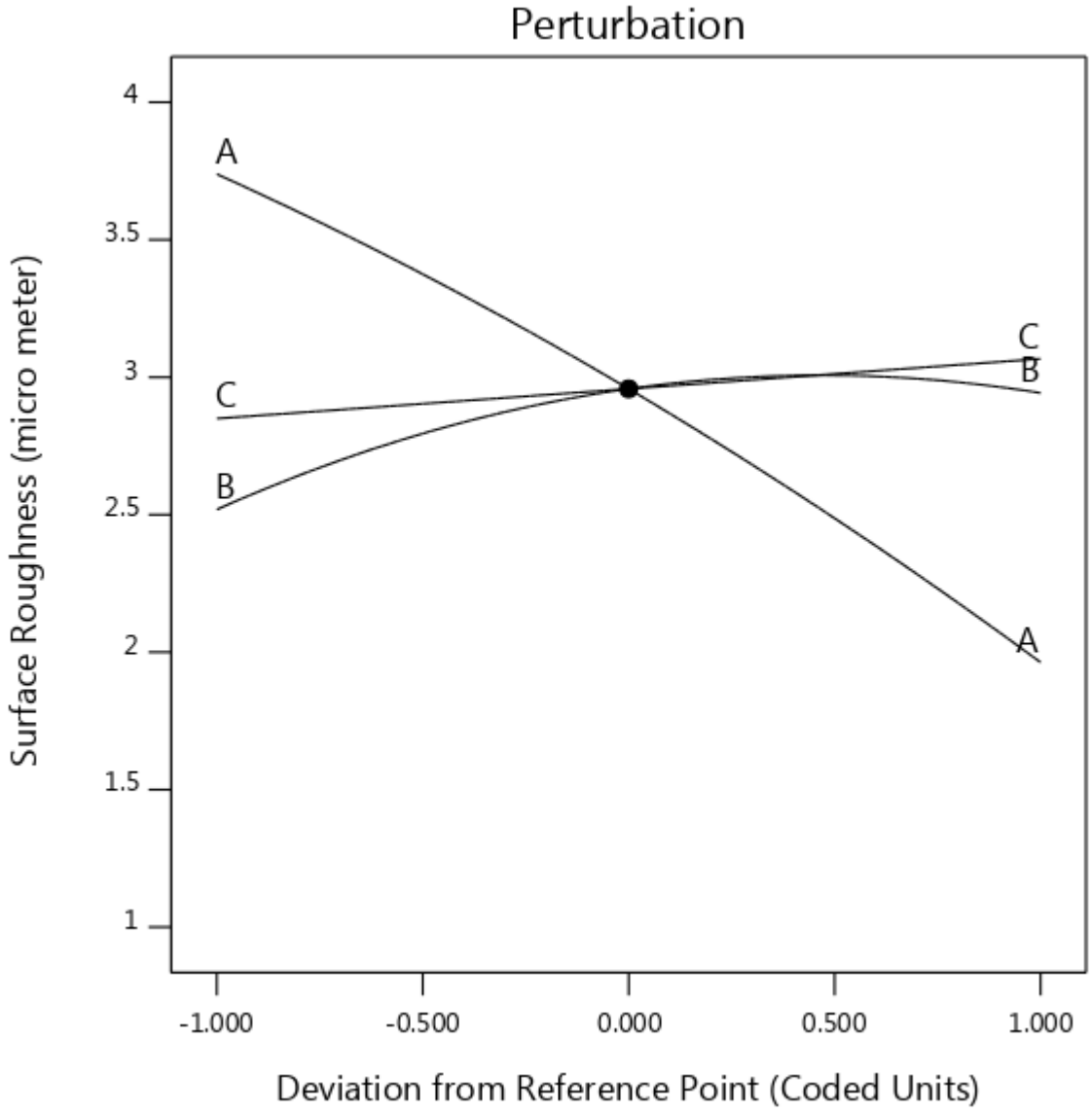

Figure 6.2: Graph represents the intersection point of SR

The graph above shows variation from the x-axis reference point while the y-axis shows surface roughness. This chart is called the curve of disturbance. In this graph, at one stage, three distinct classification variables labeled A, B and C intersect.

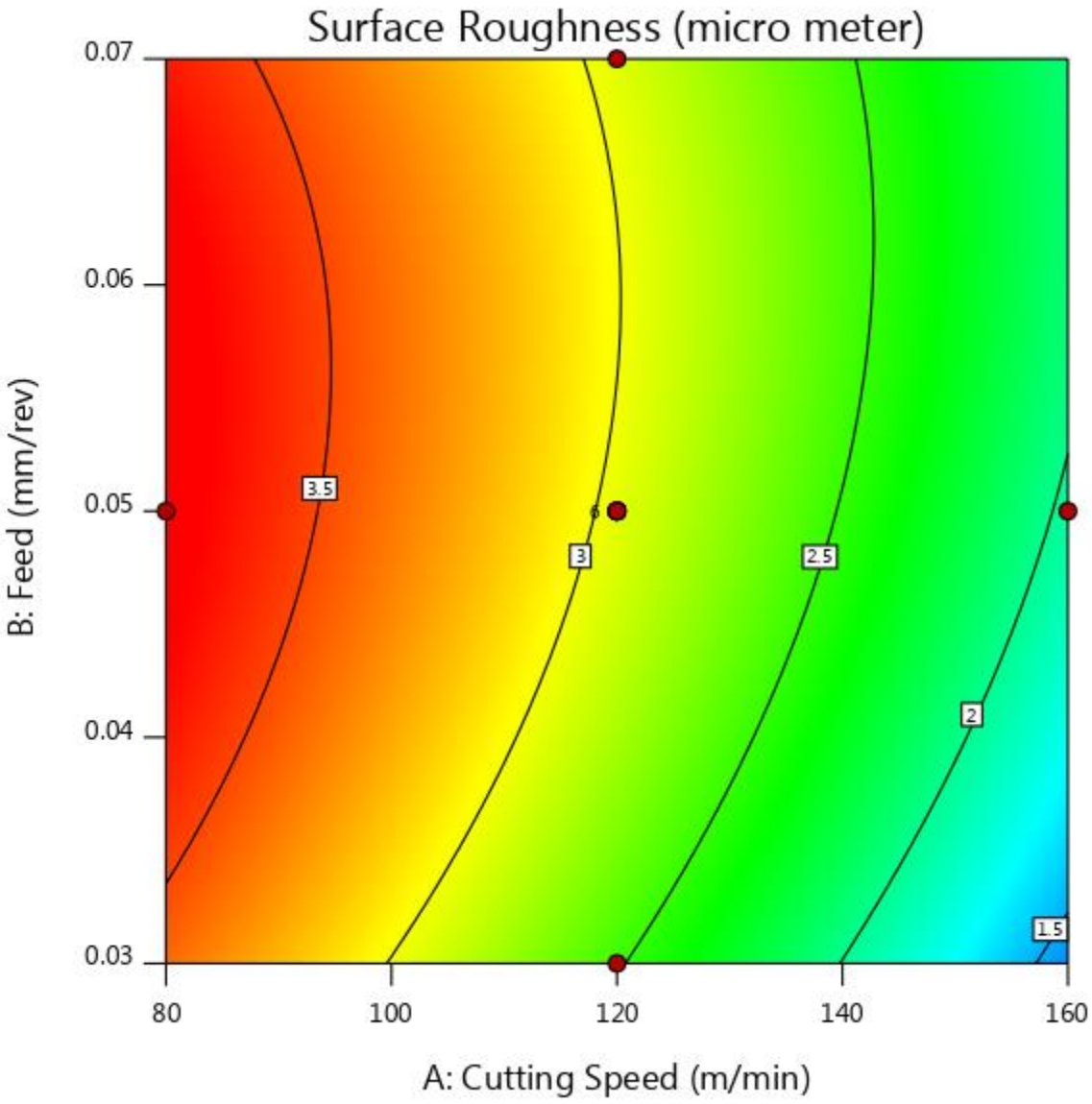

Figure 6.3: Contour plot of SR between CS and FR

This graph shows, on thex-axis, cutting speed (m / min) while on the y-axis feed (mm / rev). Surface ruggedness level is attained on this curve. Red regions depict the highest surface roughness range (3.679μm), while red regions depict the minimum surface ruggedness levels (1.05μm). The 2-D response surfaces are described by the contour charts. Contour plots have an important role to play in researching the edges of the reaction. Once produced through Software,

you can predict the ground image and accurately achieve optimized results.

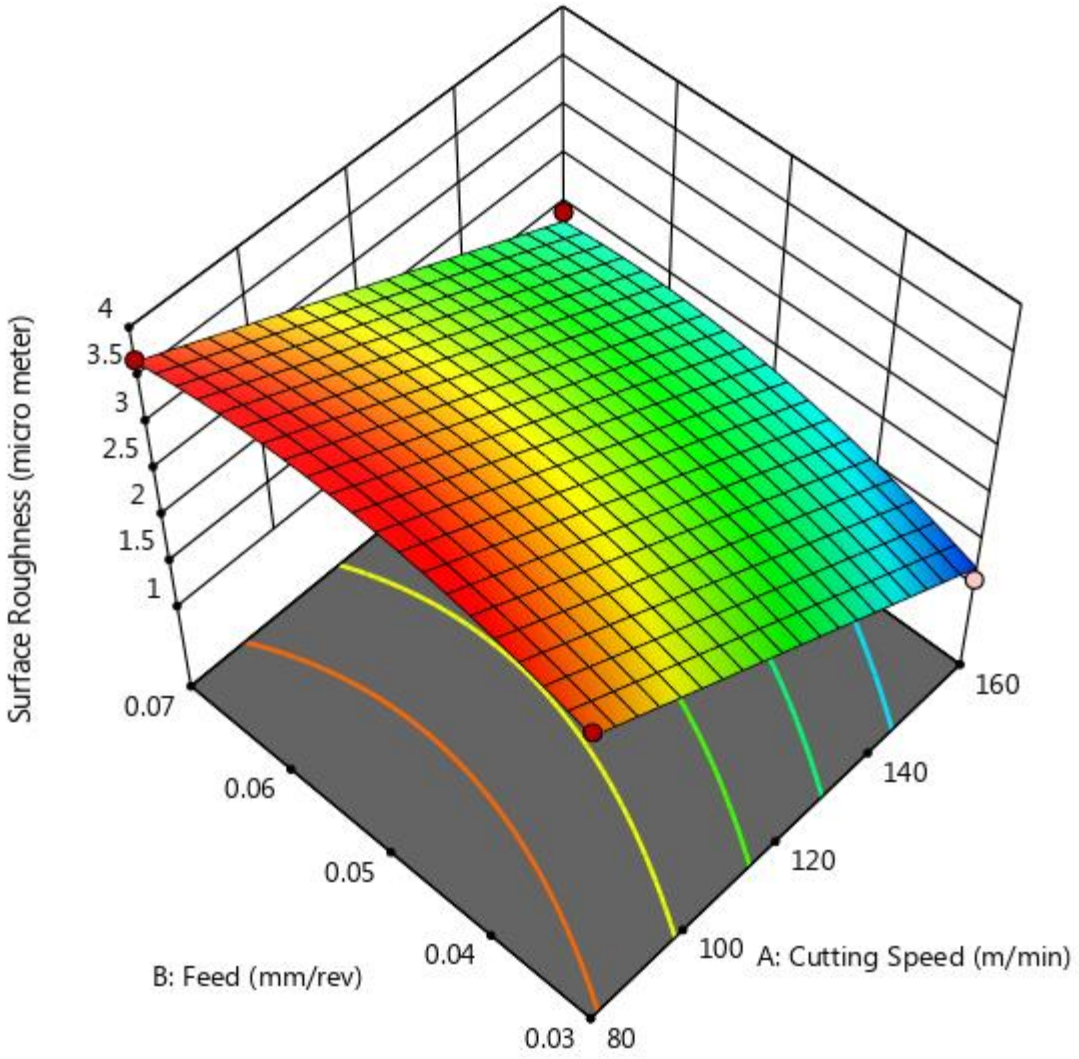

Figure 6.4: 3 D response surface graph of SR between CS and FR

This graph portrays cutting speed as x_1-axis while Feed on the x_2-axis, and lastly on the y-axis surface roughness. The response surface geometry of the response is 3-D in design.

6.1.2 Effect of analysis on Residual Stress

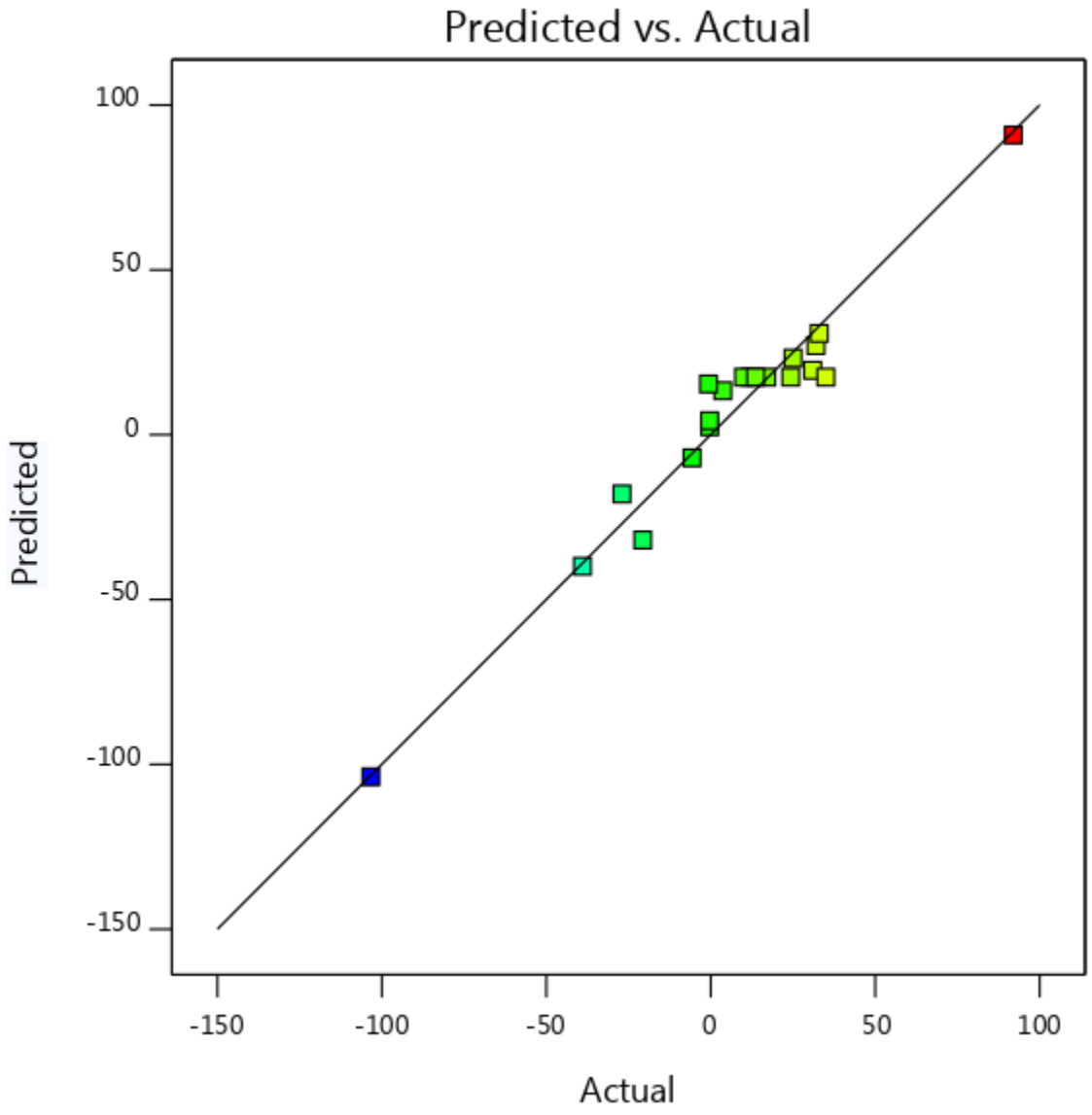

Figure 6.5: A plot between Predicted vs. Actual points of RS

The graph above shows Actual information on the x-axis of residual stress while predicting information on the y-axis of residual stress. Red spot are the largest residual stress ratio while a blue spot is the lowest residual stress rate. It is obvious from the graph that the real information is similar to the expected information. The graph demonstrates the predicted and actual information scores correlation.

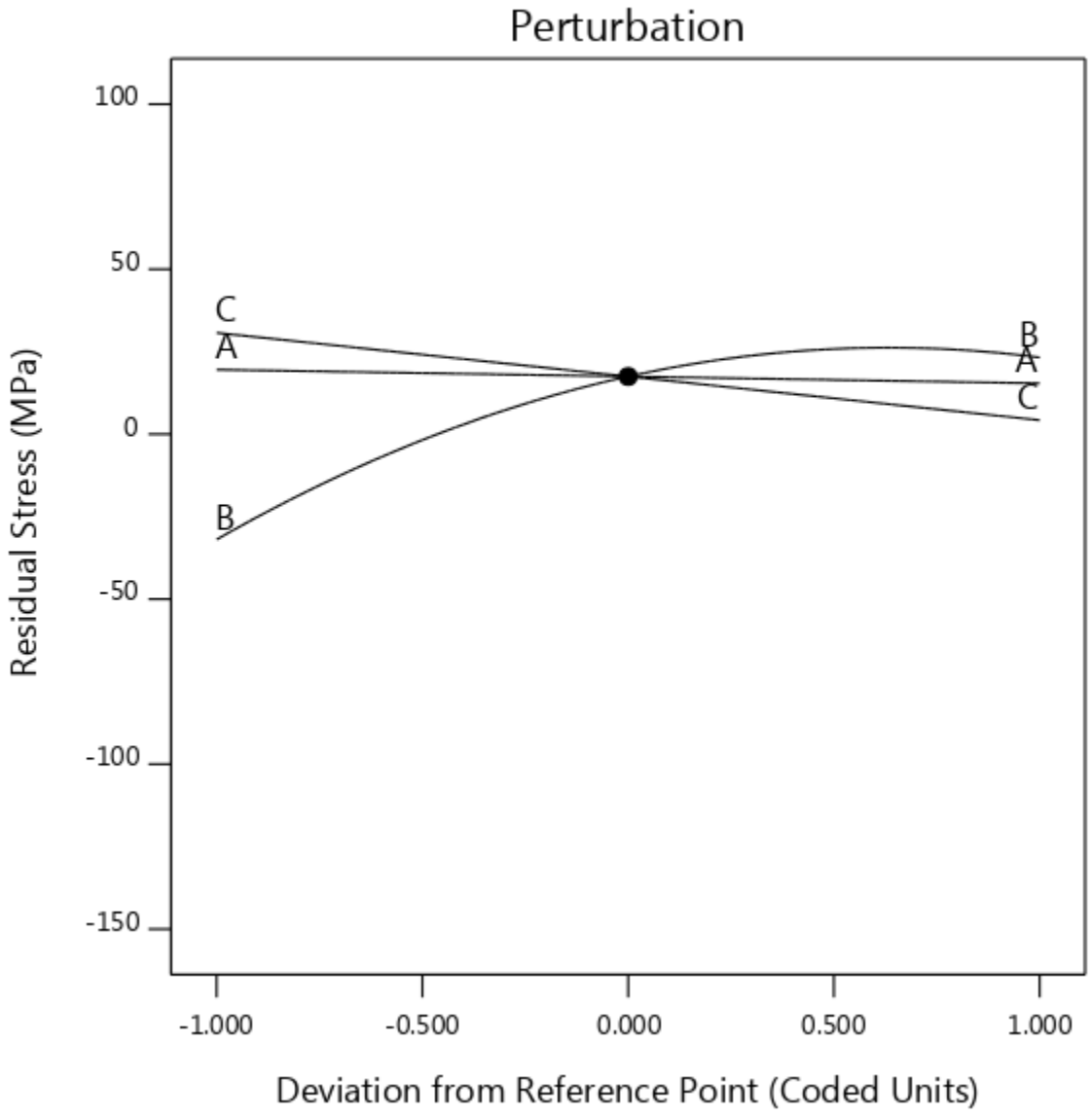

Figure 6.6: Graph represents the intersection point of RS

The graph above shows deviation from reference point on the x-axis reference point while the y-axis shows residual stress. This graph is called the curve of disturbance. In this graph, at one stage, three distinct classification variables labeled A, B and C intersects.

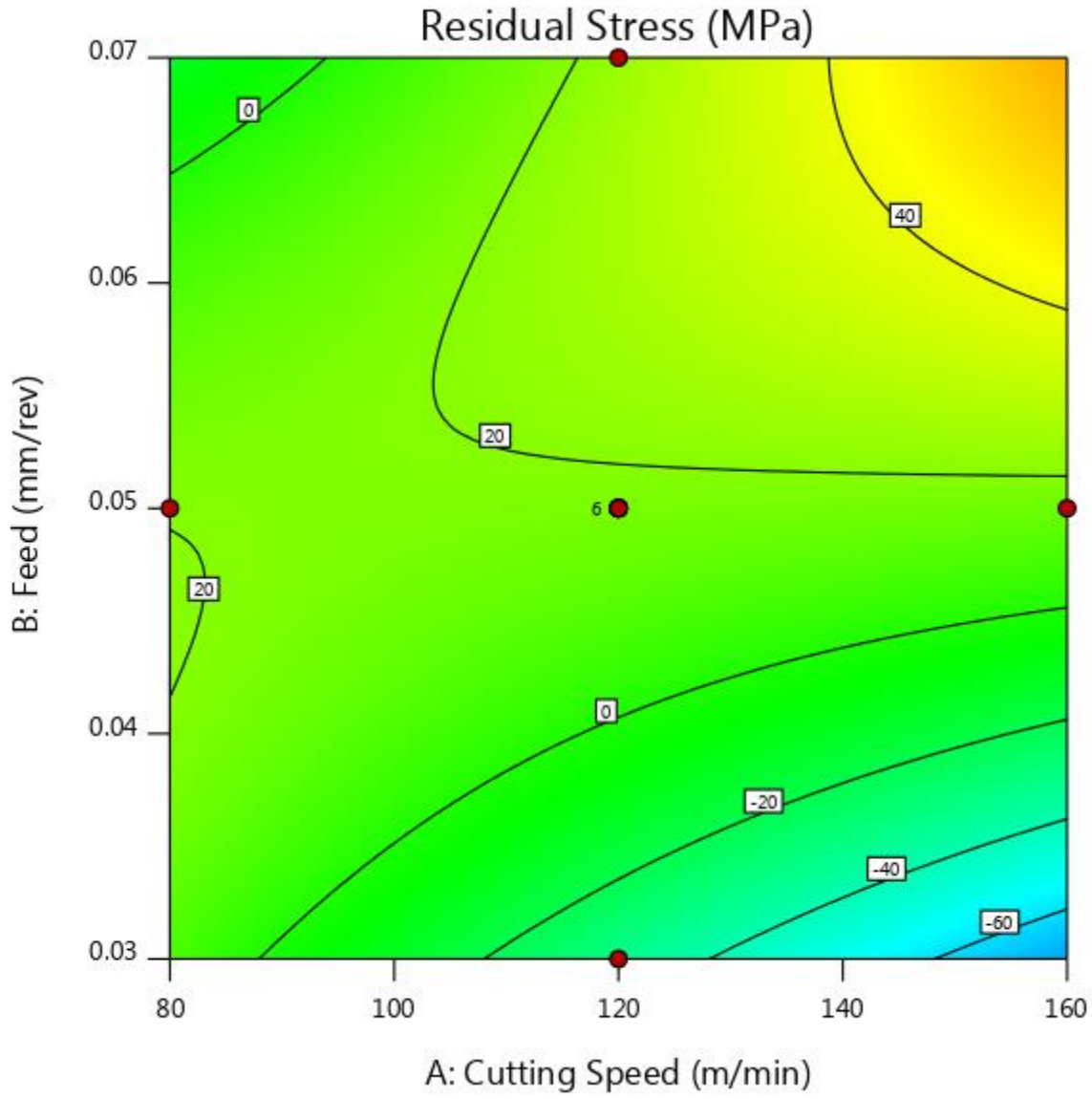

Figure 6.7: Contour plot of RS between CS and FR

This graph shows, on the x-axis, cutting speed (m / min) while on the y-axis feed (mm / rev). Residual stress level is attained on this curve. Red regions are the highest residual stress range (92MPa), while blue regions are the minimum residual stress levels (-103.333MPa). The 2-D response surfaces are described by the contour charts. Contour plots have an important role to play in researching the edges of the reaction. Once produced through Software, you can predict the response surface image and accurately achieve optimized results.

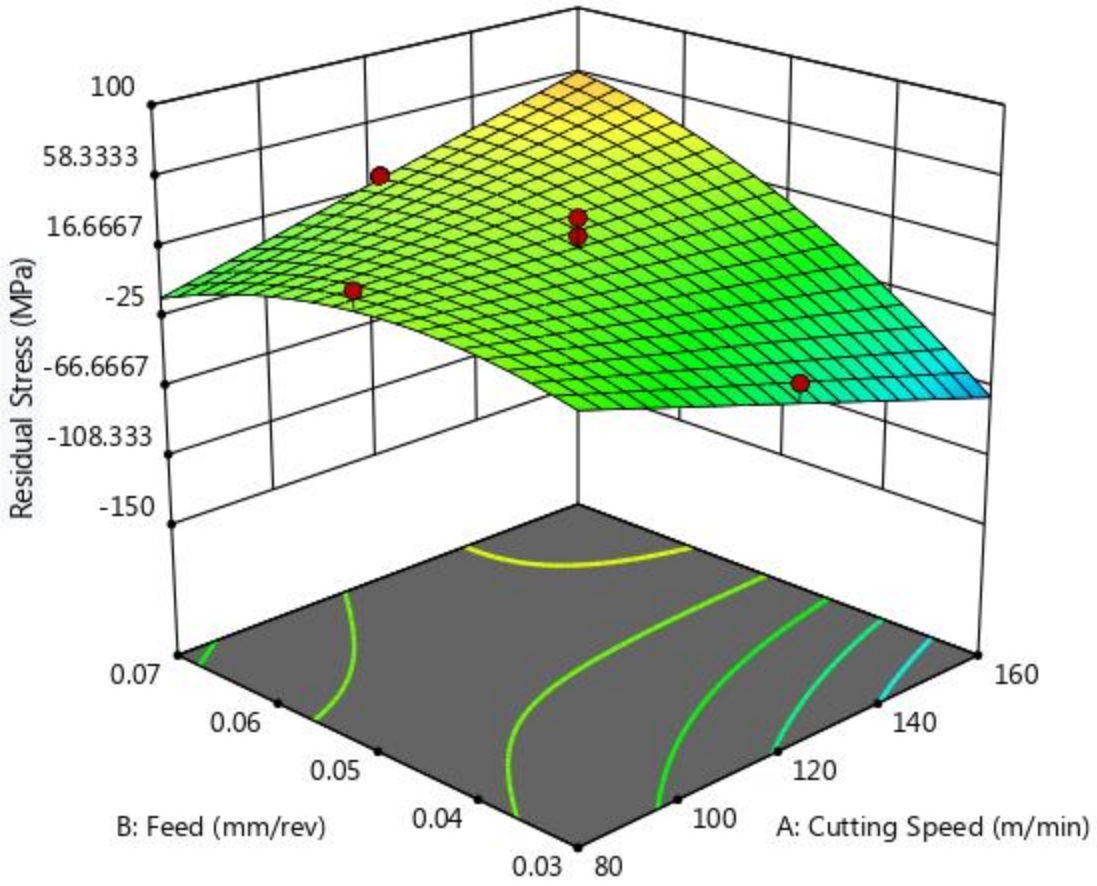

Figure 6.8: 3 D response surface graph of RS between CS and FR

This graph portrays the cutting speed as x_1-axis while Feed on the x_2-axis, and lastly the y-axis residual stress. The response surface geometry of the response is 3-D in design.

6.2 Optimization of Result

The important step is the optimization of result of the experiment. Optimizations of different response parameter are described following below:

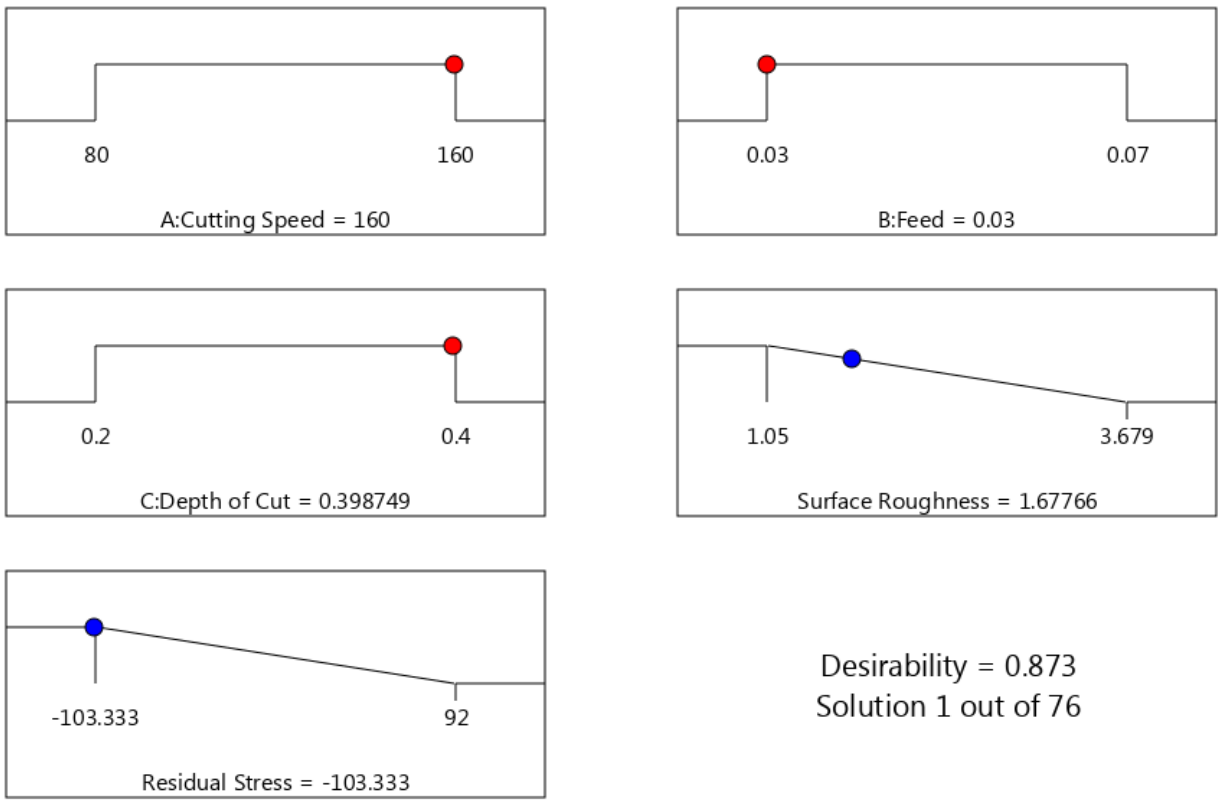

Figure 6.9: Optimum Result of Factors

The optimum result has obtained at maximum value of CS =160 m/min, minimum value of FR = 0.03 mm/rev and maximum value of DOC = 0.398 mm. The optimum values are for SR = 1.677µm and RS = -103.333 MPa with the desirability 87.30 %.

6.3 Point Prediction

This Table 5.1 describe the predict the mean of response parameter, Std Dev , 95% CI low for Mean and 95% CI high for Mean on the basis of data points of responses. The point predictions of Responses are following below in the Table 5.1:

Table 6.1: Predict the mean of Response parameter

Response	Predicted Mean	Std Dev	95% CI low for Mean	95% CI high for Mean
Surface Roughness	1.677	0.12459	1.46159	1.89373
Residual Stress	-103.333	9.66189	-120.089	-86.5772

6.4 Discussion

From the results, two significant samples were considered; first sample carries the maximum tensile residual stress while the second sample occupies the maximum compressive residual stress.

6.4.1 Maximum Compressive Residual Stress (Optimum Residual Stress)

Point 1

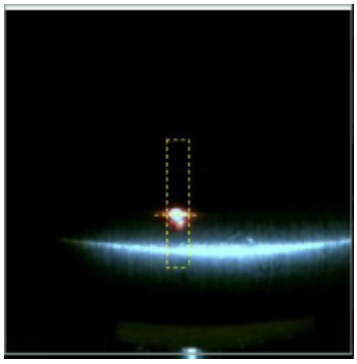

Figure 6.10: Camera image of point1 for maximum Compressive Residual Stress

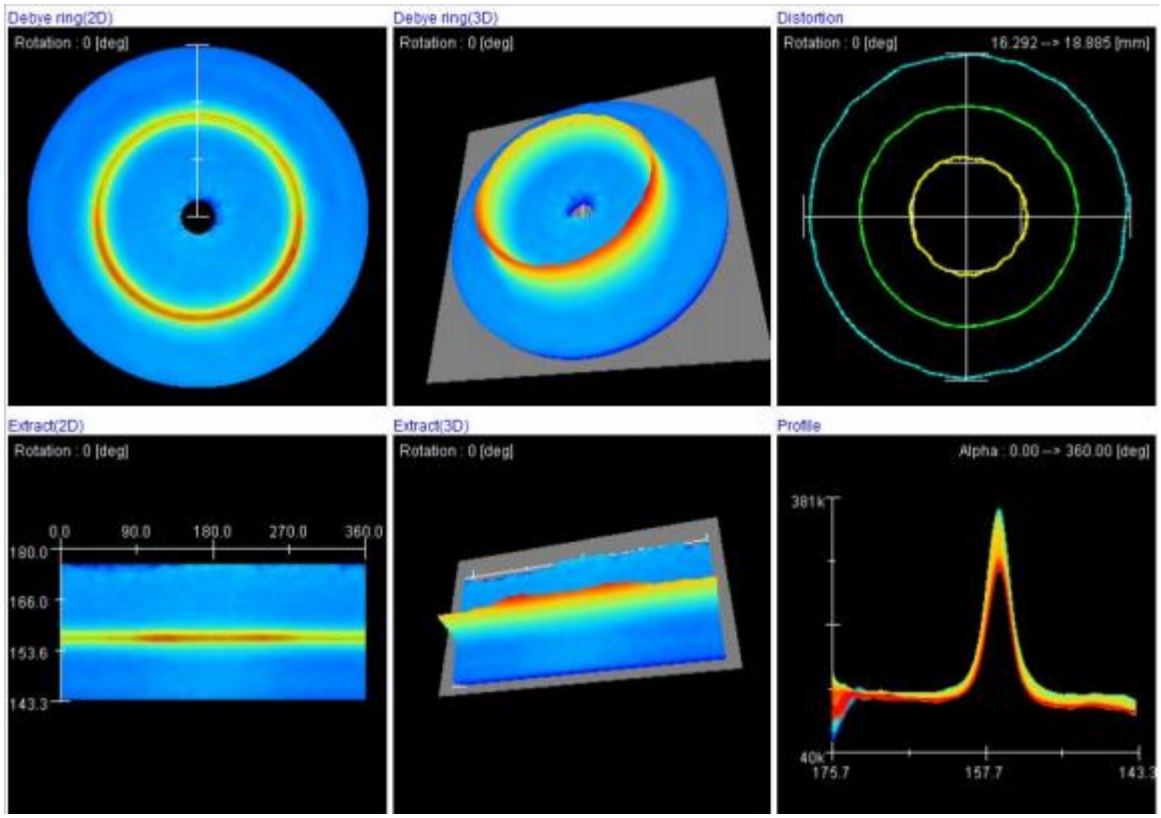

Figure 6.11: Map of Residual Stress of point 1 for maximum Compressive Residual Stress

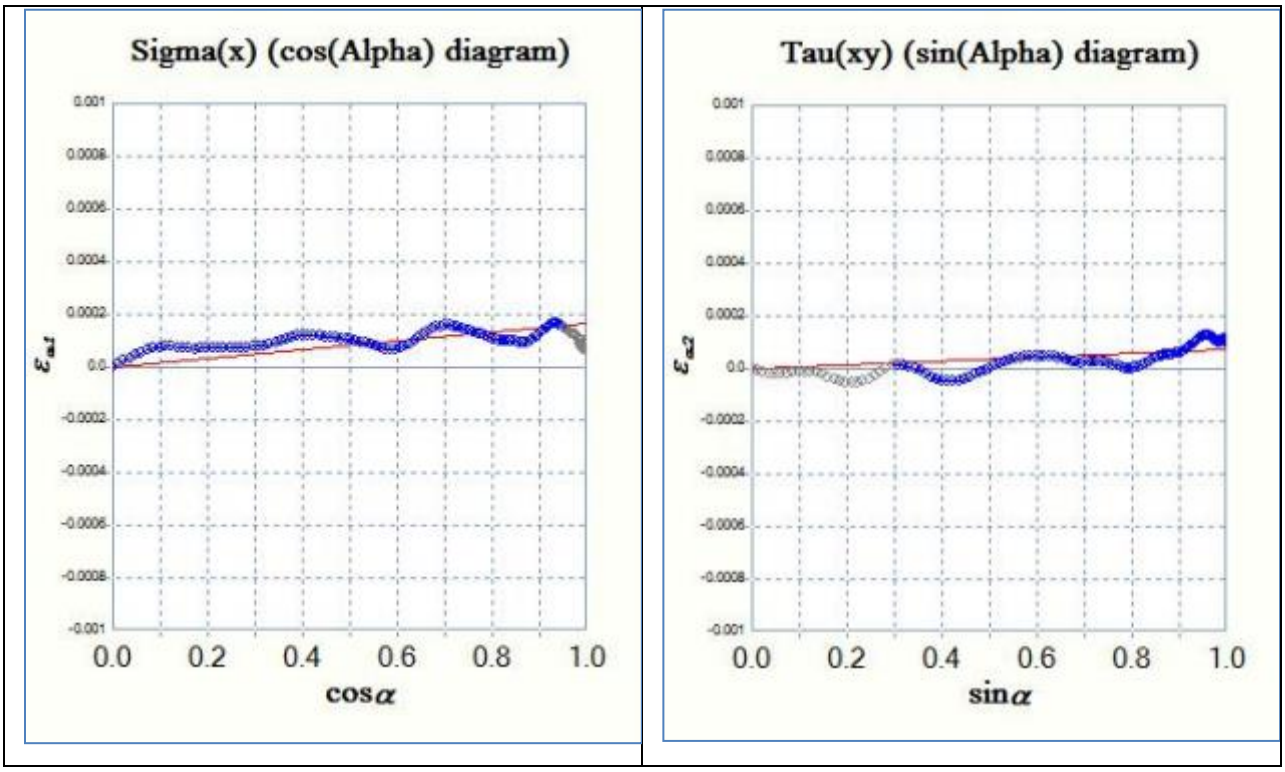

Figure 6.12: Residual Stress graph of point 1 for maximum Compressive Residual Stress

Residual Stress are as follows:-

Normal stress = (-) 75 MPa

Shear stress = (+) 26 MPa

Point 2

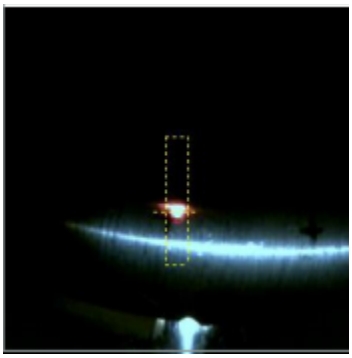

Figure 6.13: Camera image of point 2 for maximum Compressive Residual Stress

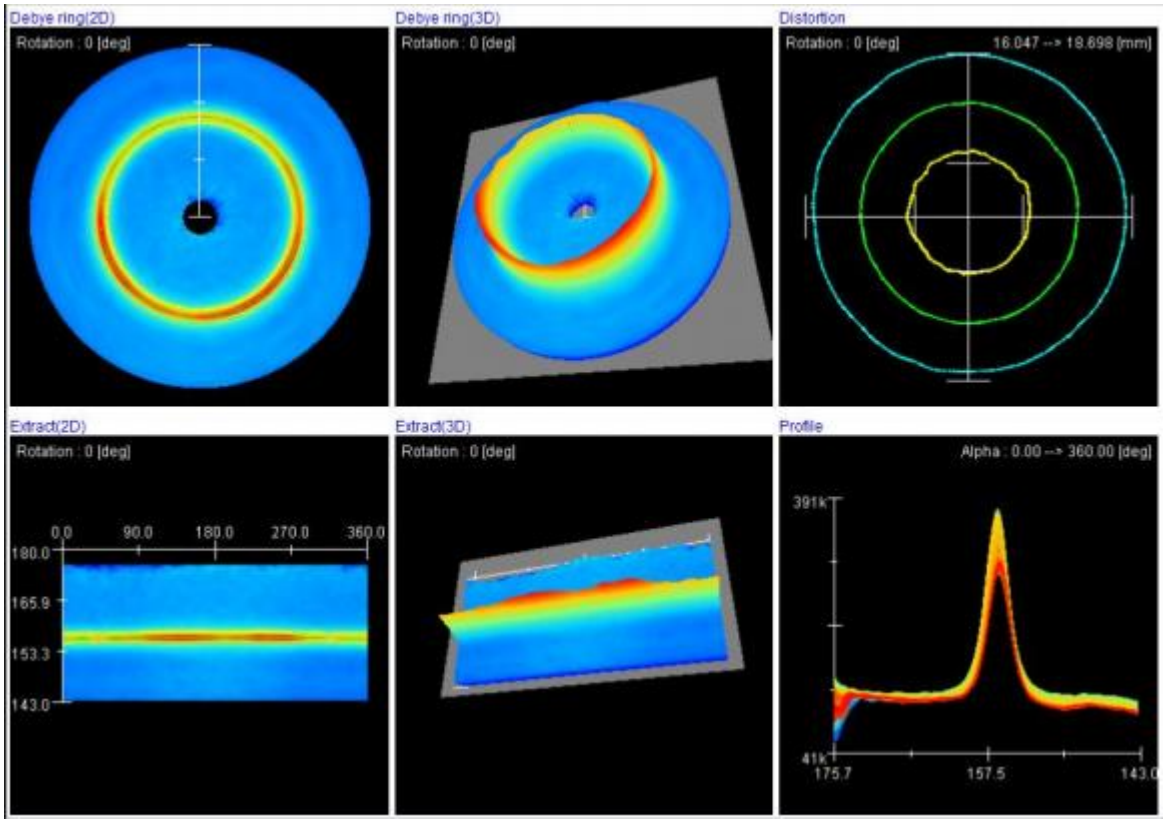

Figure 6.14: Map of Residual Stress of point 2 for maximum Compressive Residual Stress

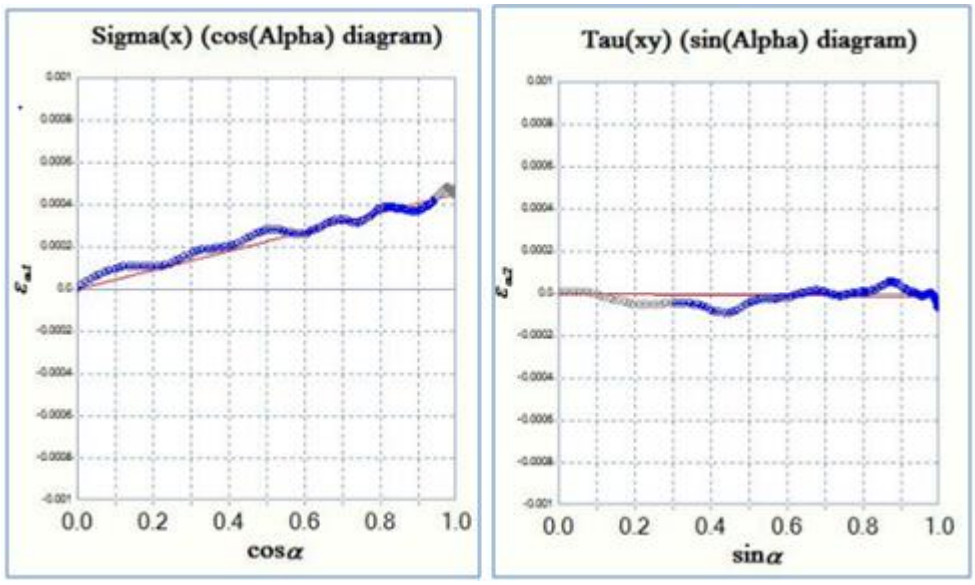

Figure 6.14: Residual Stress graph of point 2 for maximum Compressive Residual Stress

Residual Stress are as follows:-

Normal stress = (-) 209 MPa

Shear stress = (-) 6 MPa

Point 3

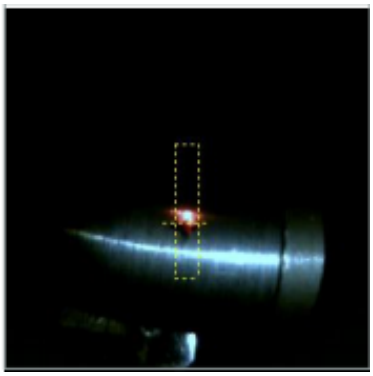

Figure 6.15: Camera image of point 3 for maximum Compressive Residual Stress

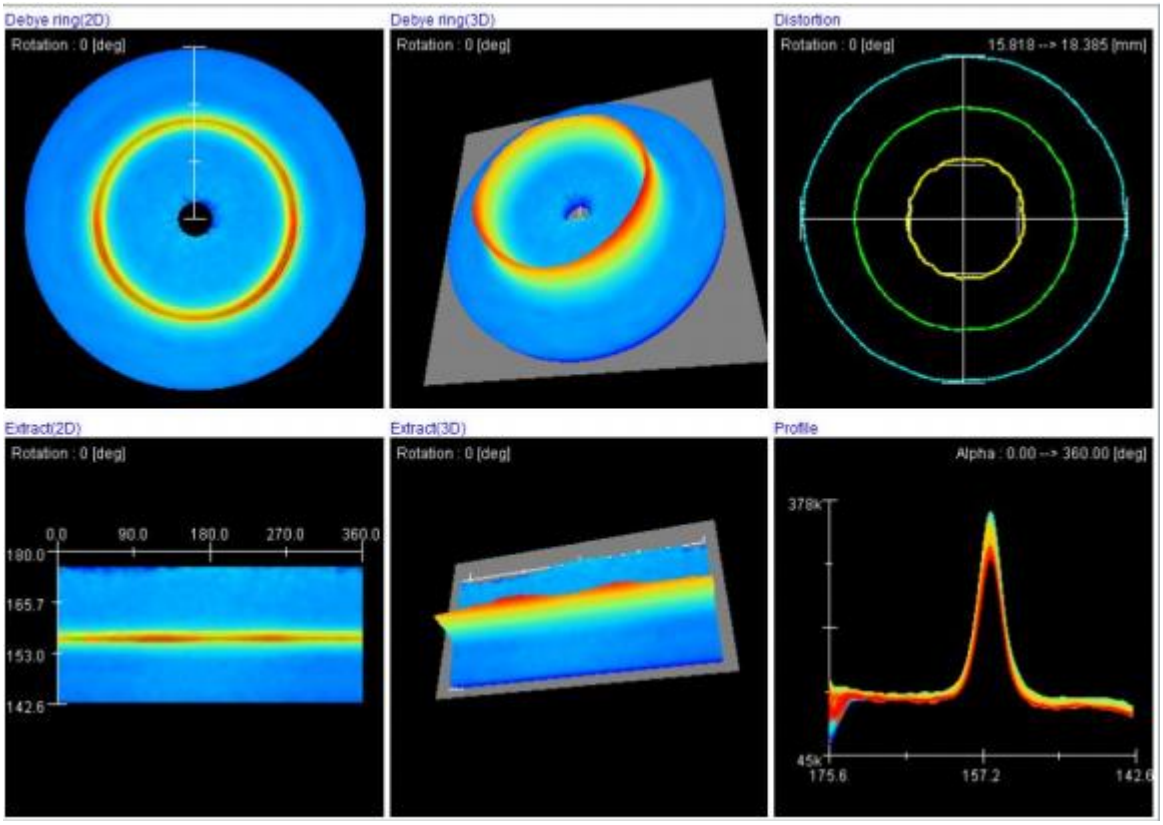

Figure 6.16: Map of Residual Stress of point 3 for maximum Compressive Residual Stress

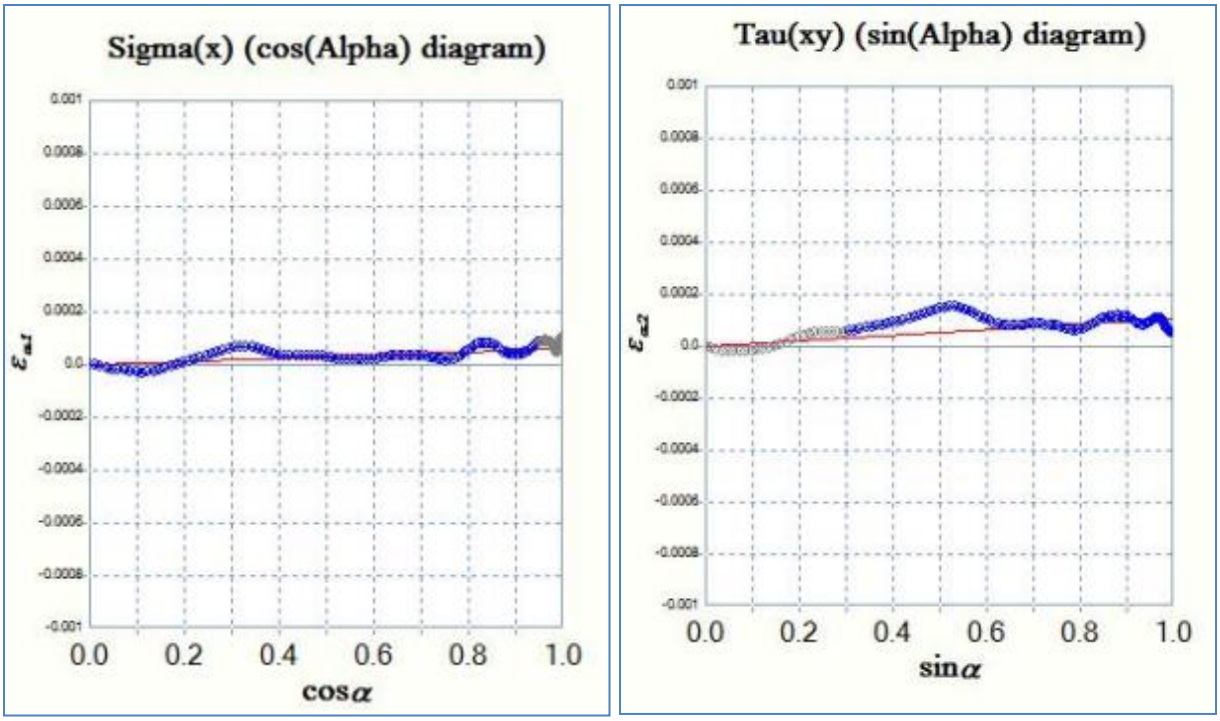

Figure 6.17: Residual Stress graph of point 3 for maximum Compressive Residual Stress

Residual Stress are as follows:-

Normal stress = (-) 26 MPa

Shear stress = (+) 40 MPa

Average Minimum Residual Stress = (-) 103.333 MPa

Explanation of arousal of maximum compressive residual stress

- From the above results, we conclude that Residual Stress depends on both the process parameters and material characteristics.
- If cutting speed is maintained high while the feed rate is maintained low, compressive residual stresses are generated.
- If cutting speed is maintained higher, then chips occupy higher heat value which gets carried away, thus the entire process remains adiabatic, which further leads to generation of compressive stresses.

6.4.2 Maximum Tensile Residual Stress

Point 1

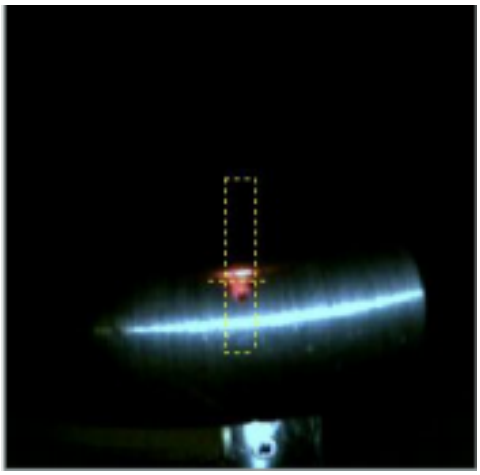

Figure 6.18: Camera image of point1 for maximum Tensile Residual Stress

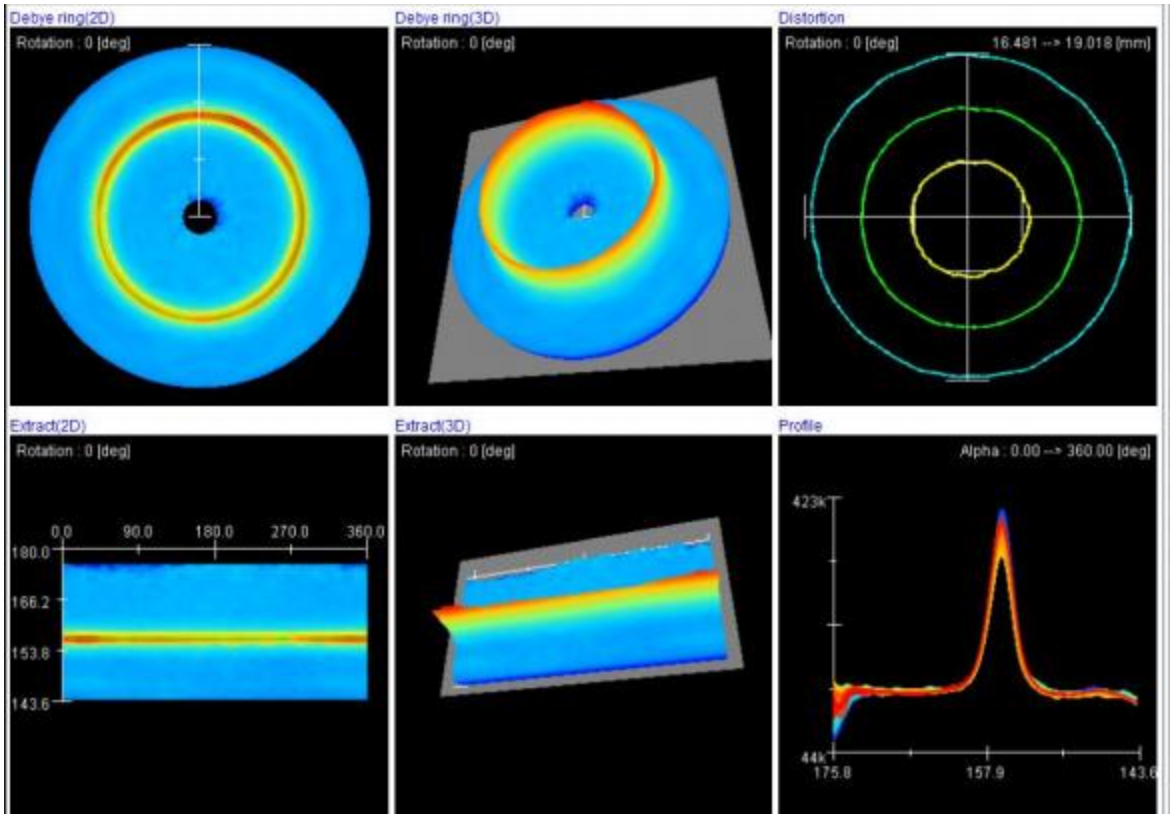

Figure 6.19: Map of Residual Stress of point 1 for maximum Tensile Residual Stress

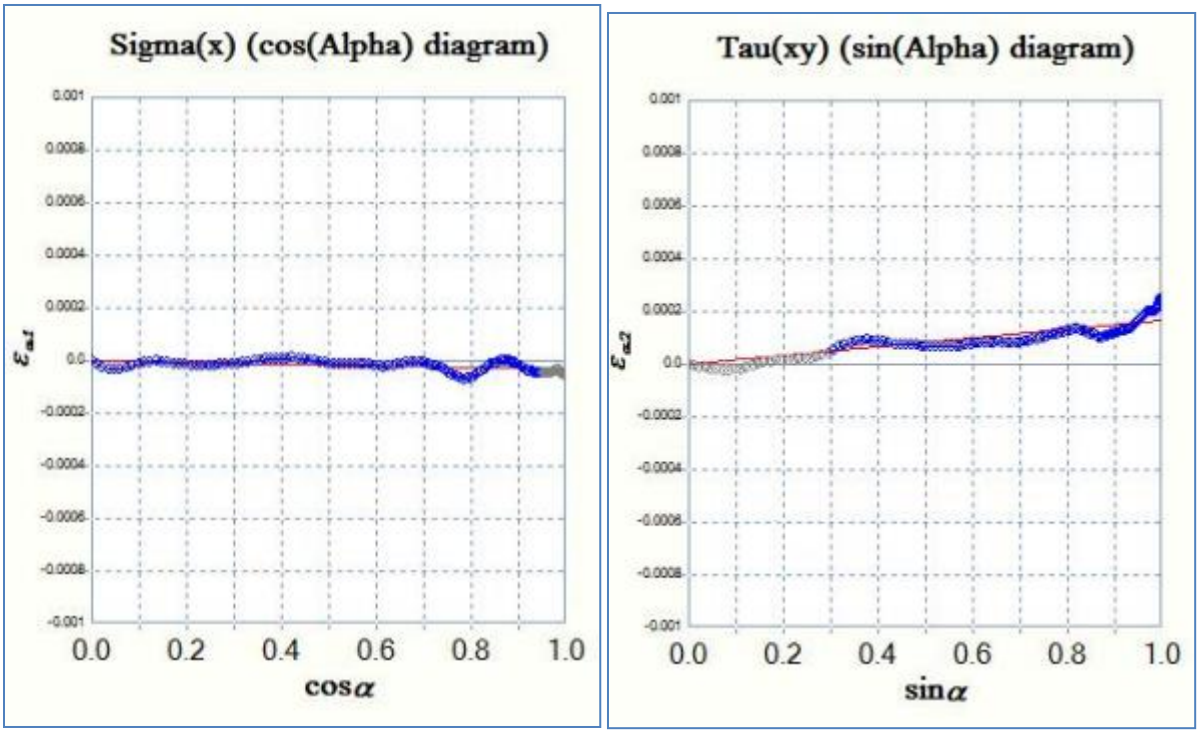

Figure 6.20: Residual Stress graph of point 1for maximum Tensile Residual Stress

Residual Stress are as follows:-

Normal stress = (+) 17 MPa

Shear stress = (+) 62 MPa

Point 2

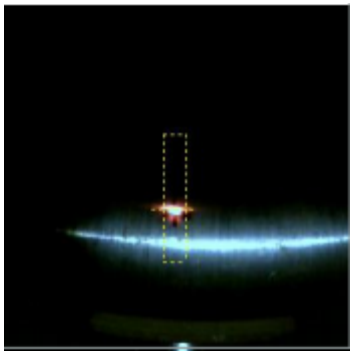

Figure 6.21: Camera image of point 2 for maximum Tensile Residual Stress

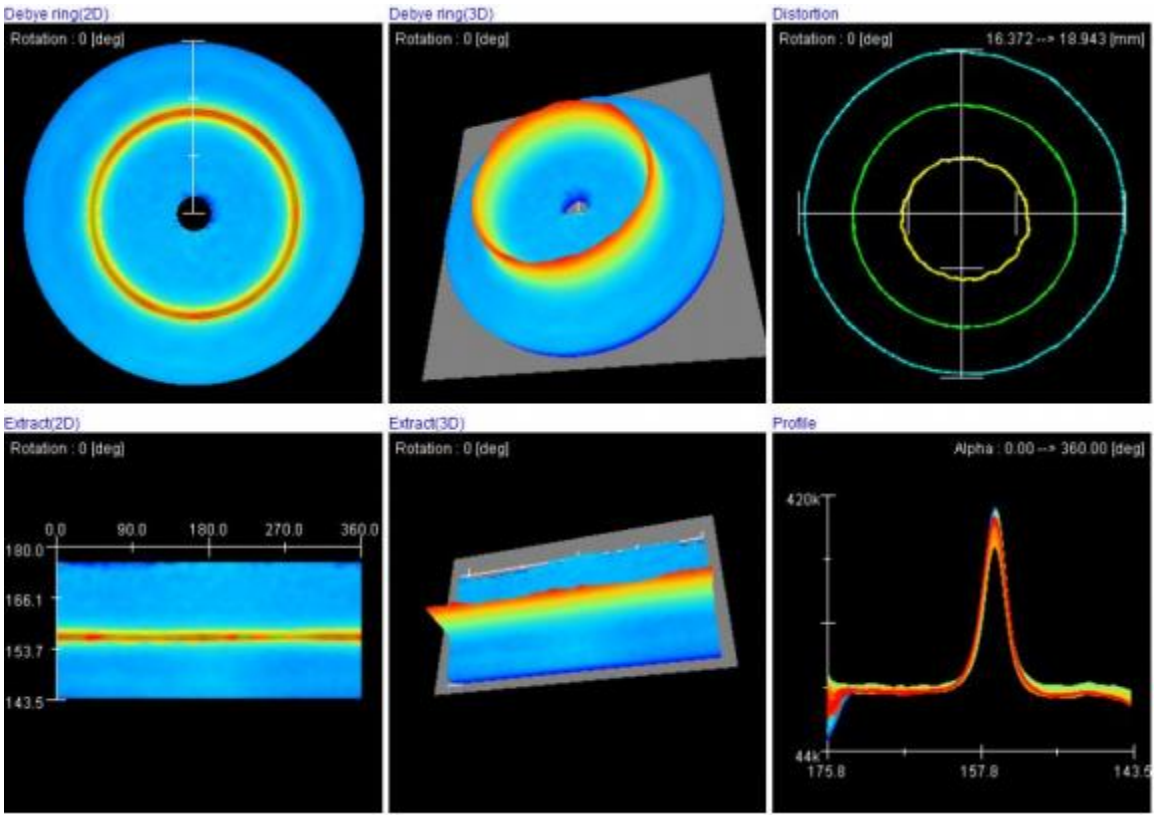

Figure 6.22: Map of Residual Stress of point 2 for maximum Tensile Residual Stress

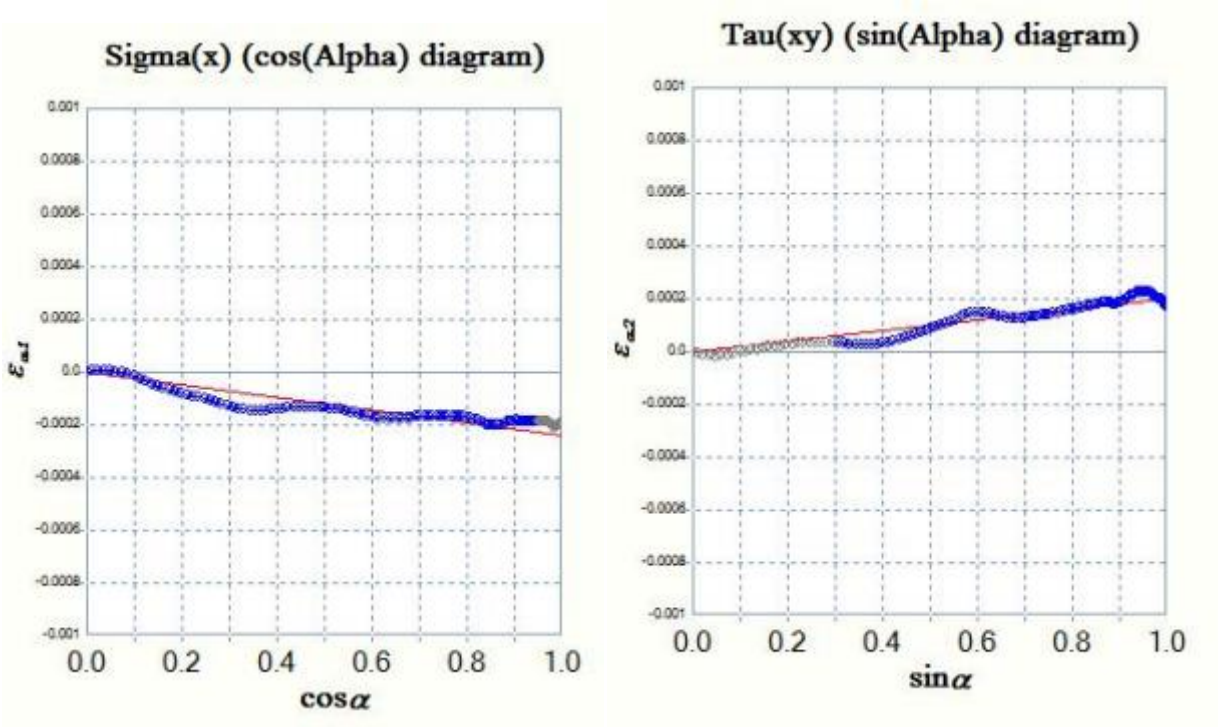

Figure 6.23: Residual Stress graph of point 2 for maximum Tensile Residual Stress

Residual Stress are as follows:-

Normal stress = (+) 113 MPa

Shear stress = (+) 76 MPa

Point 3

Figure 6.24: Camera image of point 3 for maximum Tensile Residual Stress

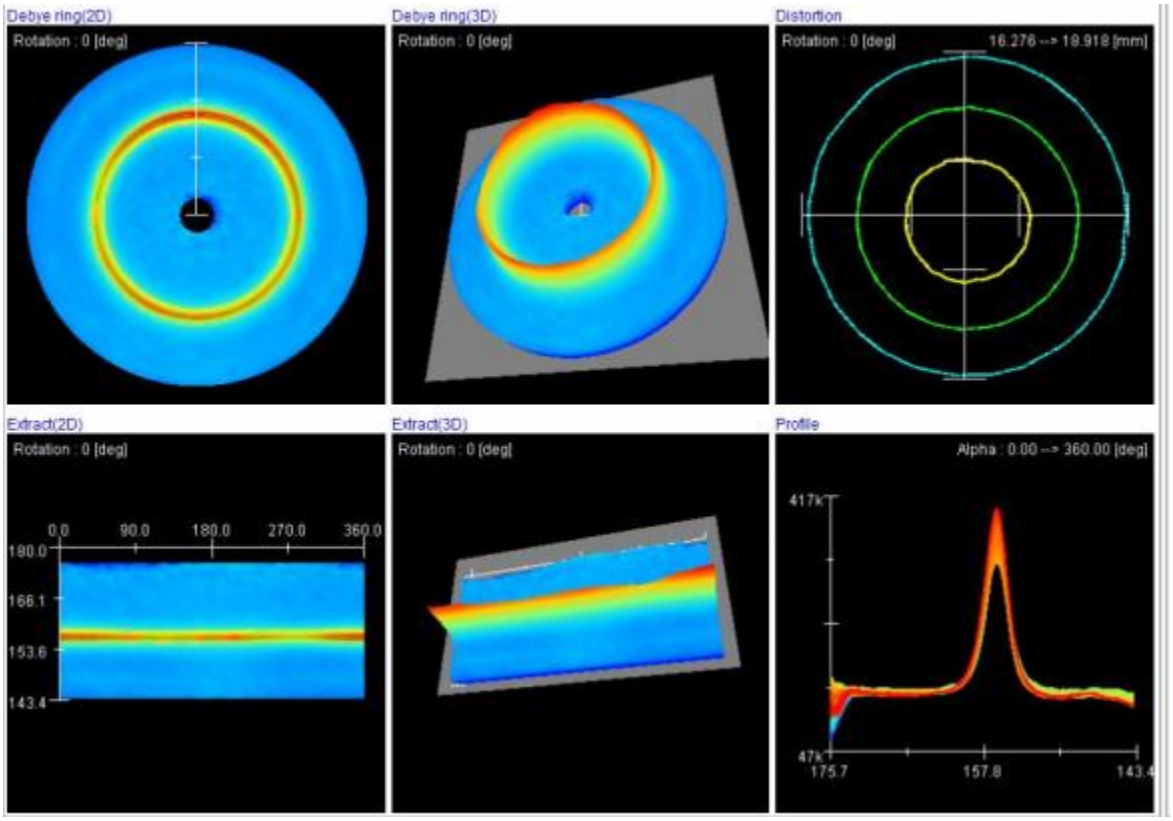

Figure 6.25: Map of Residual Stress of point 3 for maximum Tensile Residual Stress

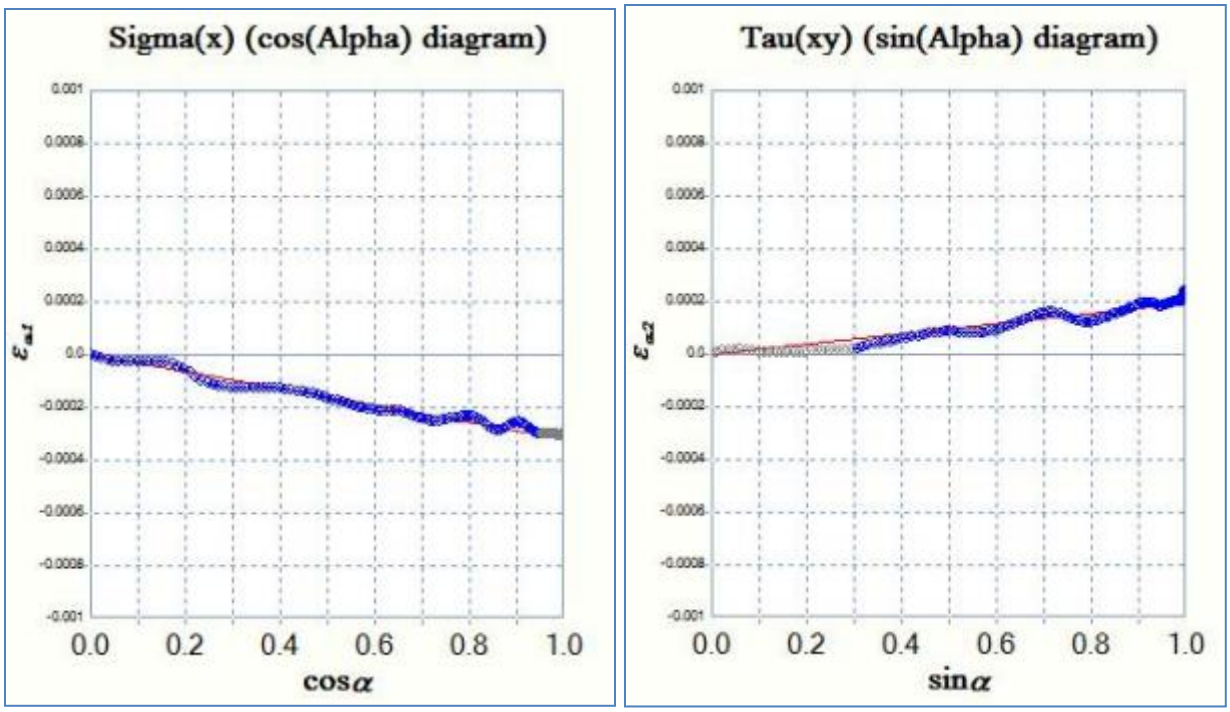

Figure 6.26: Residual Stress graph of point 3 for maximum Tensile Residual Stress

Residual Stress are as follows:-

Normal stress = (+) 150 MPa

Shear stress = (+) 72 MPa

Average Maximum Residual Stress = (+) 93.333 MPa

Explanation of arousal of maximum tensile residual stress

- It is seen that as the feed rate is raised, generation of heat will occur which further leads to increase of tensile residual stresses.
- As the cutting speed is lowered, the process turns out to be less adiabatic which further raises the tensile residual stress.
- As the feed rate is raised, it is observed that poor surface finish is achieved while higher tensile residual stress is obtained.

CHAPTER 7

CONCLUSION AND FUTURE SCOPE OF STUDY

7.1 Conclusions

This dissertation presented the work for the optimization of CNC turning using AISI 8620 steel with multi performance characteristics through RSM. Results were generated, on account of which following conclusions can be drawn as:-

- Results presented that Surface Roughness has major influential role primarily from Cutting Speed having F value of 507.88, followed by Feed with F value of 28.93 and finally Depth of Cut having F value of 7.60.
- Results presented that Residual Stress has major influential role primarily from Feed having F value of 81.61, followed by Depth of cut with F value of 18.76 and finally Cutting Speed having F value of 0.4570.
- The optimum result has obtained at maximum value of CS =160 m/min, minimum value of FR = 0.03 mm/rev and maximum value of DOC = 0.398 mm. The optimum values are for SR = 1.677µm and RS = -103.333 MPa with the desirability 87.30 %.
- The interactions between CS and FR (A×B), CS and DOC (A×C) significantly affect the performance characteristics.
- As the cutting speed is raised and feed rate is mitigated, it is observed that
  - Higher compressive residual stresses are generated.
  - Better surface finish is obtained.

7.2 Future Scope of Study

Turning process possesses huge possibilities of research and development.

- Research needs to be focused on other parameters such as tool geometry, tool material, machine vibration for calculating its effect on cutting performance.
- Further analysis can be considered to evaluate tool life and temperature rise in turning method.
- Furthermore, research can be pushed forward with investigating the cutting tool edge condition and effect on rake angle respectively.
- Tool wear can also be remarked as one of the huge possibility in terms of research area under various working environment.

Steps have been taken to ensure process with more effectiveness and productivity by irradicating the involved difficulties of the process.

REFERENCES

[1] Tzeng, C. J., & Chen, R. Y. (2013). Optimization of electric discharge machining process using the response surface methodology and genetic algorithm approach. *International journal of precision engineering and manufacturing*, *14*(5), 709-717.

[2] Nalbant, M., Gökkaya, H., & Sur, G. (2007). Application of Taguchi method in the optimization of cutting parameters for surface roughness in turning. *Materials & design*, *28*(4), 1379-1385.

[3] Arbizu, I. P., & Perez, C. L. (2003). Surface roughness prediction by factorial design of experiments in turning processes. *Journal of Materials Processing Technology*, *143*, 390-396.

[4] Abouelatta, O. B., & Madl, J. (2001). Surface roughness prediction based on cutting parameters and tool vibrations in turning operations. *Journal of materials processing technology*, *118*(1-3), 269-277.

[5] Nian, C. Y., Yang, W. H., & Tarng, Y. S. (1999). Optimization of turning operations with multiple performance characteristics. *Journal of Materials Processing Technology*, *95*(1-3), 90-96.

[6] Montgomery, D. C. (2017). *Design and analysis of experiments*. John wiley & sons.

[7] http://www.astmsteel.com/product/aisi-8620-steel-alloy/, 24/07/2019, 1:15 PM.

[8] Bisht, H., Gupta, J., Pal, S. K., & Chakraborty, D. (2005). Artificial neural network based prediction of flank wear in turning. *International Journal of Materials and Product Technology*, *22*(4), 328-338.

[9] Karkalos, N. E., Galanis, N. I., & Markopoulos, A. P. (2016). Surface roughness prediction for the milling of Ti–6Al–4V ELI alloy with the use of statistical and soft computing techniques. *Measurement*, *90*, 25-35.

[10] Rossini, N. S., Dassisti, M., Benyounis, K. Y., & Olabi, A. G. (2012). Methods of measuring residual stresses in components. *Materials & Design*, *35*, 572-588.

[11] Kumar, M. V., Kumar, B. K., & Rudresha, N. (2018). Optimization of Machining Parameters in CNC Turning of Stainless Steel (EN19) By TAGUCHI'S Orthogonal Array Experiments. *Materials Today: Proceedings*, *5*(5), 11395-11407.

[12] Plaza, E. G., & López, P. N. (2018). Analysis of cutting force signals by wavelet packet transform for surface roughness monitoring in CNC turning. *Mechanical Systems and Signal Processing*, *98*, 634-651.

[13] Gadekula, R. K., Potta, M., Kamisetty, D., Yarava, U. K., Anand, P., & Dondapati, R. S. (2018). Investigation on Parametric Process Optimization of HCHCR in CNC Turning Machine Using Taguchi Technique. *Materials Today: Proceedings*, *5*(14), 28446-28453.

[14] Routara, B. C., Sahoo, A. K., Parida, A. K., & Padhi, P. C. (2012). Response surface methodology and genetic algorithm used to optimize the cutting condition for surface roughness parameters in CNC turning. *Procedia engineering*, *38*, 1893-1904.

[15] Kumar, N. S., Shetty, A., Shetty, A., Ananth, K., & Shetty, H. (2012). Effect of spindle speed and feed rate on surface roughness of Carbon Steels in CNC turning. *Procedia Engineering*, *38*, 691-697.

[16] Nataraj, M., Balasubramanian, K., & Palanisamy, D. (2018). Influence of Process Parameters on CNC Turning of Aluminium Hybrid Metal Matrix Composites. *Materials Today: Proceedings*, *5*(6), 14499-14506.

[17] Venkatesana, K., Mathewb, A. T., Devendiranc, S., Ghazalyd, N. M., Sanjithe, S., & Raghulf, R. (2018). Machinability study and multi-response optimization of cutting force, Surface roughness and tool wear on CNC turned Inconel 617 superalloy using Al2O3 Nanofluids in Coconut oil.

[18] Tulasi, R., Singh, R., & Ali, M. I. (2018). Optimizing Surface Roughness in Turning Operation Using Taguchi Technique. *Materials Today: Proceedings*, *5*(9), 19043-19048.

[19] He, C. L., Zong, W. J., & Zhang, J. J. (2018). Influencing factors and theoretical modeling methods of surface roughness in turning process: state-of-the-art. *International Journal of Machine Tools and Manufacture*, *129*, 15-26.

[20] Palanisamy, D., & Senthil, P. (2018). Application of Grey-Fuzzy Approach for Optimization of CNC Turning Process. *Materials Today: Proceedings*, *5*(2), 6645-6654.

[21] Saini, S. K., & Pradhan, S. K. (2014). Optimization of multi-objective response during cnc turning using taguchi-fuzzy application. *Procedia Engineering*, *97*, 141-149.

[22] Rao, K. S. S., & Allamraju, K. V. (2017). Effect on Micro-Hardness and Residual Stress in CNC Turning Of Aluminium 7075 Alloy. *Materials Today: Proceedings*, *4*(2), 975-981.

[23] Das, S. R., Panda, A., & Dhupal, D. (2018). Hard turning of AISI 4340 steel using coated carbide insert: Surface roughness, tool wear, chip morphology and cost estimation. *Materials Today: Proceedings*, *5*(2), 6560-6569.

[24] Palanisamy, D., Devaraju, A., Harikrishnan, S., & Manikandan, N. (2018). Machinability Studies on CNC Turning of PH Stainless Steel with Coated Inserts. *Materials Today: Proceedings*, *5*(6), 14520-14525.

[25] Prakash, P. B., Raju, K. B., Subbaiah, K. V., Krishnamachary, P. C., ManiKandan, N., & Ramya, V. (2018). Application of Taguchi based Grey Method for Multi Aspects Optimization on CNC Turning of AlSi7 Mg. *Materials Today: Proceedings*, *5*(6), 14292-1

[26] Bharilya, R. K., Malgaya, R., Patidar, L., Gurjar, R. K., & Jha, A. K. (2015). Study of optimised process parameters in turning operation through force dynamometer on CNC machine. *Materials Today: Proceedings*, *2*(4-5), 2300-2305.4301.

[27] Srinivas, K., & Devaraj, C. (2018). Optimization of Residual Stresses in Hard Turning of Super Alloy Inconel 718. *Materials Today: Proceedings*, *5*(2), 4592-4600.

[28] Patel, V. D., & Gandhi, A. H. (2019). Analysis and modeling of surface roughness based on cutting parameters and tool nose radius in turning of AISI D2 steel using CBN tool. *Measurement*, *138*, 34-38.

[29] Parida, A. K., & Maity, K. (2019). Modeling of machining parameters affecting flank wear and surface roughness in hot turning of Monel-400 using response surface methodology (RSM). *Measurement*, *137*, 375-381.

[30] Yang, A., Han, Y., Pan, Y., Xing, H., & Li, J. (2017). Optimum surface roughness prediction for titanium alloy by adopting response surface methodology. *Results in Physics*, *7*, 1046-1050.

[31] Prasath, K. M., Pradheep, T., & Suresh, S. (2018). Application of Taguchi and Response Surface Methodology (RSM) in Steel Turning Process to Improve Surface Roughness and Material Removal Rate. *Materials Today: Proceedings*, *5*(11), 24622-24631.

[32] Ma, L., Cai, C., Tan, Y., Gong, Y., & Zhu, L. (2019). Theoretical model of transverse and longitudinal surface roughness and study on brittle-ductile transition mechanism for turning Fluorophlogopite ceramic. *International Journal of Mechanical Sciences*, *150*, 715-726.

[33] Leo Kumar, S.P. (2019). Measurement and uncertainty analysis of surface roughness and material removal rate in micro turning operation and process parameters optimization. *Measurement, 140*,538-547.

[34] Subramanian, M., Vallavi, A., Nachimuthu, M. D. G., & Cinnasamy, V. (2017). Assessment of cutting force and surface roughness in LM6/SiCp using response surface methodology. *Journal of applied research and technology*, *15*(3), 283-296.

[35] Rubio, E. M., Bericua, A., de Agustina, B., & Marín, M. M. (2019). Analysis of the surface roughness of titanium pieces obtained by turning using different cooling systems. *Procedia CIRP*, *79*, 79-84.

[36] Joardar, H. (2018). Optimization for Turning of Aluminium and Titanium Di Boride Cast Composites Using Response Surface Methodology. *Materials Today: Proceedings*, *5*(11), 23576-23585.

[37] He, C. L., Zong, W. J., & Zhang, J. J. (2018). Influencing factors and theoretical modeling methods of surface roughness in turning process: state-of-the-art. *International Journal of Machine Tools and Manufacture*, *129*, 15-26.

[38] Makadia, A. J., & Nanavati, J. I. (2013). Optimisation of machining parameters for turning operations based on response surface methodology. *Measurement*, *46*(4), 1521-1529.

[39] Tomov, M., Kuzinovski, M., & Cichosz, P. (2016). Modeling and prediction of surface roughness profile in longitudinal turning. *Journal of Manufacturing Processes*, *24*, 231-255.

[40] Neşeli, S., Yaldız, S., & Türkeş, E. (2011). Optimization of tool geometry parameters for turning operations based on the response surface methodology. *Measurement*, *44*(3), 580-587.

[41] Parida, A. K., Routara, B. C., & Bhuyan, R. K. (2015). Surface roughness model and parametric optimization in machining of GFRP composite: Taguchi and Response surface methodology approach. *Materials Today: Proceedings*, *2*(4-5), 3065-3074.

[42] He, C. L., Zong, W. J., & Sun, T. (2016). Origins for the size effect of surface roughness in diamond turning. *International Journal of Machine Tools and Manufacture*, *106*, 22-42.

[43] Rao, C. P., & Bhagyashekar, M. S. (2014). Effect of machining parameters on the surface roughness while turning particulate composites. *Procedia Engineering*, *97*, 421-431.

[44] Kumar, R., Sahoo, A. K., Das, R. K., Panda, A., & Mishra, P. C. (2018). Modelling of flank wear, surface roughness and cutting temperature in sustainable hard turning of AISI D2 steel. *Procedia Manufacturing*, *20*, 406-413.

[45] Xavierarockiaraj, S., & Kuppan, P. (2014). Investigation of cutting forces, surface roughness and tool wear during laser assisted machining of SKD11Tool steel. *Procedia Engineering*, *97*, 1657-1666.

[46] Srivastava, A. K., Nag, A., Dixit, A. R., Scucka, J., Hloch, S., Klichová, D., ... & Tiwari, S. (2019). Hardness measurement of surfaces on hybrid metal matrix composite created by turning using an abrasive water jet and WED. *Measurement*, *131*, 628-639.

[47] Araújo, R. P., Rolim, T. L., Oliveira, C. A., Moura, A. E., & Silva, J. C. A. (2019). Analysis of the surface roughness and cutting tool wear using a vapor compression assisted cooling system to cool the cutting fluid in turning operation. *Journal of Manufacturing Processes*, *44*, 38-46.

[48] Moganapriya, C., Rajasekar, R., Ponappa, K., Venkatesh, R., & Jerome, S. (2018). Influence of coating material and cutting parameters on surface roughness and material removal rate in turning process using Taguchi method. *Materials Today: Proceedings*, *5*(2), 8532-8538.

[49] Sahu, S., & Choudhury, B. B. (2015). Optimization of surface roughness using taguchi methodology & prediction of tool wear in hard turning tools. *Materials Today: Proceedings*, *2*(4-5), 2615-2623.

[50] Sarıkaya, M., & Güllü, A. (2014). Taguchi design and response surface methodology based analysis of machining parameters in CNC turning under MQL. *Journal of Cleaner Production*, *65*, 604-616.

[51] Asiltürk, I., & Akkuş, H. (2011). Determining the effect of cutting parameters on surface roughness in hard turning using the Taguchi method. *Measurement*, *44*(9), 1697-1704.

[52] Pontes, F. J., de Paiva, A. P., Balestrassi, P. P., Ferreira, J. R., & da Silva, M. B. (2012). Optimization of Radial Basis Function neural network employed for prediction of surface roughness in hard turning process using Taguchi's orthogonal arrays. *Expert Systems with Applications*, *39*(9), 7776-7787.

[53] Asiltürk, I., Neşeli, S., & Ince, M. A. (2016). Optimisation of parameters affecting surface roughness of Co28Cr6Mo medical material during CNC lathe machining by using the Taguchi and RSM methods. *Measurement*, *78*, 120-128.

[54] Asiltürk, I., & Neşeli, S. (2012). Multi response optimisation of CNC turning parameters via Taguchi method-based response surface analysis. *Measurement*, *45*(4), 785-794.

[55] Khare, S. K., & Agarwal, S. (2017). Optimization of machining parameters in turning of AISI 4340 steel under cryogenic condition using Taguchi technique. *Procedia CIRP*, *63*, 610-614.

[56] Moreira, L. C., Li, W. D., Lu, X., & Fitzpatrick, M. E. (2019). Supervision controller for real-time surface quality assurance in CNC machining using artificial intelligence. *Computers & Industrial Engineering*, *127*, 158-168.

[57] Debnath, S., Reddy, M. M., & Yi, Q. S. (2016). Influence of cutting fluid conditions and cutting parameters on surface roughness and tool wear in turning process using Taguchi method. *Measurement*, *78*, 111-119.

[58] Agrawal, A., Goel, S., Rashid, W. B., & Price, M. (2015). Prediction of surface roughness during hard turning of AISI 4340 steel (69 HRC). *Applied Soft Computing*, *30*, 279-286.

[59] Razavykia, A., Yusof, N. M., & Yavari, M. R. (2015). Determining the effects of machining parameters and modifier on surface roughness in dry turning of Al-20% Mg2Si-PMMC using design of experiments (DOE). *Procedia Manufacturing*, *2*, 280-285.

[60] Valera, H. Y., & Bhavsar, S. N. (2014). Experimental investigation of surface roughness and power consumption in turning operation of EN 31 alloy steel. *Procedia Technology*, *14*, 528-534.

[61] Ezugwu, E. O., Fadare, D. A., Bonney, J., Da Silva, R. B., & Sales, W. F. (2005). Modelling the correlation between cutting and process parameters in high-speed machining of Inconel 718 alloy using an artificial neural network. *International Journal of Machine Tools and Manufacture*, *45*(12-13), 1375-1385.

[62] Gadekula, R. K., Potta, M., Kamisetty, D., Yarava, U. K., Anand, P., & Dondapati, R. S. (2018). Investigation on Parametric Process Optimization of HCHCR in CNC Turning Machine Using Taguchi Technique. *Materials Today: Proceedings*, *5*(14), 28446-28453.

[63]https://www.renishaw.com/cmmsupport/knowledgebase/en/surface-finish-measurement--22135, 24/07/2019, 12:22 PM.

[64] https://www.qualitymag.com/articles/84505-quality-101-surface-finish-measurement-basics, 24/07/2019, 12:31 PM.

[65] https://wiki.anton-paar.com/en/x-ray-diffraction-xrd/, 24/07/2019, 12:51 PM.

[66] Choi, K. J., Yoo, S. C., Ham, J., Kim, J. H., Jeong, S. Y., & Choi, Y. S. (2018). Fatigue behavior of AISI 8620 steel exposed to magnetic field. *Journal of Alloys and Compounds*, *764*, 73-79.

APPENDIX

In this appendix, Residual stress graphs are shown of the respected data points. Residual stress graphs are following below:-

5.1

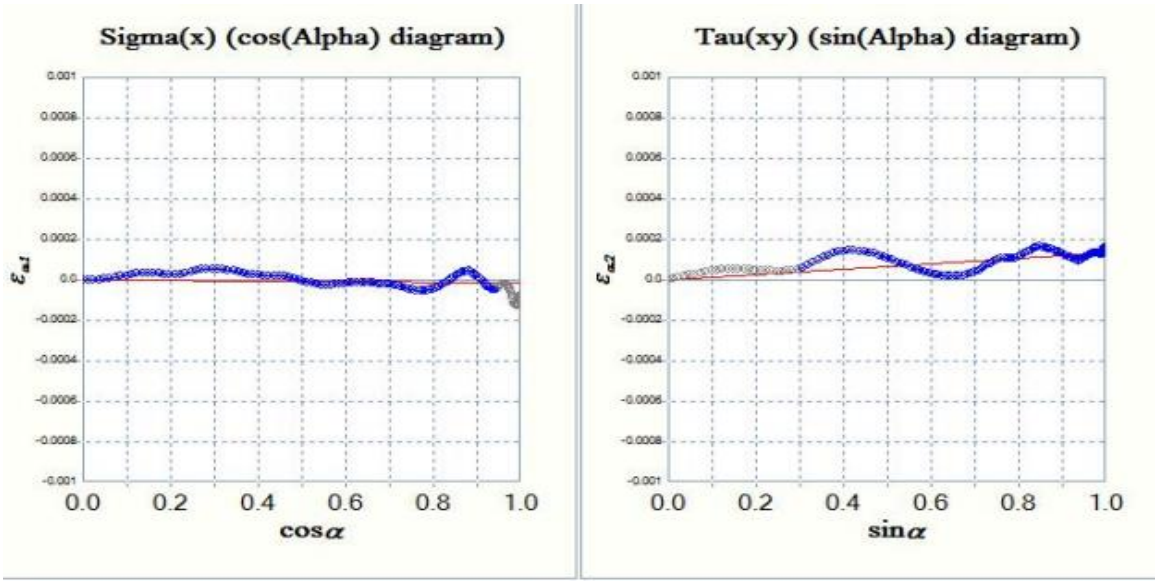

Normal Stress = (+) 7 MPa

Shear Stress = (+) 50 MPa

5.2

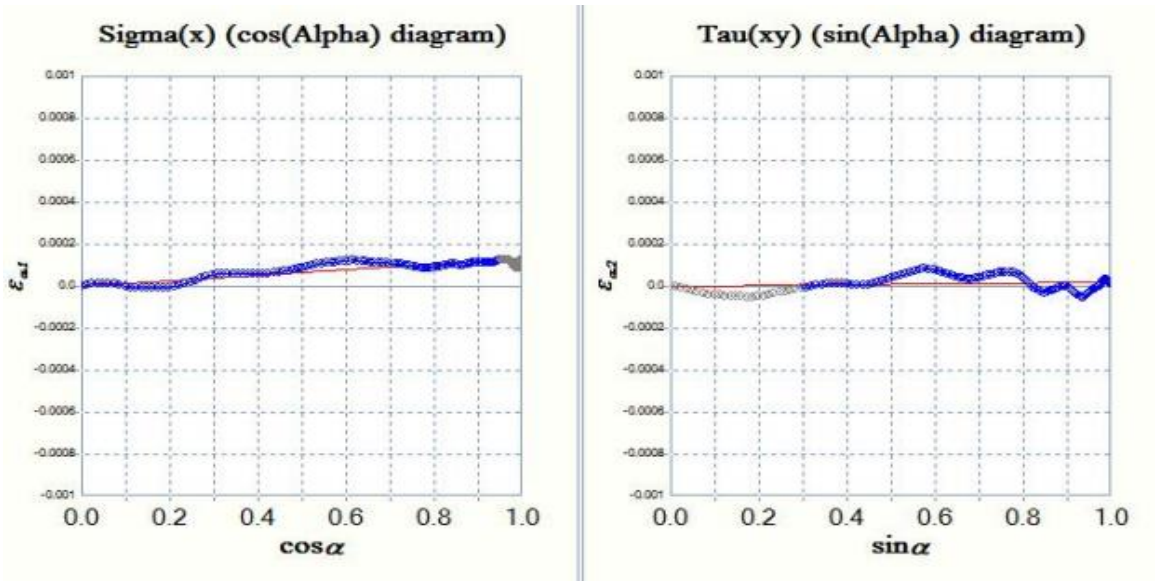

Normal Stress = (-) 62 MPa

Shear Stress =(+) 5 MPa

5.3

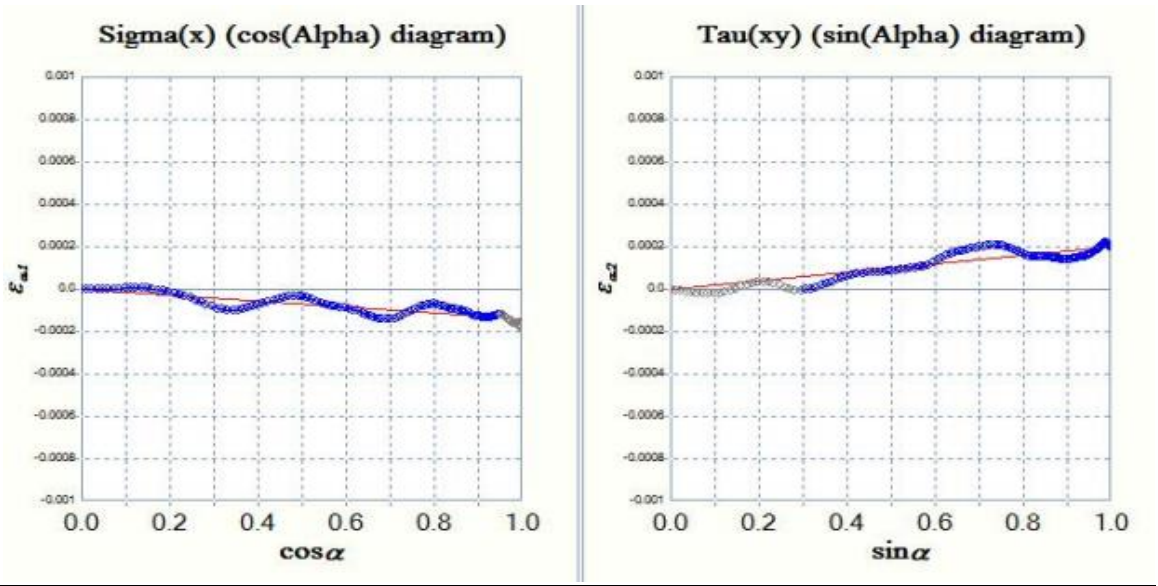

Normal Stress = (+) 66 MPa

Shear Stress = (+) 74 MPa

Average Residual Stress of 3 points = (+) 3.666 MPa

7.1

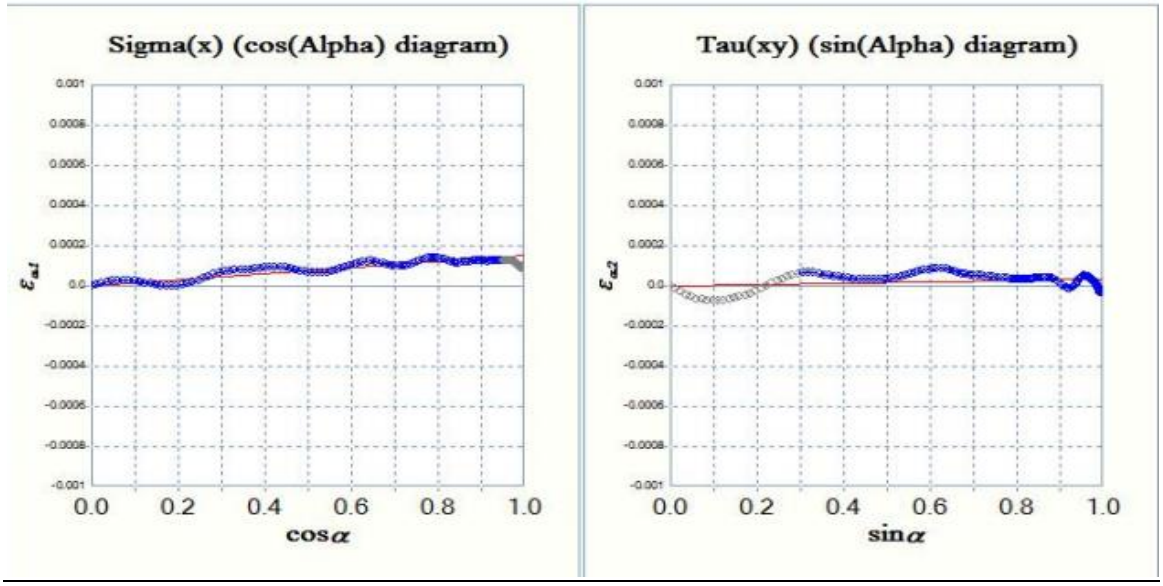

Normal Stress = (-) 68 MPa

Shear Stress = (+) 12 MPa

7.2

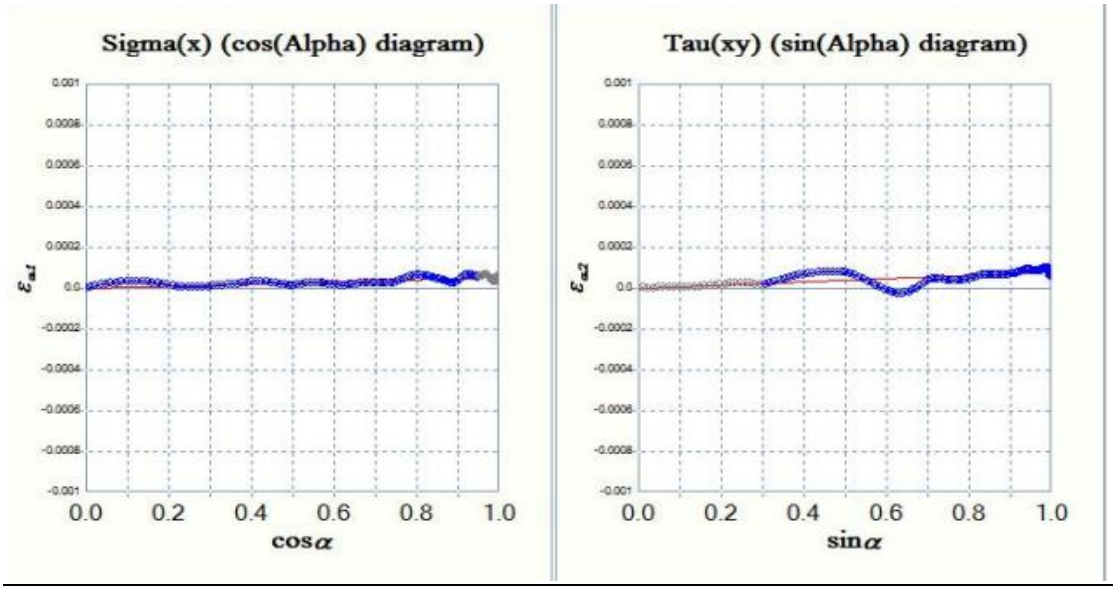

Normal Stress = (-) 22 MPa

Shear Stress = (+) 28 MPa

7.3

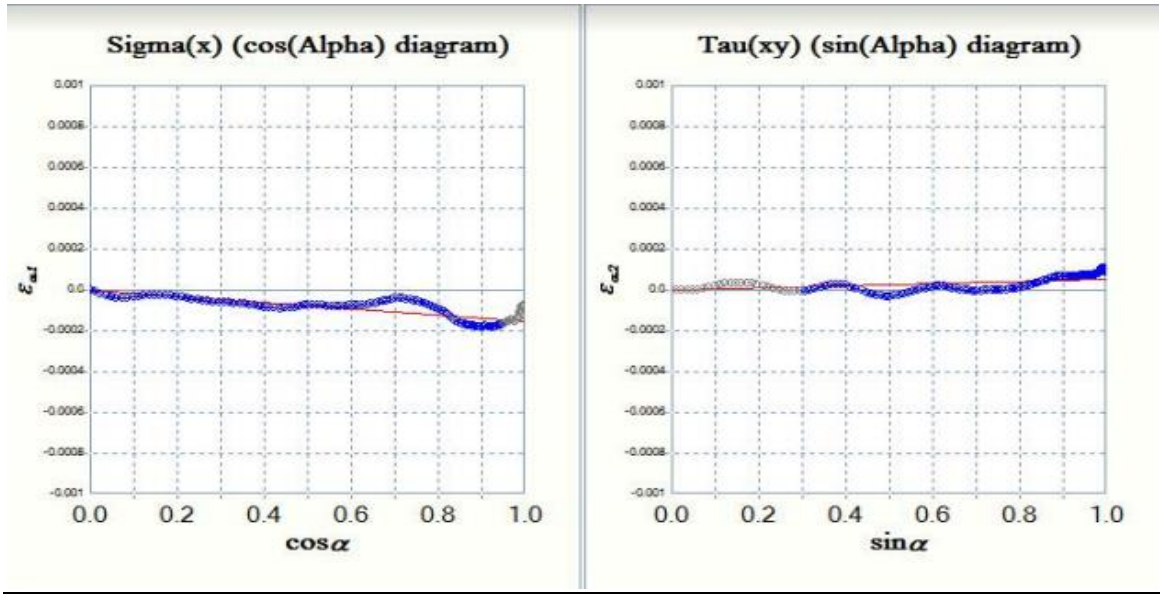

Normal Stress = (+) 73 MPa

Shear Stress = (+) 20 MPa

Average Residual Stress of 3 points = (-) 5.666 MPa

9.1

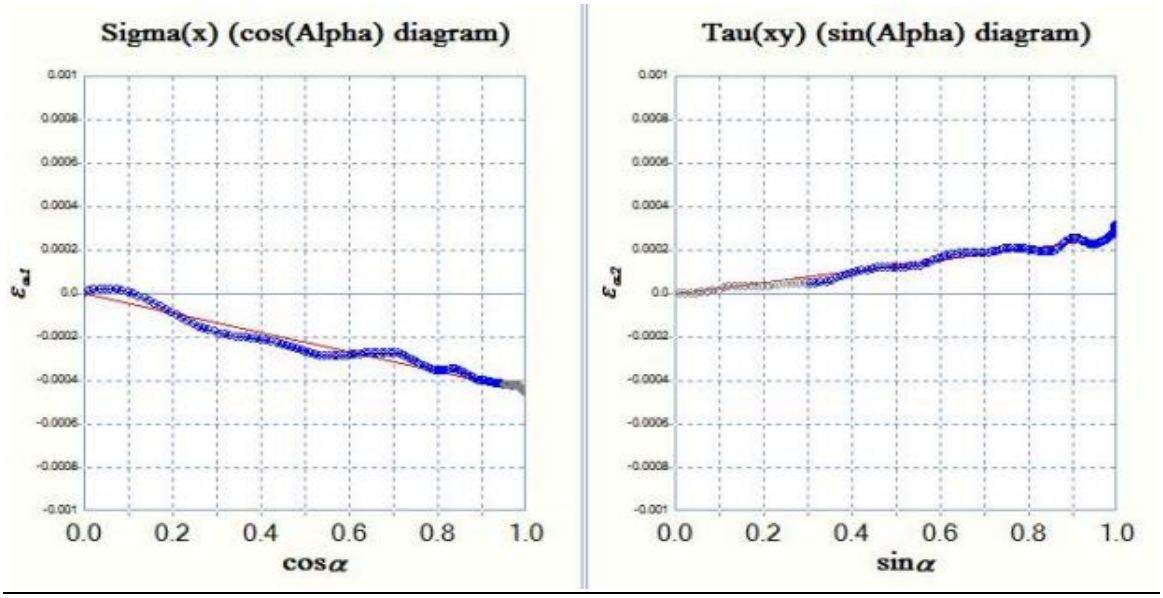

Normal Stress = (+) 209 MPa

Shear Stress = (+) 98 MPa

9.2

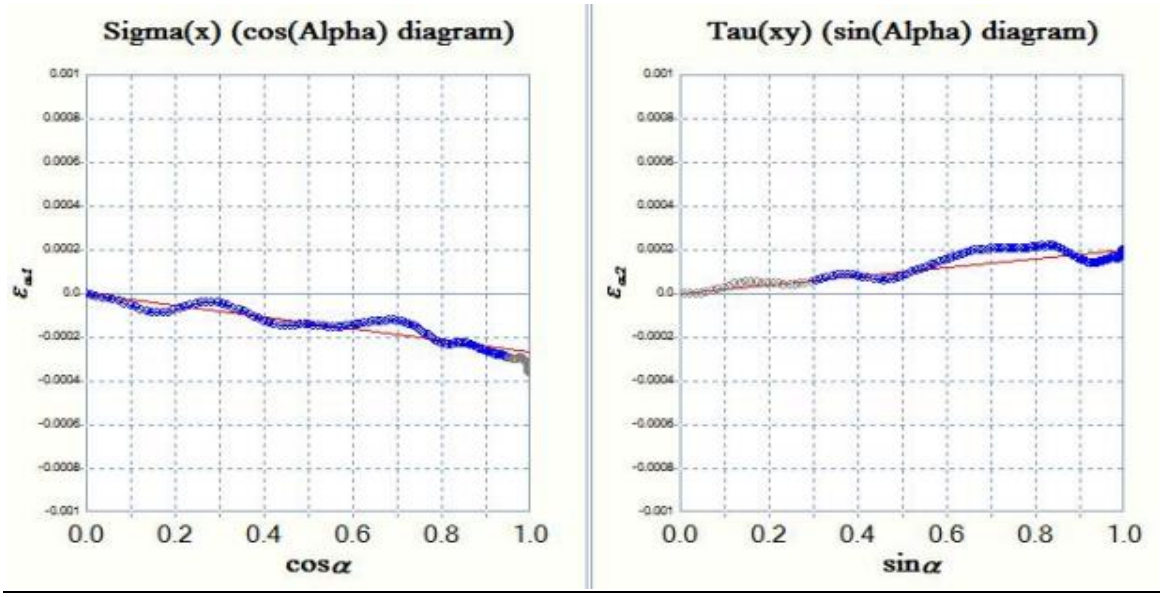

Normal Stress = (+) 125 MPa

Shear Stress = (+) 76 MPa

9.3

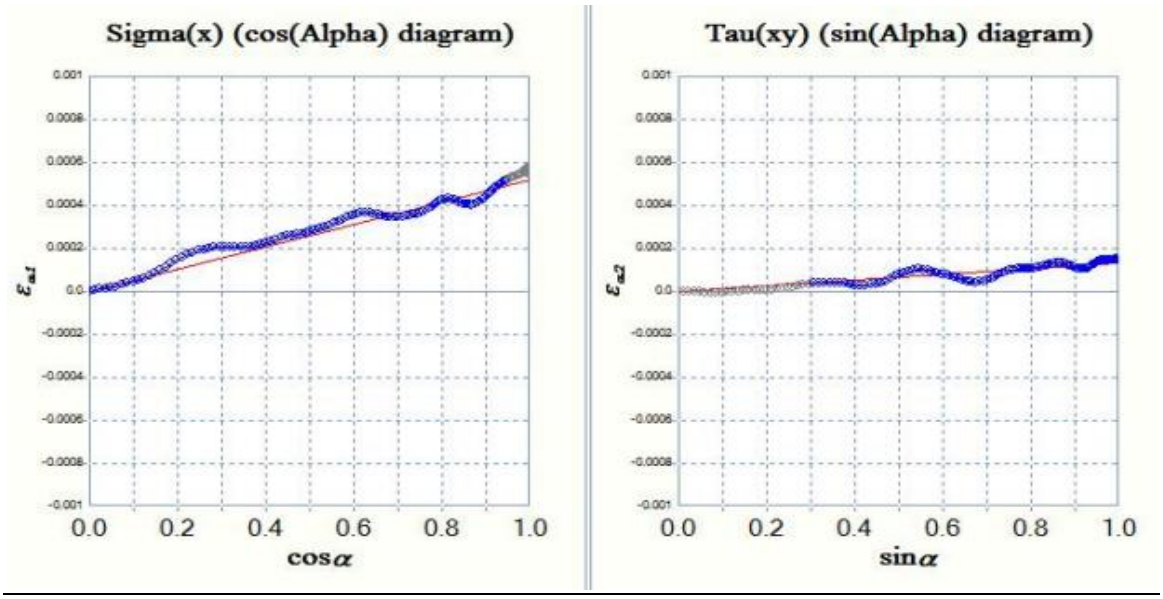

Normal Stress = (-) 241 MPa

Shear Stress = (+) 50 MPa

Average Residual Stress of 3 points = (+) 31 MPa

10.1

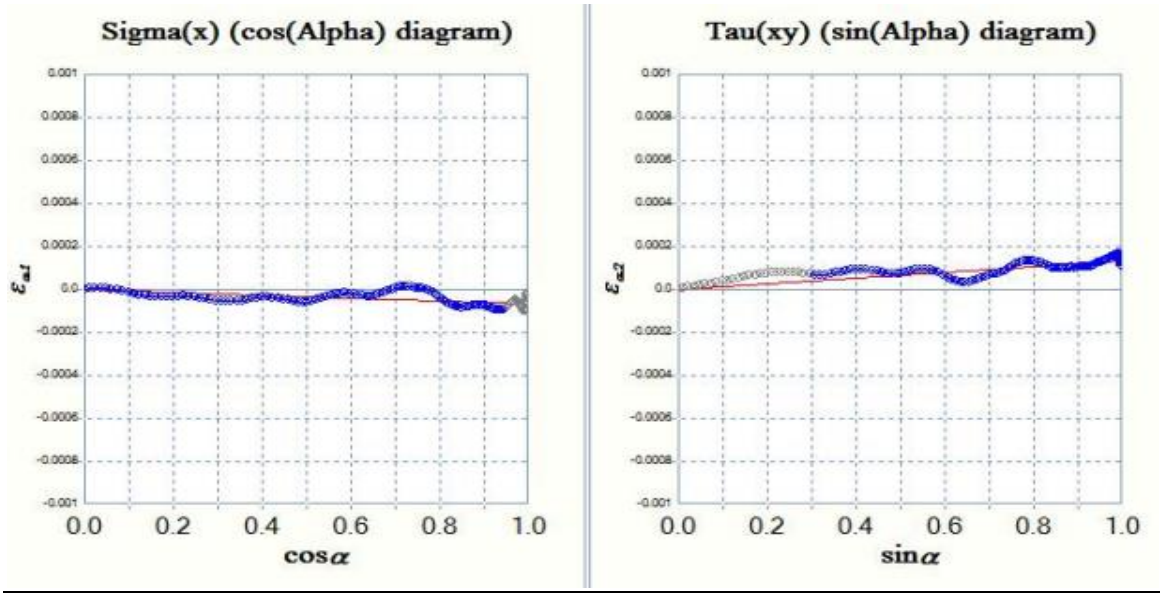

Normal Stress = (+) 33 MPa

Shear Stress = (+) 50 MPa

10.2

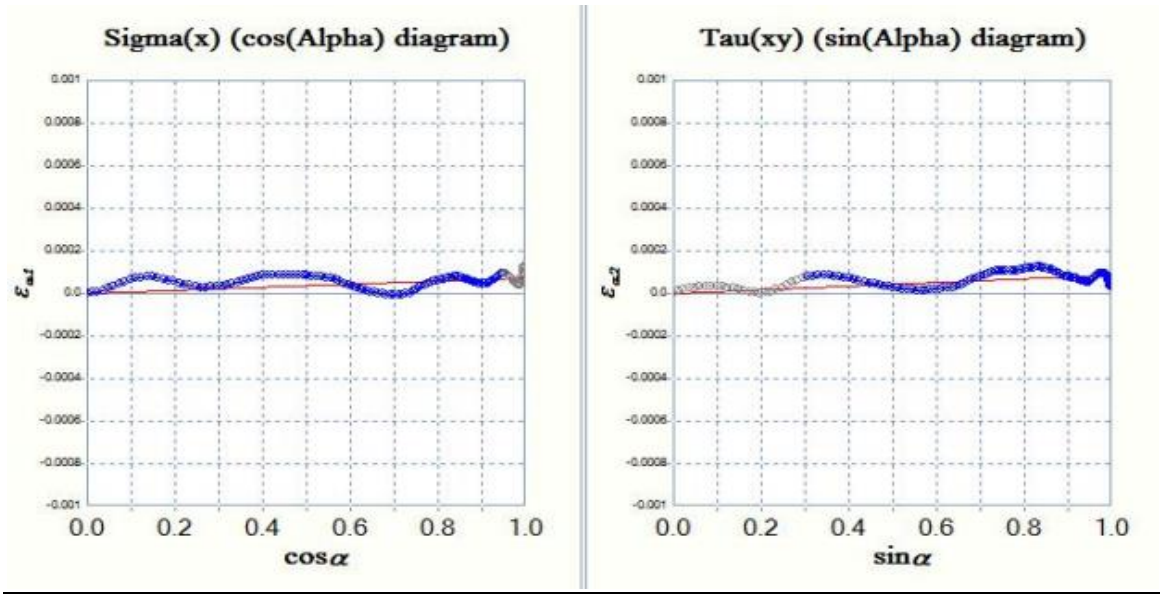

Normal Stress = (-) 32 MPa

Shear Stress =(+) 33 MPa

10.3

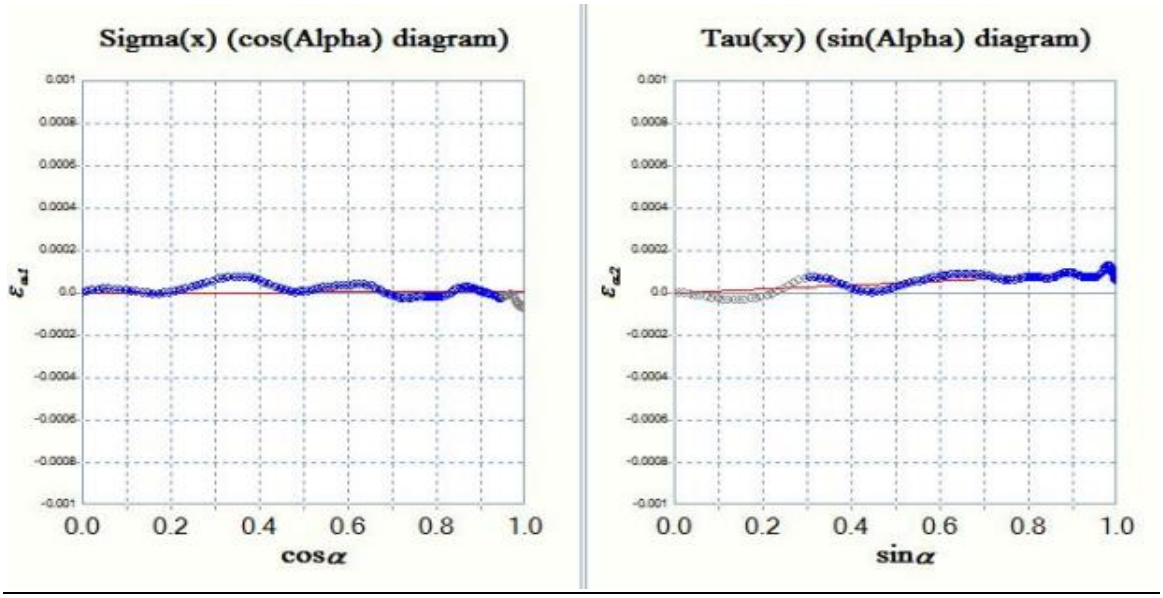

Normal Stress = (-) 3 MPa

Shear Stress =(+) 34 MPa

Average Residual Stress of 3 points = (-) 0.666 MPa

11.1

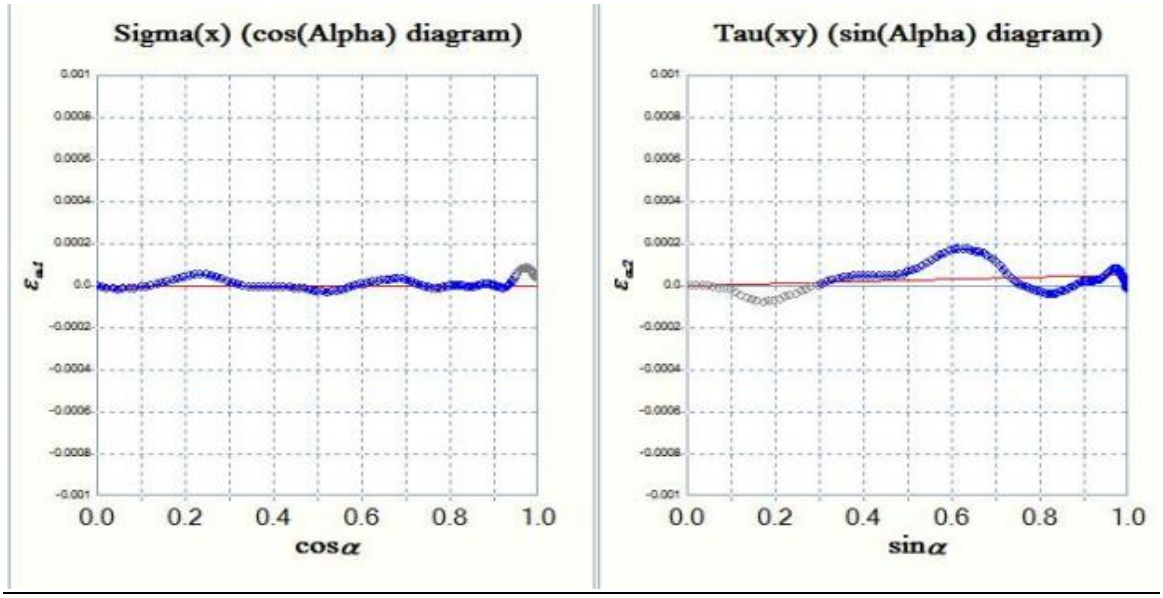

Normal Stress = (+) 1 MPa

Shear Stress = (+) 19 MPa

11.2

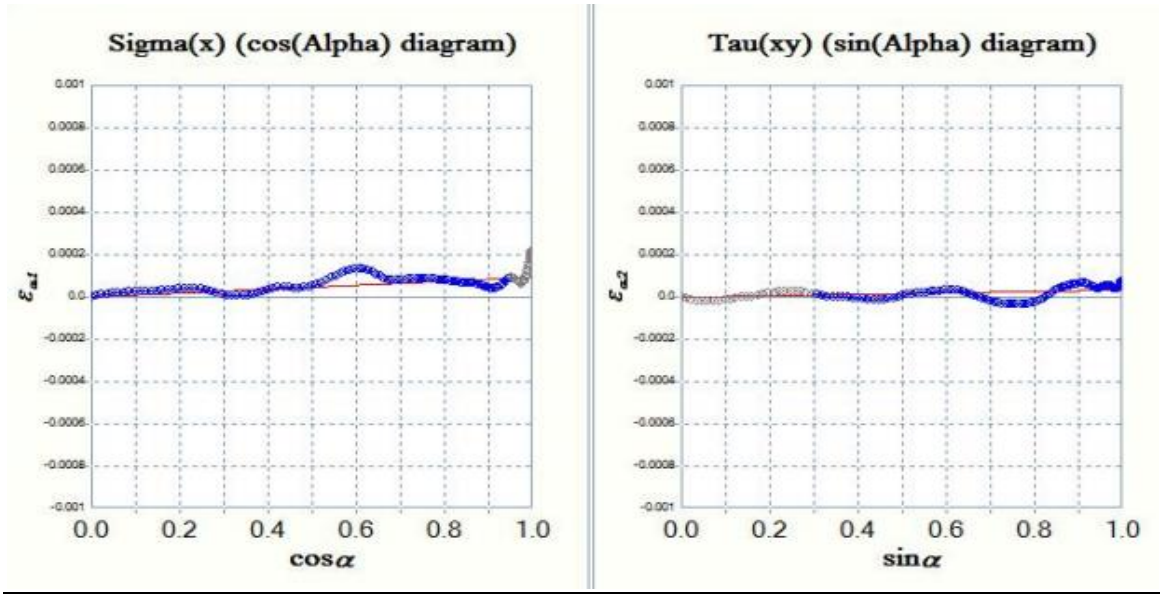

Normal Stress = (-) 43 MPa

Shear Stress =(+) 11 MPa

11.3

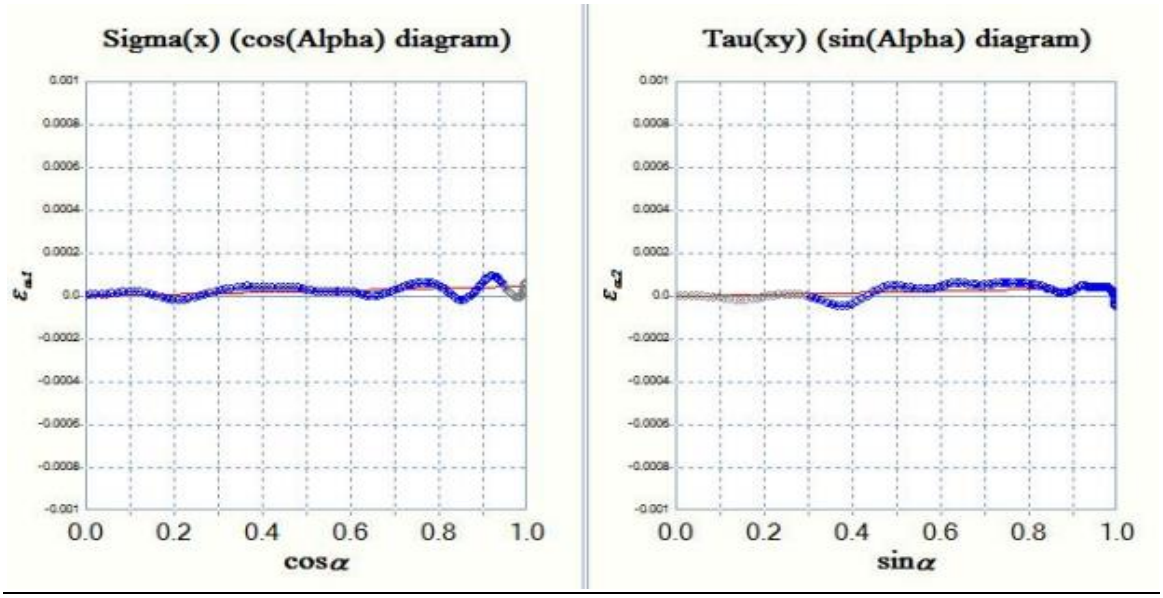

Normal Stress = (-) 20 MPa

Shear Stress = (+) 13 MPa

Average Residual Stress of 3 points = (-) 20.666 MPa

14.1

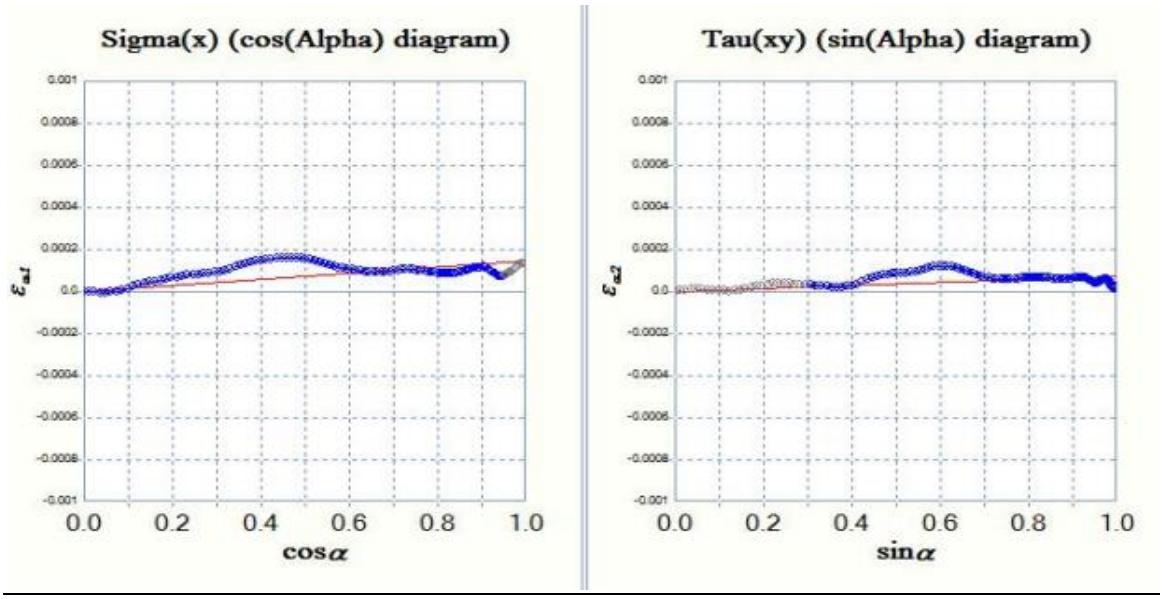

Normal Stress = (-) 67 MPa

Shear Stress = (+) 26 MPa

14.2

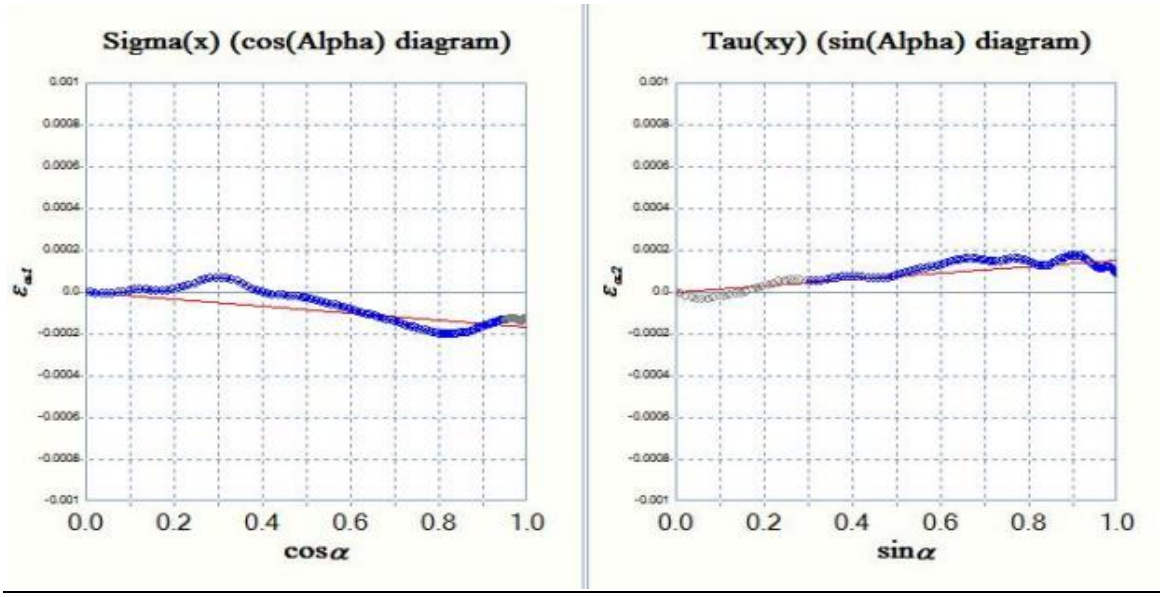

Normal Stress = (+) 80 MPa

Shear Stress = (+) 58 MPa

14.3

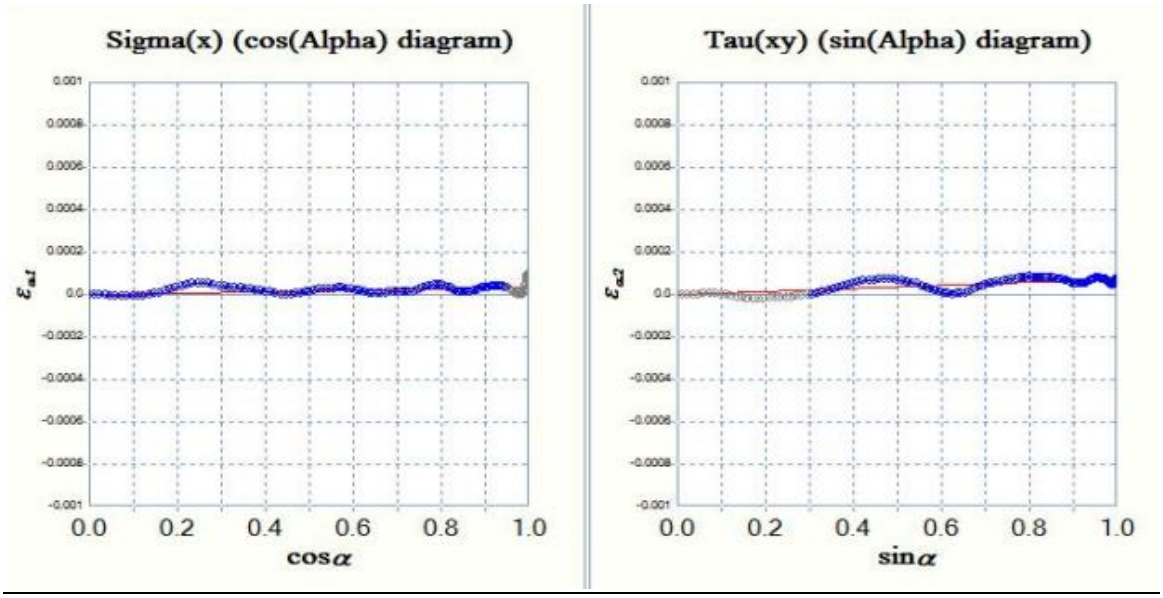

Normal Stress = (-) 14 MPa

Shear Stress = (+) 26 MPa

Average Residual Stress of 3 points = (-) 0.333 MPa

17.1

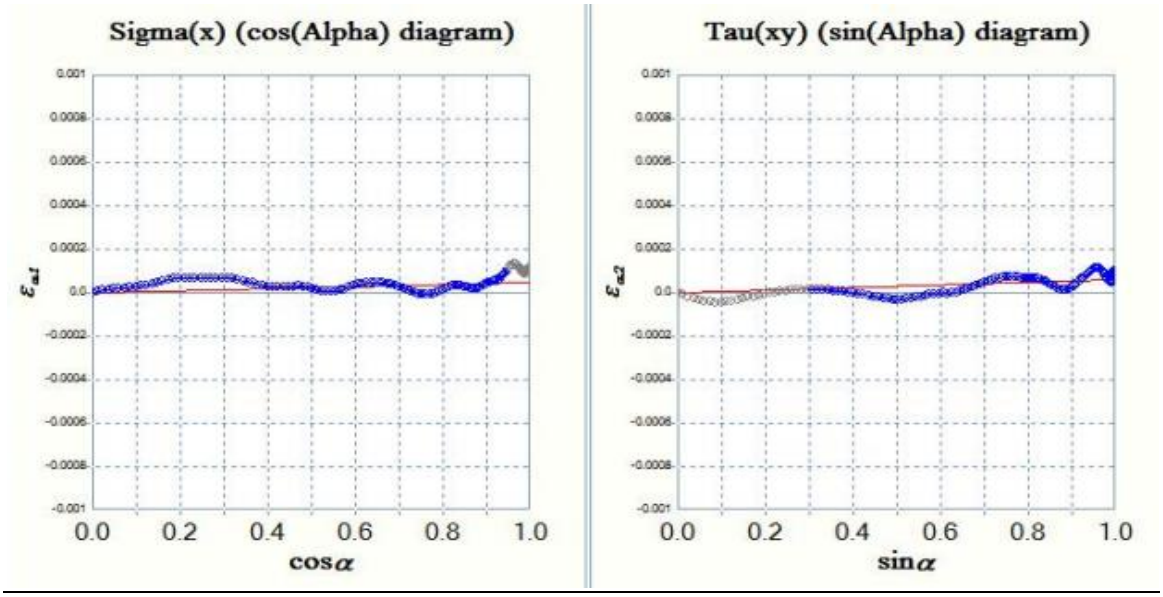

Normal Stress = (-) 20 MPa

Shear Stress = (+) 21 MPa

17.2

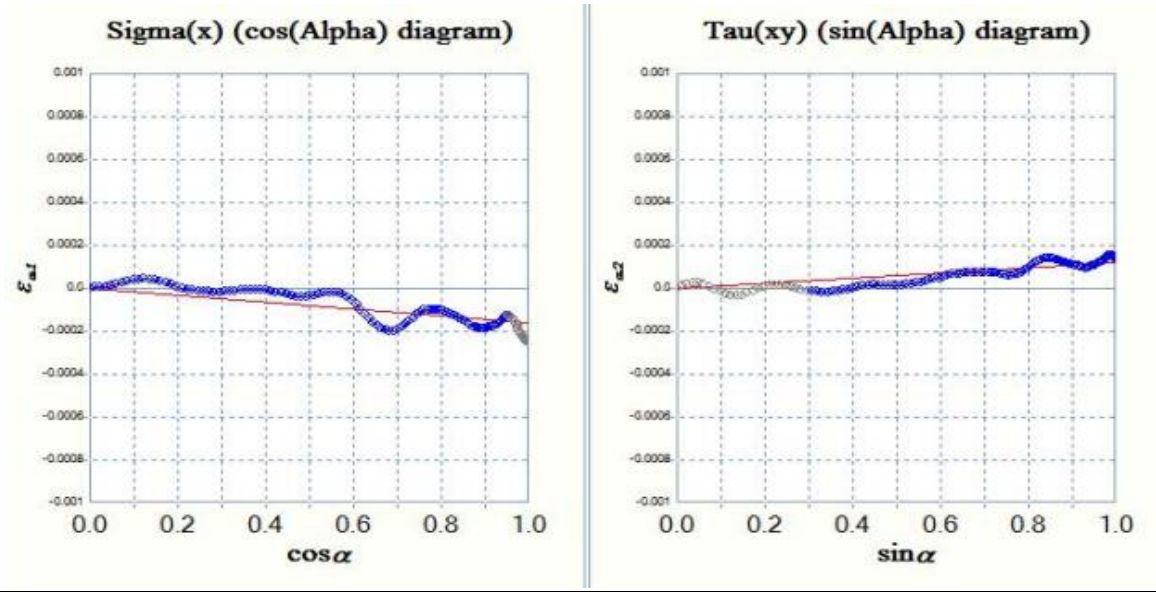

Normal Stress = (+) 77 MPa

Shear Stress = (+) 44 MPa

17.3

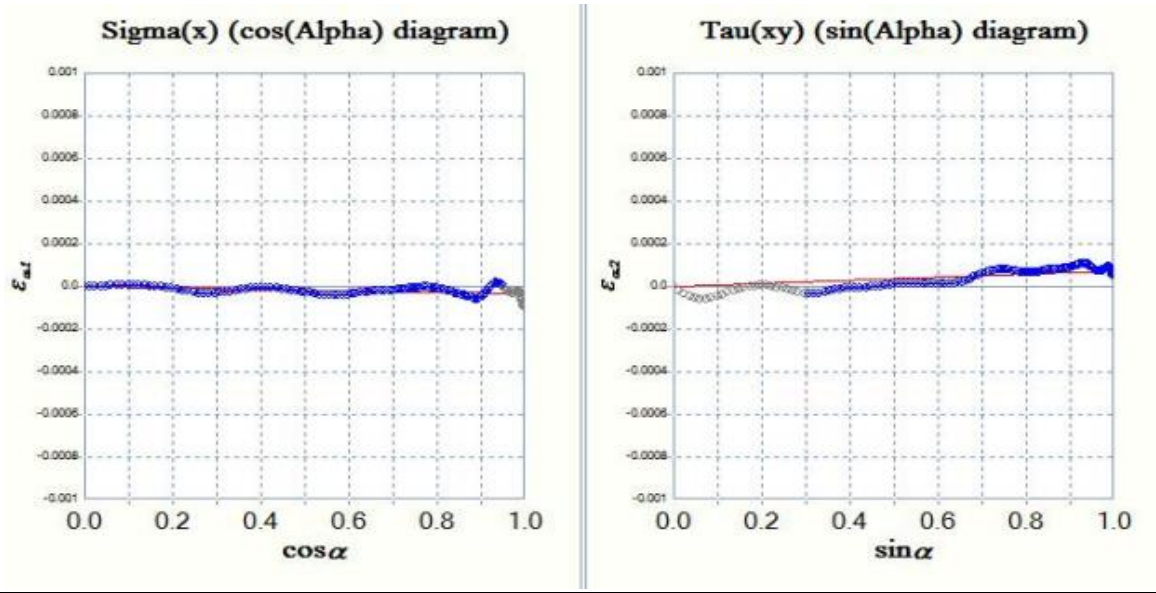

Normal Stress = (+) 16 MPa

Shear Stress = (+) 28 MPa

Average Residual Stress of 3 points = (+) 24.333 MPa

19.1

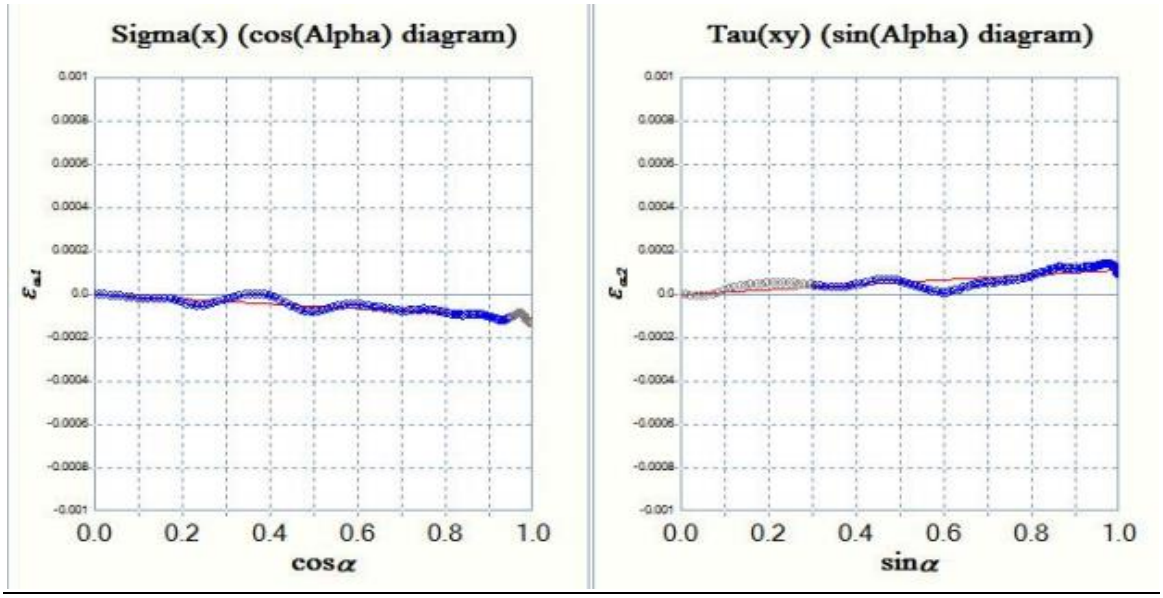

Normal Stress = (+) 52 MPa

Shear Stress = (+) 42 MPa

19.2

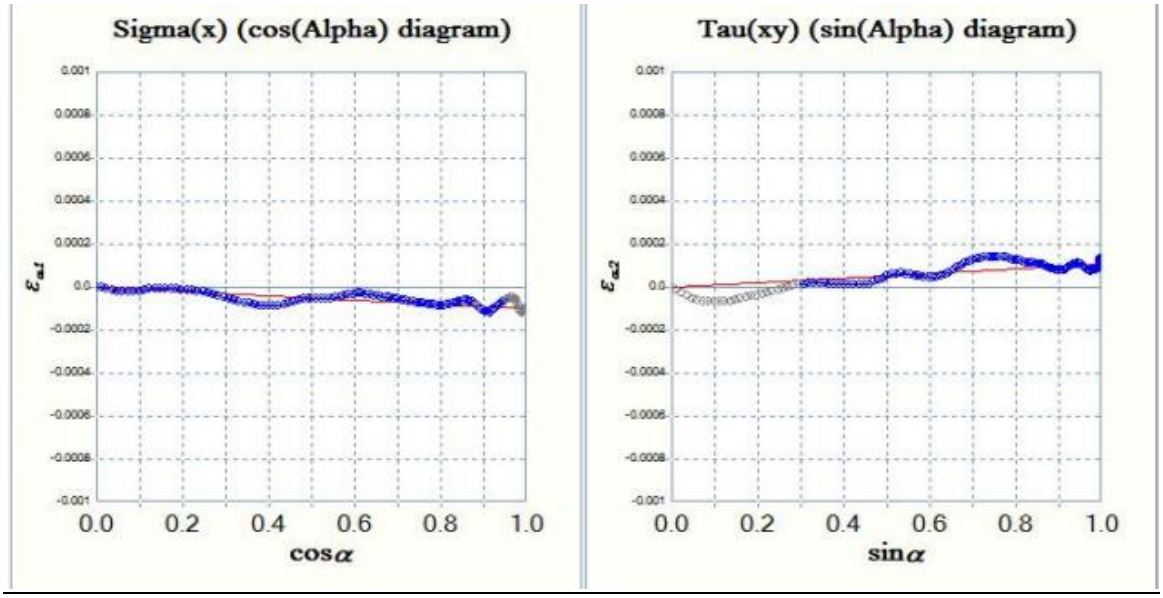

Normal Stress = (+) 47 MPa

Shear Stress = (+) 41 MPa

19.3

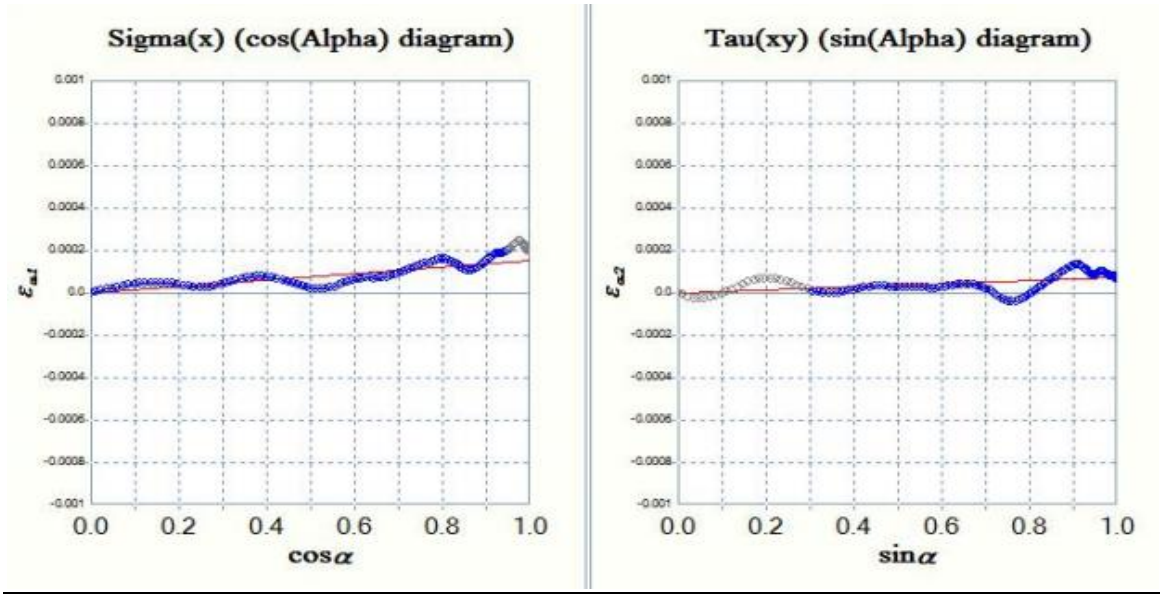

Normal Stress = (-) 69 MPa

Shear Stress = (+) 25 MPa

Average Residual Stress of 3 points = (+) 10 MPa

20.1

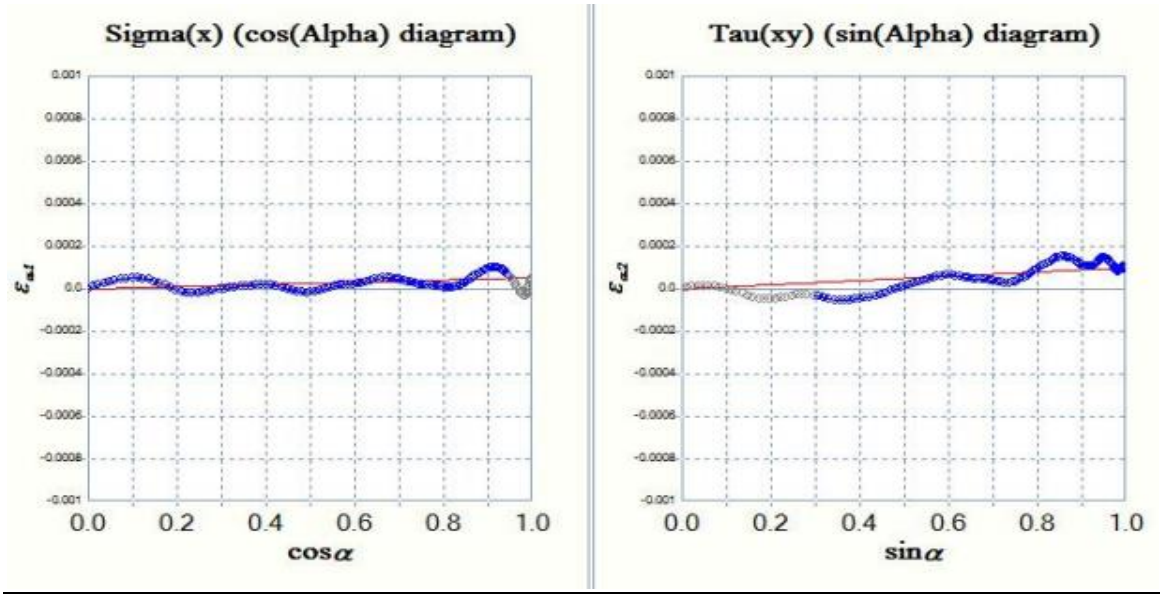

Normal Stress = (-) 23 MPa

Shear Stress = (+) 37 MPa

20.2

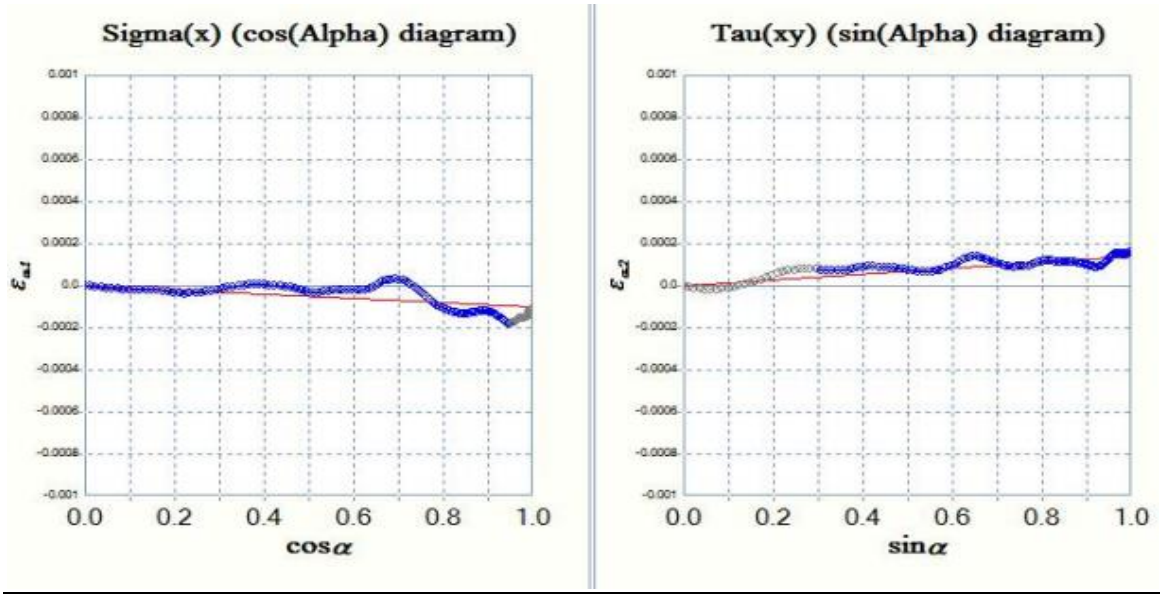

Normal Stress = (+) 47 MPa

Shear Stress = (+) 53 MPa

20.3

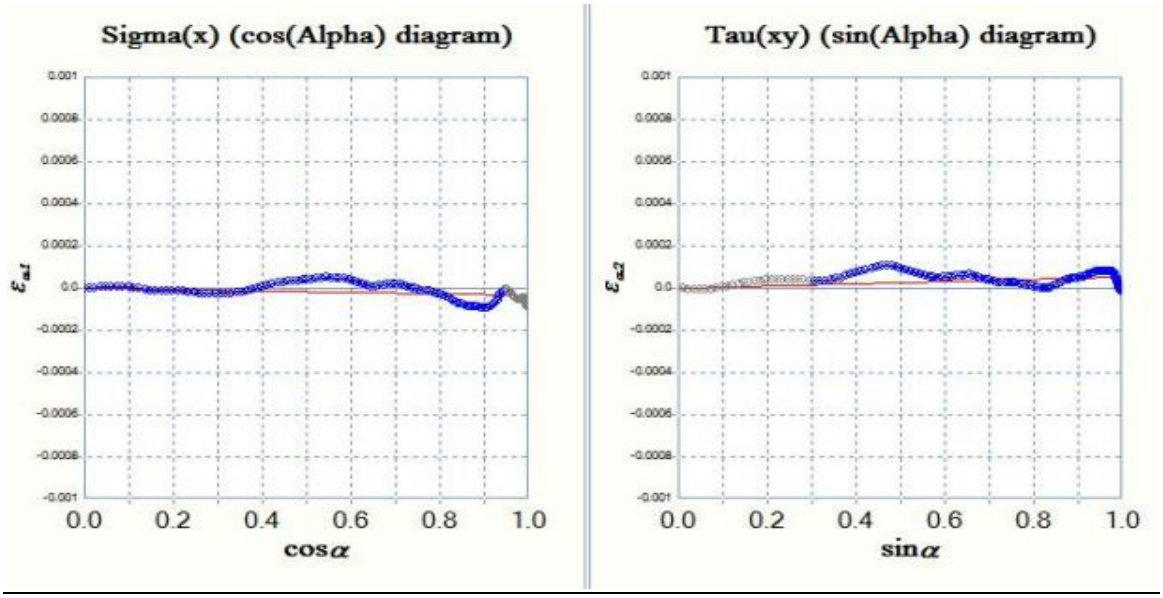

Normal Stress = (+) 17 MPa

Shear Stress = (+) 19 MPa

Average Residual Stress of 3 points = (+) 13.666 MPa

the machined components

ORIGINALITY REPORT

16%	12%	7%	12%
SIMILARITY INDEX	INTERNET SOURCES	PUBLICATIONS	STUDENT PAPERS

PRIMARY SOURCES

1	core.ac.uk Internet Source	1%
2	Mei-Jiau Huang. "An Investigation of the Thermal Stresses Induced in a Thin-Film Thermoelectric Cooler", Journal of Thermal Stresses, 05/2008 Publication	1%
3	www.starrett.com Internet Source	1%
4	Submitted to Visvesvaraya Technological University Student Paper	1%
5	docplayer.net Internet Source	1%
6	Submitted to Caledonian College of Engineering Student Paper	1%
7	willrich.com Internet Source	1%

Submitted to Savitribai Phule Pune University

8	Student Paper	1%
9	Submitted to Bharati Vidyapeeth Deemed University College Of Engineering Student Paper	<1%
10	en.wikipedia.org Internet Source	<1%
11	www.astmsteel.com Internet Source	<1%
12	doras.dcu.ie Internet Source	<1%
13	digital.lib.washington.edu Internet Source	<1%
14	www.ijert.org Internet Source	<1%
15	BERBER, Adnan. "Mathematical Model for Fuel Flow Performance of Diesel Engine", Selçuk Üniversitesi Alaeddin Keykubat Kampüsü Teknik Eğitim Fakültesi Selçuklu / Konya, 2016. Publication	<1%
16	www.ukessays.com Internet Source	<1%
17	Submitted to The RCY Colleges & Institutes Student Paper	<1%

18	www.slideshare.net Internet Source	<1%
19	Submitted to Royal Melbourne Institute of Technology Student Paper	<1%
20	ijari.org Internet Source	<1%
21	www.predev.com Internet Source	<1%
22	Submitted to Wawasan Open University Student Paper	<1%
23	Submitted to Universiti Kebangsaan Malaysia Student Paper	<1%
24	f-di.hu Internet Source	<1%
25	Submitted to University of Malaya Student Paper	<1%
26	www.tech.plym.ac.uk Internet Source	<1%
27	Submitted to National Kaohsiung University of Applied Science Student Paper	<1%
28	Submitted to Institute of Technology, Nirma University	<1%

Student Paper

29	"Modeling of Metal Forming and Machining Processes", Springer Nature, 2008 Publication	<1%
30	Kyoung Joon Choi, Seung Chang Yoo, Junhyuk Ham, Ji Hyun Kim, Soo Yeol Jeong, Yeon Suk Choi. "Fatigue behavior of AISI 8620 steel exposed to magnetic field", Journal of Alloys and Compounds, 2018 Publication	<1%
31	Kalipada Maity, Swastik Pradhan. "Study of Chip Morphology, Flank Wear on Different Machinability Conditions of Titanium Alloy (Ti-6Al-4V) Using Response Surface Methodology Approach", International Journal of Materials Forming and Machining Processes, 2017 Publication	<1%
32	Eva M. Rubio, Alfonso Bericua, Beatriz de Agustina, Marta M. Marín. "Analysis of the surface roughness of titanium pieces obtained by turning using different cooling systems", Procedia CIRP, 2019 Publication	<1%
33	ijoer.in Internet Source	<1%
34	www.ijirset.com Internet Source	<1%

35	archive.org Internet Source	<1%
36	Submitted to Deakin University Student Paper	<1%
37	www.ganpatiinstitutions.com Internet Source	<1%
38	V Gunaraj, N Murugan. "Application of response surface methodology for predicting weld bead quality in submerged arc welding of pipes", Journal of Materials Processing Technology, 1999 Publication	<1%
39	Sahu, Neelesh Ku., and A. B. Andhare. "Optimization of Surface Roughness in Turning of Ti-6Al-4V Using Response Surface Methodology and TLBO", Volume 4 20th Design for Manufacturing and the Life Cycle Conference 9th International Conference on Micro- and Nanosystems, 2015. Publication	<1%
40	G. kartheek, Kolla Srinivas, Ch. Devaraj. "Optimization of Residual Stresses in Hard Turning of Super Alloy Inconel 718", Materials Today: Proceedings, 2018 Publication	<1%
41	Submitted to Visvesvaraya National Institute of	

	Technology Student Paper	<1%
42	Senthilkumar, N., T. Tamizharasan, and V. Anandakrishnan. "Experimental investigation and performance analysis of cemented carbide inserts of different geometries using Taguchi based grey relational analysis", Measurement, 2014. Publication	<1%
43	P. Sivaiah, D. Chakradhar. "Analysis and Modeling of Cryogenic Turning Operation Using Response Surface Methodology", Silicon, 2018 Publication	<1%
44	vssut.ac.in Internet Source	<1%
45	link.springer.com Internet Source	<1%
46	pt.scribd.com Internet Source	<1%
47	Submitted to Universiti Teknologi MARA Student Paper	<1%
48	Aruna, M., and V. Dhanalakshmi. "Optimisation of turning parameters of Inconel 718 alloy using RSM", International Journal of Manufacturing Technology and Management, 2012. Publication	<1%

49	Submitted to Maharshi Dayanand University Student Paper	<1%
50	Submitted to Modern Education Society's College of Engineering, Pune Student Paper	<1%
51	www.ijaerd.co.in Internet Source	<1%
52	www.cs.iusb.edu Internet Source	<1%
53	Submitted to Maulana Azad National Institute of Technology Bhopal Student Paper	<1%
54	Submitted to Walchand College of Engg Sangli Maharastra Student Paper	<1%
55	V.P. Bhemuni, S.R. Chalamalasetti. "A Review on Hard Turning by using Design of Experiments", Journal for Manufacturing Science & Production, 2013 Publication	<1%
56	Submitted to Institute of Research & Postgraduate Studies, Universiti Kuala Lumpur Student Paper	<1%
57	Submitted to Vels University Student Paper	<1%

58	www.pertanika2.upm.edu.my Internet Source	<1%
59	Submitted to Coventry University Student Paper	<1%
60	S. Ramesh, L. Karunamoorthy, K. Palanikumar. "Surface Roughness Analysis in Machining of Titanium Alloy", Materials and Manufacturing Processes, 2008 Publication	<1%
61	Submitted to Higher Education Commission Pakistan Student Paper	<1%
62	Submitted to VIT University Student Paper	<1%
63	於2012-01-01提交至Caledonian College of Engineering Student Paper	<1%
64	www.irjet.net Internet Source	<1%
65	Submitted to Chindwin College Student Paper	<1%
66	www.scribd.com Internet Source	<1%
67	www.trp.org.in Internet Source	<1%

68	Submitted to Malaviya National Institute of Technology Student Paper	<1%
69	E. García Plaza, P.J. Núñez López. "Application of the wavelet packet transform to vibration signals for surface roughness monitoring in CNC turning operations", Mechanical Systems and Signal Processing, 2018 Publication	<1%
70	cutting-tools-dealers-in-chennai.blogspot.my Internet Source	<1%
71	C. Ezilarasan. "Surface roughness analysis on machining of nimonic C-263 alloy using ANN and RSM techniques", International Journal of Precision Technology, 2011 Publication	<1%
72	Submitted to British University in Egypt Student Paper	<1%
73	Submitted to University of Newcastle upon Tyne Student Paper	<1%
74	Submitted to Cankaya University Student Paper	<1%
75	jchps.com Internet Source	<1%
76	Korimilli Surya Sundara Rao, K. Viswanath	

	Allamraju. "Effect on Micro-Hardness and Residual Stress in CNC Turning Of Aluminium 7075 Alloy", Materials Today: Proceedings, 2017 Publication	<1%
77	www.iaeme.com Internet Source	<1%
78	Submitted to Nanyang Technological University, Singapore Student Paper	<1%

Exclude quotes	On	Exclude matches	< 10 words
Exclude bibliography	On		